



Light-Curing Polymer Systems
As Novel Pressure-Sensitive Adhesives
With Innovative Crosslinking Mechanisms

Inaugural-Dissertation

for the attainment of the title of
Doctor in Natural Sciences (Dr. rer. nat.)
from the Faculty of Mathematics and Natural Sciences
of the Heinrich Heine University in Dusseldorf

presented by

Moritz Arnold

born in Leverkusen

Düsseldorf, November 2024

Printed with the permission of the
Faculty of Mathematics and Natural Sciences
Heinrich-Heine-University Düsseldorf

Supervisor: Prof. Dr. Laura Hartmann
Co-supervisor: Priv.-Doz. Dr. Klaus Schaper

Date of the oral examination: 6th of November 2024

Declaration of authorship

I hereby declare that the thesis submitted is my own work without making use of impermissible aids, considering the "Rules on the Principles for Safeguarding Good Scientific Practice at Heinrich Heine University Düsseldorf". All direct or indirect sources used are acknowledged in the bibliography as references. I further declare that I have not submitted this nor a similar thesis at any other examination board in order to obtain a degree.



02.12.2024

Moritz Arnold

Date

“If you can’t fix it with duct tape,
then you ain’t using enough duct tape.”

Will Sawyer (2018)

Content

List of patents and publications

Abstract

1. Introduction	1
2. Theoretical background	3
2.1 Pressure sensitive adhesives	3
2.2 Polymerization and polymer design for acrylic PSA.....	8
2.3 UV curing and sustainability.....	12
2.4 UV crosslinking of acrylic hotmelts: Free radical	15
2.5 UV crosslinking of acrylic hotmelts: Cationic	19
2.6 Sensitizers for onium salts	26
2.7 Silanes in cationic curing PSA.....	29
3. Motivation and aims	31
4. Results and discussion	32
4.1 Cationic curing PSA.....	32
4.2 Cationic curing: Photoinitiator possibilities.....	35
4.3 Sensitizers for improved LED curing.....	44
4.4 Optimization of cationic curing.....	53
4.5 Upscaling of LED curable cationic PSA.....	58
4.6 Free radical curing LED PSA.....	61
4.7 Polymerizable free radical LED photoinitiator	71
4.8 Reducing oxygen inhibition of free radical PSA.....	79
4.9 Migration study on AC-ITX.....	83
4.10 Silane promoted cationic curing PSA.....	86

5. Conclusion and outlook.....	106
6. Experimental part.....	111
6.1 Polymerization of cationic curable PSA	111
6.2 Polymerization of free radical curable PSA	113
6.3 Synthesis of AC-ITX.....	115
6.4 Migration test for AC-ITX PSA.....	119
6.5 Formulations for Silane promoted cationic PSA	120
6.6 PSA test methods	121
6.6.1 Shear adhesion failure test (SAFT).....	121
6.6.2 Peel test	123
6.6.3 UV rheology	125
6.7 Analytical methods	126
6.7.1 Gel permeation chromatography (GPC)	126
6.7.2 Infrared spectroscopy (IR).....	127
6.7.3 Nuclear Magnetic Resonance (NMR).....	127
6.7.4 Differential Scanning Calorimetry (DSC)	127
6.7.5 UV/VIS Absorption.....	127
6.7.6 Dynamic mechanical analysis (DMA)	128
6.7.7 Soxhlet extraction	128
6.7.8 Atomic force microscopy (AFM)	128
6.8 PSA sample preparation and UV curing	129
7. References	130
8. Appendix.....	144
8.1 List of abbreviations.....	144
8.2 Acknowledgements.....	147

List of patents and publications

The content of this PhD thesis has been patented by the author via Henkel AG & Co. KGaA and shall not be copied or reproduced.

WO 2023208833 (published) – UV LED curable hotmelt pressure sensitive adhesive composition, its production as well as an article – M. Arnold, A. Taden, A. Schneider and T. Roschkowski

Contribution: Development of Suitable photoinitiator combination for fast LED curing with 365nm. Improving the curing efficiency and enabling a commercializable LED curable hotmelt PSA. *Planning, investigation, experiments, patent draft.*

EP 22214076.6 (published) – UV LED Free Radical curable Hotmelt Pressure sensitive adhesive – M. Arnold, A. Taden, A. Schneider and T. Roschkowski

Contribution: Development of a free radical curable LED PSA including tests procedures, experiments, investigations and patent draft. Ensuring reduced oxygen inhibition by finding suitable synergists. *Planning, investigation, experiments, patent draft.*

EP 22214079.0 (published) – Polymerizable Photoinitiator for LED curing products M. Arnold, A. Taden and A. Schneider

Contribution: Planning and realization of a synthesis route for the preparation of a copolymerizable photoinitiator suitable for enhanced LED curing. *Planning, investigation, synthesis, patent draft, upscaling supervision.*

2023ID00217 (Internal number, filed) – UV curable pressure sensitive adhesive M. Arnold, S. Liu, A. Schneider, E. Silverberg, P. Ernst and A. Taden

Contribution: Development of a high cohesion PSA for excellent plastic adhesion. Enabling transfer coating applications, with low viscosity LED curable hotmelt for a more sustainable PSA. *Planning, investigation, experiments.*

Arnold, M.; Schneider, A.; Taden, A. Novel LED cationic curable hotmelt pressure sensitive adhesive (PSA). *ACS Macro Letters* **presumably 2025**.

Contribution: Investigation of suitable commercially available cationic photoinitiators for LED curable cationic polymerization of epoxy acrylate hotmelt polymers used in PSA applications. *Planning, investigation, synthesis, publication draft.*

Arnold, M.; Schneider, A.; Taden, A. Energy efficient LED curing of cationic pressure sensitive adhesive (PSA) with suitable photosensitizers. *ACS Macro Letters* **presumably 2025**.

Contribution: Investigation of suitable commercially available sensitizers for improving cationic photoinitiators used for LED curable cationic polymerization of epoxy acrylate hotmelt polymers used in PSA applications. *Planning, investigation, synthesis, publication draft.*

Arnold, M.; Schneider, A.; Taden, A. The role of Thioxanthone in novel LED curing hotmelt pressure sensitive adhesives (PSA). *ACS Macro Letters* **presumably 2025**.

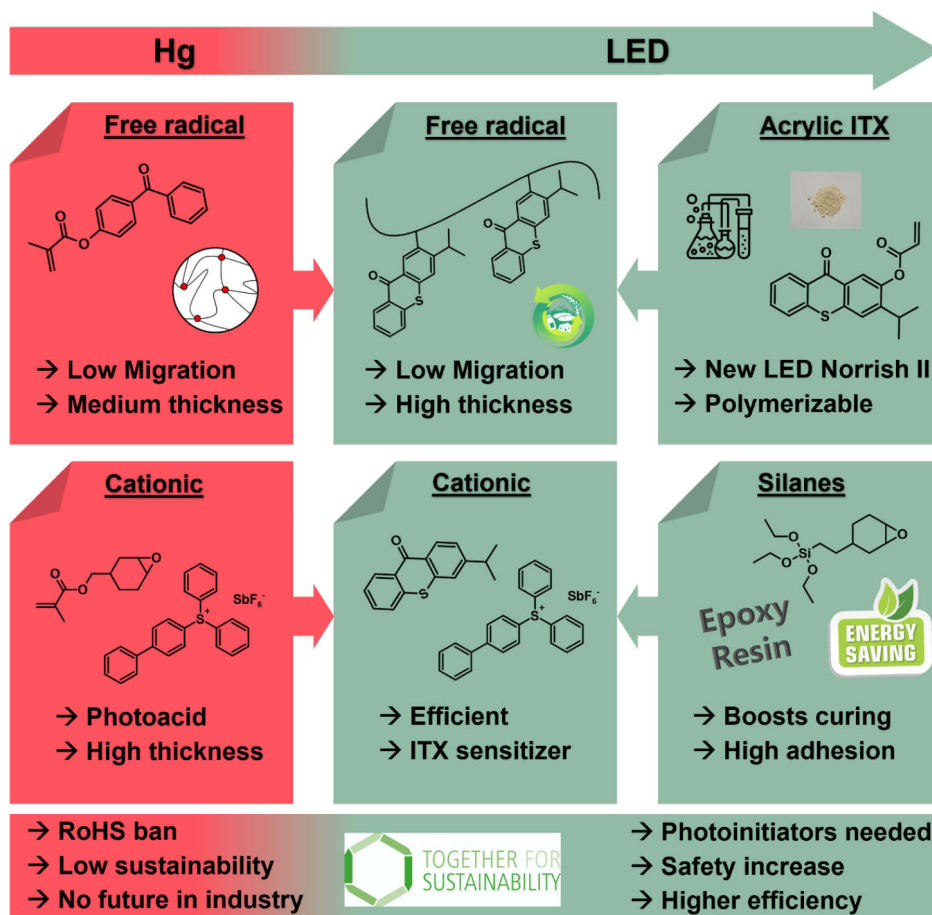
Contribution: Planning and realization of a synthesis route for the preparation of a copolymerizable photoinitiator suitable for enhanced LED curing. Implementation of novel copolymerizable LED photoinitiator into acrylic PSA Hotmelt. *Planning, investigation, synthesis, publication draft.*

Abstract

UV curing of inks, coatings and adhesives developed to one of the fundamental curing mechanisms during the past decades as it is known as a rapid and comparable sustainable curing technology, compared to competitive hardening processes. The curing via UV irradiation produced by mercury bulb technologies became known as the robust curing method, combined with reduced oxygen inhibition and better surface curing as the byproduct ozone which is generated and quenches the oxygen molecules reliable. However, since the world strives for a more sustainable and economically friendly industry including not only the origin of energy but also the technologies used by it, the future of mercury bulb curing is more than uncertain. This is not only connected to the fact that with LEDs a worthy replacement was developed, but also by the fact that especially the European Union puts a lot of pressure on the mercury bulb technology and already bans them in several industry sectors. Even though there is still an exemption for the adhesive market so the mercury bulbs can still be used there, it is expected to come to an end in the next years and adhesive customers are more than willing to change to LED curing technology.

Since the switch to LED technology is connected to a reduction in the broadness of the wavelength where photons are emitted, a simple switch from mercury bulb curing to LED cannot be simply achieved by changing the UV source only. As the overall curing behavior strongly depends on the photoinitiator technology, it is necessary to have suitable photoinitiators available which show a high reactivity at the wavelength the LED emits. When having a look onto the printing industry, in which it is very common to cure prints with UV irradiation, the switch to LED technology did already take place in the past years. Since the formulations consist of unsaturated monomeric and oligomeric systems here, they can be cured well with commercially available Norrish Type I photoinitiators like BAPO, TPO, etc. Of course, this was not done by simply switching the photoinitiator, but also the concern of oxygen inhibition at the surface needed to be considered and was achieved by using synergistic monomer formulations reducing oxygen inhibition. In the market of pressure sensitive adhesive (PSA), where UV hotmelt based PSA have a not to be neglected share, the switch from mercury bulb curing to LED curing cannot be achieved by using the same photoinitiators which are

used by the printing industry. However, as the UV hotmelt PSA market share is expected to rise tremendously in the future, mainly because there is a big pressure on solvent based PSA because of sustainability reasons, the switch from mercury bulb curing to LED is essential to enable a UV hotmelt technology which is not only viable in the future but also is truly dedicated to the idea of being more sustainable.



Scheme 1: Overview of chapters dealt with in this PhD thesis

Within this thesis, the state of the art for LED curable hotmelts has been investigated including possibilities for rapid LED curing with commercially available photoinitiators. Since there is a big pressure on the change to LED technology for the UV hotmelt market and it is expected to happen during the next few years already, it is essential to keep the process as close to the possibility of commercialization in the next years, including the fact that for UV hotmelt PSA there is a strong limitation for the final

product price. Two different possible curing mechanisms, cationic and free radical, have been used to investigate if they are suitable for LED curing of hotmelt PSA. Both curing technologies are already known to the industry and demonstrated over the past years, that they are working properly with regard to high curing speed and curing of thick coatings for the cationic curing, as well as low migration and great product variety in case of free radical curing. Different commercially available cationic photoinitiators have been investigated if they can be used as alternative photoinitiator while keeping rapid LED curing and high temperature stability. Due to the hotmelt application process at $\approx 120^{\circ}\text{C}$ it was immediately found out that, it is not possible to use Iodonium based cationic photoinitiators since the temperature stability of this photoinitiator class is not sufficient to be used in hotmelt based PSAs. Unfortunately, this leads to the fact, that two types of recent for LED developed cationic photoinitiators cannot be used. Following that, the only solution is to use Sulfonium based cationic photoinitiators, however, it was shown that they alone are not sufficient to enable rapid LED curing while keeping the temperature stability high. Here the implementation of a sensitizer enables a more rapid curing while sticking to the same amount of cationic photoinitiator. Again, focusing on commercial availability, different potential photosensitizers have been investigated in combination with the best cationic photoinitiator and it was possible to speed up the curing tremendously. With that combination and a slight change in the polymer composition it was possible to achieve an UV LED curable hotmelt which not only cures as fast as the mercury cured reference but also shows very similar PSA performance. During the investigation it could be observed that a combination of cationic curing and silane technology leads to even faster curing, enabling lower viscosities which result in reduced application temperature while enabling new performance characteristics on plastic substrates.

In case of free radical curing PSA, it was quickly shown that simply formulating a polyacrylate with a Norrish Type I or Type II photoinitiator which demonstrates reactivity at the LED photon emission spectrum did not enable LED curable hotmelt PSAs with sufficient adhesive performance. It is expected that the photoinitiator molecules favor recombination reactions with the activated polymer chains since they are more mobile in the matrix than the polymer chain. This thesis showed the boundaries of commercially available photoinitiator technology. Using only the already

commercially available photoinitiator technology it is not possible to achieve LED curable hotmelt PSA showing low migration and sufficient PSA performance. Following that, a new copolymerizable photoinitiator has been developed which enables low migration and rapid curing. The new LED photoinitiator is copolymerized with other acrylic monomers, eliminating any competing recombination reaction of loose photoinitiator molecules. When switching to the new LED photoinitiator, it is possible to cure thicker coatings than before while staying at a very high level of performance and a proven low level of migration. This technology can be used in a variety of different products and opens the door for a sustainable UV LED hotmelt technology in the future as the application range can be seen as very broad, ranging from tapes and labels to medical and food contact for those adhesives.

1. Introduction

In the modern well industrialized world pressure sensitive adhesives (PSA) are considered more and more as a granted technology as it is part of many people's daily life. Not only at home in DIY applications but also in many professional areas like building and construction, PSA are used weekly if not daily. Although the application of PSA is very simple with the touch of a finger, it is easy to forget that a high-tech product lies behind it.

The ability to stick to different surfaces with tremendous stability of the bond, depending on the applications, even though the original bonding only took seconds if not less than that plays a special role inside the adhesive technology. For that to happen the adhesive needs well-tuned characteristics consisting of not only viscous- but also elastic behavior. The viscos part is needed for the ability to stick to surfaces while the elastic part is essential to remain on that surface with a certain amount of resistance. With these characteristics different PSAs can be designed depending on the later application. To gain the elastic behavior it is often necessary to have a curing mechanism to build up a certain molecular weight and network, which enables high shear and high temperature applications. Inside the acrylic based PSAs, the main curing mechanisms can be summarized by coagulation (water-based PSA), physical crosslinking (solvent-based PSA) and covalent crosslinking induced e.g., by UV irradiation. Crosslinking via UV irradiation became more and more popular as the B2B customer purchases a 100% solid system without any solvents which is not even a dangerous good. The adhesive is coated at elevated temperatures as simple hotmelt material and UV irradiated afterwards. Until now standard mercury bulbs are used to generate a broad UV spectrum allowing the excitation of the photoinitiator inside the adhesive. As climate change makes technology changes essential, not only the mining of mercury but also its use in certain products gets more and more regulated pushing the switch to light emitting diode (LED) systems in the future. This switch brings various challenges with it as the UV spectrum is not broad anymore as LEDs are almost monochromatic. The wavelength window where energy transfer onto the photoinitiator is possible, gets shortened by the technology switch. Following that, the shortened photon emission area leads to the problem, that some of the used

photoinitiators cannot be used anymore, since the absorption of the photoinitiator and the emission of the UV LED do not overlap anymore. This makes it essential to adapt the technology behind the curing of the adhesive, so the usage of LEDs is possible including economic curing speeds.

2. Theoretical background

2.1 Pressure sensitive adhesives

As already mentioned in the introduction the fundamental significance of PSAs lays in their balance between viscous and elastic behavior. The viscous part not only allows the initial tack of the adhesive but also leads to continuous adhesion on the substrate while the elastic part improves not only shear values but also adhesion resistance.¹⁻³

The interaction of cohesion and adhesion in PSA technology can be explained by the Dahlquist criterium. This theory combines the appearance of a tacky surface with rheologic properties, especially the storage modulus G' . Dahlquist found out that a polymer with a dynamic shear modulus less than 3×10^5 Pa has a tacky surface which will stick to substrates.^{1,3} However, it is important to notice that this rule is only applicable if the frequency is set to 1s^{-1} which is approximately the timeframe of deformation when pressing the PSA with e.g., a finger onto a substrate.^{1,3} Considering this as given for a material it generally sticks to any surface and any material. Yet a given pressure sensitive adhesive has higher adhesion and sticks better to one material compared to a different material. This can be explained by the fact that the strength of adhesion and the possibility to adhere to a tacky surface is not only depending on the adhesive but also on the substrate and the substrate's surface. For instance, surface energy plays an important role when it comes to adhesion strength and the pattern of the substrate surface.^{1,4} Generally for users of adhesives, bonding often is connected to roughing the surface to increase their real surface and increasing the bonding area. However, in case of PSAs it is important to consider the rheological behavior of the adhesive which determines its surface wetting possibilities.^{1,4,5} If the adhesive is not viscous enough to flow into surface dales but only sticks to the surface humps the bonding area is smaller instead of larger.⁵

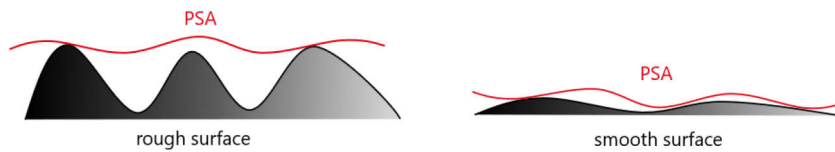


Figure 1: effect of substrate surface roughness on wetting

In fact, this explains why in most cases smooth surfaces are preferred when it comes to bonding with PSA.² This might be completely different for other adhesive technologies like liquid adhesives which have the necessary flow and low viscosity. Once the surface wetting is done, the adhesive stays on the surface of the substrate and needs a force to be debonded.^{1,4}

As different parts of the adhesive get burdened these forces may vary tremendously also depending on the angle of the applied force. In case of peel forces the main effect relies in surface interactions of the adhesive and the substrate.^{1,6} These interactions can be mechanical originated effects by interlocking of the polymer and the surface but also chemically based.⁶ Depending on the technology of the adhesive and the type of surface ionic and nonionic interactions are possible but also covalent bonds between adhesive and surface are common for certain systems.^{1,2,4} Which kind of interaction occurs depends on the type of adhesive and the substrate. Interlocking may only appear if the adhesive is low viscous enough to flow into dales of the substrate surface while remaining a certain amount of elastic resistance against a peel force.^{1,3} Nonionic interactions often come with nonionic surfaces which is the case for nonpolar polymer substrates e.g., like Polyethylene (PE) and Polypropylene (PP).^{1,3} As these interactions mostly rely on Van der Waals forces, the gain in adhesion strength is not that high as Van der Waal forces generally count to the lower side of chemical forces.¹ In addition to that they are heavily depending on the distance between molecules, which again shows how important proper wetting for substrates is where only Van der Waal forces help to build up adhesion.¹ Compared to that ionic interactions can be declared as much stronger than Van der Waals forces, resulting in bigger effects.¹ In this case it is essential that both, the substrate surface and the adhesive meet the requirements to build up ionic interactions. Mainly this can be achieved by the polymer design on the adhesive side by using monomers which introduce functional groups into the polymer in case of standard acrylics.¹⁻³ Several common substrate surfaces already have

functional groups inside their matrix which allow proper ionic interactions like glass or polyethylene terephthalate (PET). Even in case of non-polar substrates like PE and PP it is possible to modify them prior to the bonding in order to bring in polar groups which allow ionic interactions e.g., by Corona or Plasma treatment.¹ Due to this modification, it is also possible to achieve high peel strengths on substrates which originally had a low polarity.¹⁻⁴ However, this might not be applicable for every substrate class and in every application.

Essential for any interaction is the difference in surface energy between adhesive and substrate.^{1,4} Generally, it is easier to bond substrates which bring a high surface energy without any special modification of the adhesive. Higher surface energy increases the wetting of the adhesive, whereupon the area of possible interactions is increased as well.^{1,4-6} The strength of adhesion does not only depend on surface interactions and wetting but also on the cohesion of an adhesive.¹⁻³ This can be explained by the fact that a higher cohesion increases the adhesion resistance up to a certain point. Of course, this effect is limited and stops at the point where chain mobility is limited at such a degree that surface interaction for adhesion is hindered and the dissipation of forces is lowered.^{4,6,7} Once the applied force cannot be dissipated over a larger surface the area of interaction is lowered and peel strength will decrease.^{1,4,6,7} As a result, it is very important to adjust cohesion of a PSA very carefully as it will only help increasing adhesion up to a certain level.^{1,6} As can be seen in Figure 2, the adhesion drops after crossing this point. As tack is behaving antiproportional to cohesion it directly decreases when increasing cohesion e.g., by increasing crosslinking density.¹

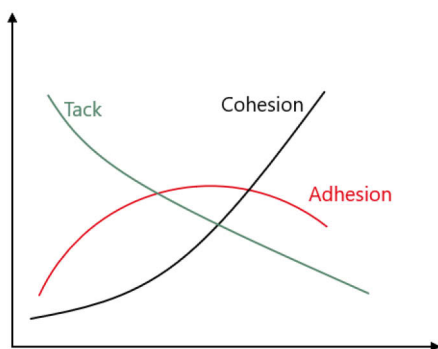


Figure 2: Relation of cohesion, adhesion and tack

Depending on the level of cohesion it is also possible to adjust a potential failure pattern of the adhesive in a peel test. If the cohesion is kept low enough to not cross the turning point, a cohesive failure (CF) will be often achieved.^{1,2,4} Cohesive failure results in adhesive residue on both, the substrate e.g., metal plate and the carrier substrate of the adhesive, e.g., PET foil. When the cohesion is increased further and the turning point is crossed, the failure mode is likely to change to an adhesion failure (AF) mode. Here the adhesive fully remains on the PET foil and there is no residue left on the substrate.¹ It cannot be stated that one or the other is favored, as this depends on the application area of the adhesive.

Increasing cohesion can be achieved by different factors which vary once the adhesive technology changes. In case of polar interactions, it is possible to increase the possibility for those interactions inside the adhesive. This can be done by implementing polar groups into the adhesive.^{1,3,4} These polar groups not only increase adhesion to certain substrates, but also increase the cohesion level and viscosity by increasing polymer chain interactions and force of chain attraction.^{1,3,4} Besides polar chain interactions of course there are also Van der Waals forces between the polymer chains. However, their proportion in cohesion is not as big as the polar forces between chains.¹ In all cases and independent of any interactions, also molecular weight plays a key role. By increasing the molecular weight, the internal strength of the polymer increases, also allowing bigger knot structures with a high level of entanglement.^{1,4,6,7} With increasing entanglement, the applied force onto the polymer can be dissipated over a wider area increasing e.g., shear strength.^{4,6,7} As the viscosity is limited in most applications to a certain value due to application procedures it is important to gain molecular weight after the application of the adhesive has taken place in many technologies. This can be achieved e.g., by coagulation of particles after evaporating the water of the dispersion in water-based systems (Figure 3, A). For solvent based PSA this is often done by e.g., complex formation of metals with polar groups, e.g., Aluminum acetylacetonate (AlAcAc) or covalent bonding with Isocyanates during the evaporation of the solvent in a drying process (Figure 3, B).^{1,2} Since water based systems and solvent based systems are not connected to a hotmelt applications process their average molecular weight often strongly exceeds the molecular weight of hotmelt PSA. This can be explained by the fact, that through the change of total solid the viscosity can be

adapted to the needed level for both technologies, which is not possible for hotmelts as there is no solvent anymore. A popular way of increasing cohesion after the application has taken place for hotmelt PSA is by UV induced crosslinking which will be used in this thesis as well.^{1,2} In this case it is common to use a photoinitiator which links the polymer chains to each other and by that forming a network.^{1,3,7}

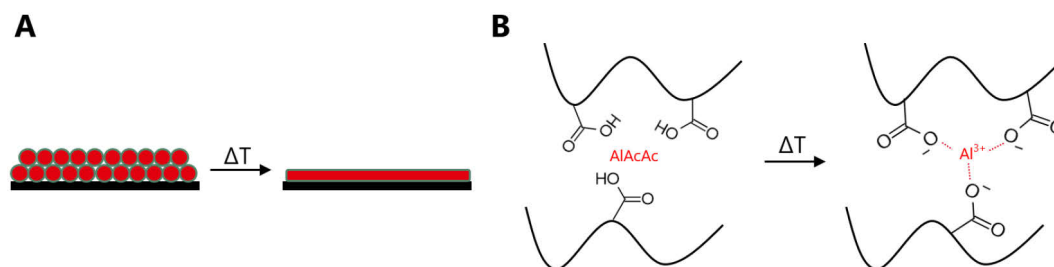


Figure 3: Curing of water-based coating (A); curing of solvent-based coating (B)

Generally, those technologies are not limited to one curing mechanism, as it is possible to combine some of them with each other.^{1,2,6} The different types of UV mechanisms and types of photoinitiators will be outlined in a separate section of this thesis. All these curing (and coagulation) technologies lead to an increasing polymer chain size and/or formation of a network. Following that, the adhesives show more of an elastic behavior compared to the same type of adhesive which have not been cured. Increasing elastic behavior leads to an increase in cohesion which is followed by better performance in e.g., shear strength tests.^{1,2,6} As already stated out before, increasing the network and network density will also have an impact on wetting and adhesion theories.^{1,4-6} Consequently, shear performance might not increase measurably as the adhesive fails with an adhesion failure even before the cohesive strength can be measured, because the increased network and connected hindered chain mobility does not allow high adhesion forces anymore. This explains why designing high cohesive PSAs showing high adhesion on certain substrates is a very challenging task in most cases.

2.2 Polymerization and polymer design for Acrylic PSA

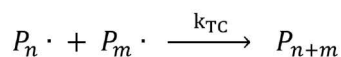
In case of hotmelt based acrylic PSA technology with a following UV curing step it is essential to design a sufficient acrylic polymer in a first step. Due to the fact that application viscosities are pretty limited it is not possible to build up a high molecular weight in the polymer design as these types of polymers would not be applicable even though they might have great performance. As a result, the molecular weight is limited and also the number of polar groups is limited as well and needs to be chosen wisely. For hotmelt acrylic PSA it is very common to polymerize the monomers via a free radical mechanism, but it would also be possible to use RAFT mechanisms, however, due to the impact on pricing it is not very common in the PSA technology.²

The free radical polymerization of acrylic monomers for PSA applications is often executed through a solution polymerization in a semi feed process. This not only leads to better control of heat, statistical copolymerization and exothermy, but it also allows chain transfer reactions with the solvent (depending on the solvent) in order to achieve a broader molecular weight distribution.^{2,8-10} To start the free radical polymerization a radical starter is needed. Usually these are either Azo types or peroxides or a combination of both, depending on the molecular weight design.^{2,8-10} The generation of radicals can either be achieved by applying heat or by means of triggering the reaction in a redox mechanism, especially in case of peroxides. After e.g. heat has triggered the initiator, it separates into radicals and follows the widely known general rules of free radical copolymerization kinetics. As the starting reaction and chain propagation reaction are following the general rules and the production of a broad molecular weight distribution for combined cohesion and adhesion is from huge interest, the chain transfer reactions are a key fact for the production of PSA polymers.^{2,8-10}

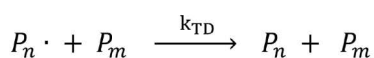
There are several different kinds of termination reactions which can occur which not only depend on the monomer and solvent composition but also on the progressively increasing viscosity of the system during the polymerization. Some of them might happen on purpose to control molecular weight distribution, while some of them might occur even though they are not planned in some reactions.^{2,8-10} When the polymer chain has grown, many radicals have been formed and the amount of unreacted monomer is decreasing there might be combination reactions of polymer chains happening (see

Equation 4).^{2,8-10} These combination reactions (k_{TC}) of polymer chains (P_n and P_m) lead to an increase in molecular weight, but it is also possible that a polymer chain recombines with a smaller radical, like a monomer or initiator radical.^{2,8-10} Once the recombination has taken place, there is no radical species left on the chain.

Recombination



Disproportionation



Chain transfer agent reaction

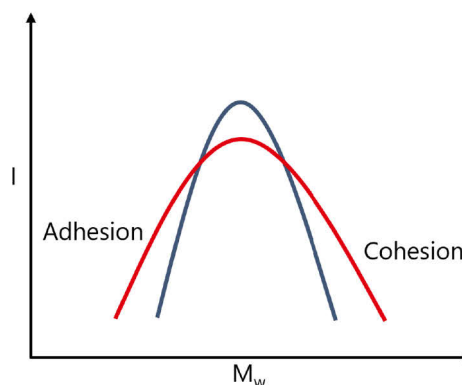
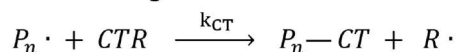


Figure 4: Different transfer reactions; Importance of broad molecular weight distribution

Apart from the combination reaction it is also possible that radicals (P_n and P_m) lose their radical order by a disproportionation reaction (k_{TD}) (see Figure 4).^{2,8-10} Following that, both radicals are quenched by a hydrogen radical abstraction reaction. One of the radicals is directly quenched by the hydrogen radical itself, losing the reactive position, the other radical is quenched by recombination reaction of two adjacent radicals.^{2,8-10} Due to the recombination of those two radicals a new double bond is formed which can be part of a new chain starting reaction. However, in case of a grown polymer chain with a high molecular mass and with that hindered mobility it is not as easy for the polymer chain to grow further than starting a new chain which has a higher mobility inside the matrix.^{2,8-10}

Another possible reaction path for a formed radical and especially for a radical on a polymer chain (P_n) is a chain transfer reaction (k_{CT}) with e.g. the solvent (CTR) (see Figure 4).^{2,8-10} Generally, these chain transfer reactions do not reduce the number of radicals inside the system, however this reaction path can reduce further molecular weight growth.^{2,8-10} Chain transfer reactions cannot only occur with the solvent but in principle with every molecule inside the reaction vessel. However, the reactivity and probability of a chain transfer reaction with the solvent can be well controlled by the

type of solvent used in the reaction.^{2,8-10} With different solvents it is possible to achieve different molecular weight distributions even though the monomer and initiator composition has not been changed. This is based on different solvents which have different types of chain transfer constants for transfer reactions with the used monomers. As a result, this is not only depending on the solvent but also the monomer type in the respective reaction.^{2,8-10}

By choosing monomers which can abstract a hydrogen radical from a chains transfer agent under the formation of a rather stabilized second radical on the monomer side it is possible to increase polymer chain transfer reactions.^{2,8-10} This is the case for several small alcohols like isopropanol acting as chain transfer agent. However, using isopropanol as the only solvent might reduce molecular weight that much that the formed polymer chains are not long enough e.g. to have proper cohesion in PSAs. In that regard it is common to only use small amounts of alcohol in combination with a solvent with a lower chain transfer reaction constant like ethylacetate.^{2,8-10} Using this it is possible to modify molecular weight and its distribution depending on the setup if the isopropanol is directly used from the beginning or dosed after some time.^{2,8-10}

Control of molecular weight and its distribution is essential for synthesizing polymers for PSAs.^{1,4,6,7} As the molecular weight has a major influence on cohesion and adhesion, it is a key factor to set up the polymer for the later application and the followed curing reaction (if there is one). Higher molecular weight leads to an increase in cohesion as the force can be dissipated over a longer polymer chain and the amount of entanglement of polymer chain is higher for a longer chain.^{4,6,7} With that it is easier for the polymer to withstand an applied force. As a drawback the mobility of chains decreases with increasing molecular weight and consequently also the adhesion to substrates.¹ As polymer chain mobility is crucial to wet the surface, it results in a smaller area of surface interaction if the polymer chain is not mobile enough to get to the surface and flow into the surface roughness.^{1,4-6} As already outlined before, cohesion can only be measured and show its effect if adhesion is strong enough for the cohesive strength to perform. Consequently, there is a high interest in not only increasing cohesion but also maintaining good adhesion characteristics.² While increasing the molecular weight, e.g. by using less initiator, the adhesion will be directly

affected in a negative way as it decreases.^{1,2} The solution is to form a polymer with a broad molecular weight distribution which contains high molecular weighted parts as well as low molecular weighted parts inside the polymer. The higher molecular weighted parts increase the cohesive strength of the PSA (see Figure 4), while the lower molecular weighted parts remain good wetting and adhesion on the surface of the substrate (see Figure 4).^{1,4,6,7} As a side effect the polymer viscosity does not increase that much even though there are high molecular weighted polymer chains inside the polymer system. As can be seen in Figure 4, the red PSA sample has a broader molecular weight distribution compared to the blue sample. Consequently, the red sample has both, a higher adhesion and a higher cohesion compared to the blue sample. However, it might have a comparable viscosity to the blue sample.^{1,4,6,7}

Yet the broadening of molecular weight is limited and cannot be executed endless to get the optimum PSA polymer. Factors like difficult bonding surfaces might have such a great influence, that there is no large improvement in adhesion to the surface even though the molecular weight has been broadened.^{5,11} In these cases, it can be helpful to use a tackifier. For acrylic polymers rosin based tackifiers are very popular as they show high compatibility with acrylics and are easy to accomplish.^{1,6,7,11} These, in comparison to the PSA polymer, low molecular weighted rosin-based structures soften the PSA polymer by loosening some of the entanglements.^{1,6,7,11} Following which the wetting of the polymer is improved as chains get more mobile again. Interactions for adhesion theorems can take place and the adhesion is improved even though the molecular weight of the PSA polymer and its composition has not been changed.^{1,6,7,11} Another advantage is that the tackifiers reduce the viscosity of PSA hotmelts. Yet the usage of tackifiers is often combined with the drawback that high temperature cohesion might decrease as the tackifier starts melting at elevated temperatures and as a consequence it is hard for polymer chains to keep the force dissipated.^{1,6,7,11}

2.3 UV curing and sustainability

While solvent-based or water-based acrylic PSA are dependent on a certain drying process which might even be connected to the evaporation of cancerogen mutagen reprotoxic (CMR) relevant solvent mixtures, UV induced crosslinking has become more and more popular in the past 60 years which is also connected to the jump in development of free radical photoinitiators in the 1960s.^{12,13} From early stages until now UV irradiation is often connected to a more economic type of curing even though this might not be exactly true and is technology dependent. Since UV mercury pressure bulbs even have been invented way earlier than that, the photoinitiator chemistry was focused to cure with mercury pressure bulbs and push absorption levels towards the excitation levels of these bulbs.^{12,13} It was found to be very advantages that the mercury pressure bulbs emit a very broad wavelength and show high output of powerful UVC light (see Figure 5). Since both, lamp and photoinitiator technologies matched perfectly to each other, the focus has always been on improving lamp power and absorption patterns of photoinitiators.^{12,13} By that it was possible to improve curing speeds over the years to make rapid curing possible.

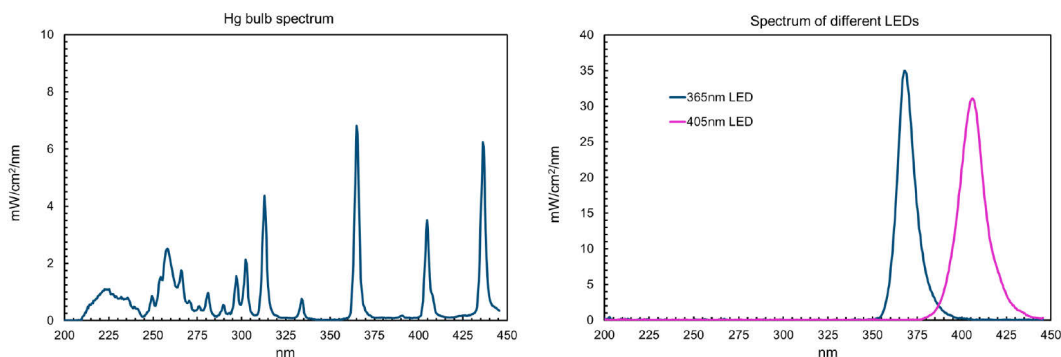


Figure 5: Emission spectrum of a mercury bulb and two different LEDs

However, as mercury bulbs consume a lot of energy, lifetime of the bulbs is limited and produce toxic ozone, besides some practical disadvantages the hunt for more economical and sustainable curing methods has started early after the first photocuring products have been developed.¹²⁻¹⁴ Consequently, even before the turn of the millennium blue and UV LEDs have been developed, though they had way less power than the well-developed mercury pressure bulbs. Besides the lower power the

difference in emission spectrum compared to the mercury pressure bulbs lead to challenges with photo curing mechanisms. As LEDs emit light by current flowing through a semiconductor which then emits photons at a characteristic wavelength, they show a nearly monochromatic emission spectrum which is only about 50nm wide (see Figure 5).¹⁵ This leads to the problem that the energy output onto the photoinitiator is limited to that wavelength area and most of the absorption spectrum of the photoinitiator cannot be used anymore.^{12,13} In the past 25 years development of UV LED technology led to a vast increase of LEDs power and still remain energy efficient as there is less heat generation compared to mercury pressure bulbs and the lifetime is way exceeding that of mercury pressure bulbs.^{14,15}

Besides the narrow emission spectrum, the development of UVC LEDs has not been that fast as the development of UVA LEDs as semiconductor technology for the UVC region seems rather challenging and due to that also very expensive.¹⁴ Consequently, the shift from mercury pressure bulbs to UVA LEDs is not only connected to the challenge that the emission spectrum is very narrow but also that it is not in the powerful UVC region. As most of the photoinitiators developed in the past have been created to be used with mercury pressure bulbs, the selection of commercially available photoinitiators which work with UVA LEDs is very limited.^{12,13} Since climate change has become a major recognized challenge for the world in the past 15 years and will be challenging for the next decades as well there is a huge interest in switching to LED technology with photo curing products. This process-reconsidering has already led to research groups focusing not only on the development of suitable new photoinitiators but also on the development of photoinitiator systems which can even be used with NIR light.¹⁶⁻¹⁸ NIR light has the advantage that it has even a higher penetration depth than UVA LEDs which are already advantageous in penetration depth compared to mercury pressure bulbs as all the emission is in the UVA region.¹⁶⁻¹⁸

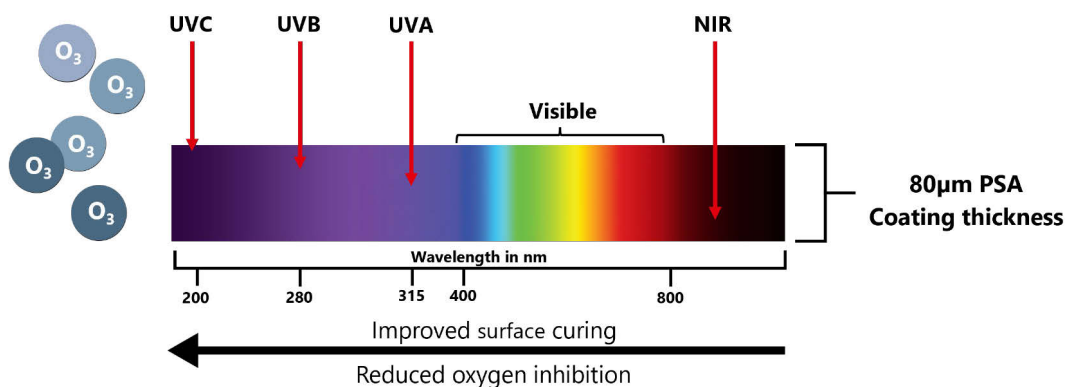


Figure 6: Penetration depth of different wavelength (not to scale)

This allows the curing of thicker coatings and making UV cured 3D printed resins possible. The drawback of the deeper penetration depth of photons is connected to the fact that surface curing might be lowered by that as UVA LEDs do not produce ozone as byproduct compared to mercury pressure bulbs. The ozone by-product can quench oxygen radicals and by that reduce oxygen inhibition on the surface.^{19,20} To reduce oxygen inhibition when curing with UVA LEDs it can either be done by switching the curing technology from free radical to cationic, which is not dependent on oxygen or by using synergists which quench the oxygen as well, e.g. amines, thiols, ethers or flushing the curing area with nitrogen before curing will improve surface curing as well.^{19,20} Besides that, the fact that less electrical energy is transferred to heat in case of LED technology there is also less temperature on the polymer which is UV cured. As nearly with every chemical reaction an increase in heat however increases reaction speed and the curing speed.²¹ Consequently, the fact that less heat is generated by the lamp which is positive for economic reasons does not really help with curing chemical wise. Again, this is a side effect which leads to naturally slower curing of polymer samples when using LED technology compared to mercury pressure bulbs without adjusting the photoinitiator or polymer composition. Of course, this could be overcome by using IR sources to heat samples up prior curing, however, this would reduce the positive economic characteristic of LEDs used in curing technology. Fortunately, in case of hotmelt PSA coatings the curing takes place at elevated temperatures anyways since the curing step directly happens after the hotmelt application. Therefore, the polymer is already heated up before the curing step and with that curing speeds are not extremely lowered by using LEDs regarding the temperature effect.

2.4 UV crosslinking of acrylic hotmelts: Free radical

As already stated out above, UV crosslinking is one of various methods to gain cohesion after the polymerization of the adhesive has been executed. UV crosslinking inside the group of PSAs can mainly be done by either a free radical or cationic mechanism with an affiliated photoinitiator.^{1,7,12,13} However, there are also some other techniques like photoinitiator free crosslinking by UVC irradiation, but they are rare even though they have some advantages.²² In case of UV induced free radial crosslinking there are two types of photoinitiators which can be used. They are split into Norrish Type I and Norrish Type II photoinitiators.^{7,12,13} Norrish Type I photoinitiators are structures which split into two radicals after excitation by the desired wavelength (see Scheme 2).^{12,13}



Scheme 2: General mechanism of Norrish Type I and Type II photoinitiators

The formed radicals can be homolytic, but they can have also other characteristics. It is also possible that a small molecule like CO₂ or O₂ is split from one of the radicals.^{12,13} Norrish Type I photoinitiators have the advantage that there is a broad variety of products available even for longer UV irradiation like UVA (see Figure 7).^{12,13} In addition to that they show a low migration since the radicals which are formed are free radicals which react with monomers and by that become part of the polymer backbone.^{12,13}

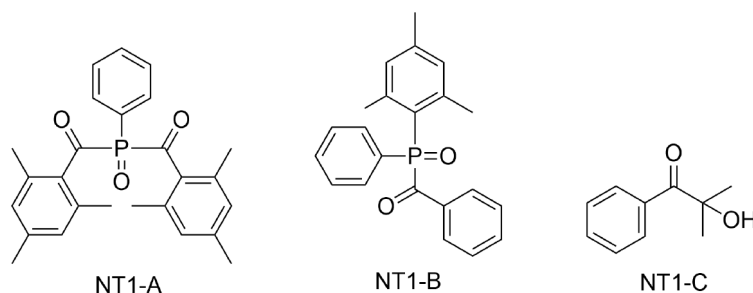


Figure 7: Structures of common Norrish Type I photoinitiators

Yet it might not be the best choice of photoinitiator when curing prepolymers where the curing mechanism is not depending on double bonds but on abstraction and transfer reactions of hydrogen radicals and polymer chains. Here Norrish Type II

photoinitiators function best as they do not form directly free radicals after excitation by UV light by abstract a hydrogen radical from another structure (see Scheme 2).^{7,12,13} For instance, this can be located in the polymer side chain.⁷ By that there is the generation of a free radical position on the polymer sidechain which can either recombine with another polymer chain which has a free radical position in the sidechain as well or there is a recombination reaction of the free radical side chain with another chain where the reactive photoinitiator has bond to.^{7,12,13} Because of that abstraction mechanism Norrish Type II photoinitiators are not that popular to polymerize unsaturated systems. Due to the abstraction reaction mechanism the nature of the molecule which splits the hydrogen radical has a big influence on reactivity.^{12,13} For instance, a hydrogen atom which is positioned at a tertiary position is more likely to be split in a radical mechanism than a primary located hydrogen atom.^{1,12,13} This needs to be taken into account when choosing raw materials for polymerization and later network formation.

In case of Norrish Type II photoinitiators there are several commercially available grades as well.^{12,13} Some of them only absorb in the UVC region, a few of them however also work with longer UV light (see Figure 8). As there is not a real generation of free radicals during the excitation, this type of photoinitiator tends to show higher migration levels compared to the Norrish Type I photoinitiators.^{12,13}

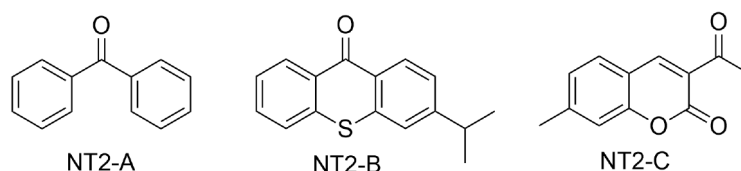


Figure 8: Structures of common Norrish Type II photoinitiators

However, there are ways to reduce the photoinitiator mobility and fix them prior to the UV curing step onto the polymer backbone.^{7,12,13} This can either be done by grafting reactions or by using Norrish Type II photoinitiators which can be copolymerized in a free radical copolymerization together with other acrylics. One of them is the Benzophenone methacrylate (BPMA), which is commercially available since many years (see Figure 9). This Norrish Type II photoinitiator can be copolymerized with other acrylics and will later cure the polymer system by forming a network after UV

irradiation via hydrogen radical abstraction reactions from another chain.⁷ As already mentioned above, at first it is important to choose comonomers where a hydrogen abstraction reaction is favored due to its molecular structure. As an example, it is popular to use the BPMA copolymerized with 2-Ethylhexyl acrylate (2-EHA) or Isobutyl acrylate (IBuA).

The BPMA rather shows absorption inside the UVC region, making it necessary to use mercury bulbs for curing.^{7,12,13} The copolymerization reduced migration possibilities tremendously, leading to safer PSA systems in order to enable food contact and medical contact applications. In case of PSA systems with a freely moving photoinitiator this will often not be the case as not properly reacted photoinitiators molecules will keep migrating. For systems with Norrish Type I photoinitiators this might be different as the highly reactive radicals might at least form oligomers, reducing migration possibilities.^{7,12,13}

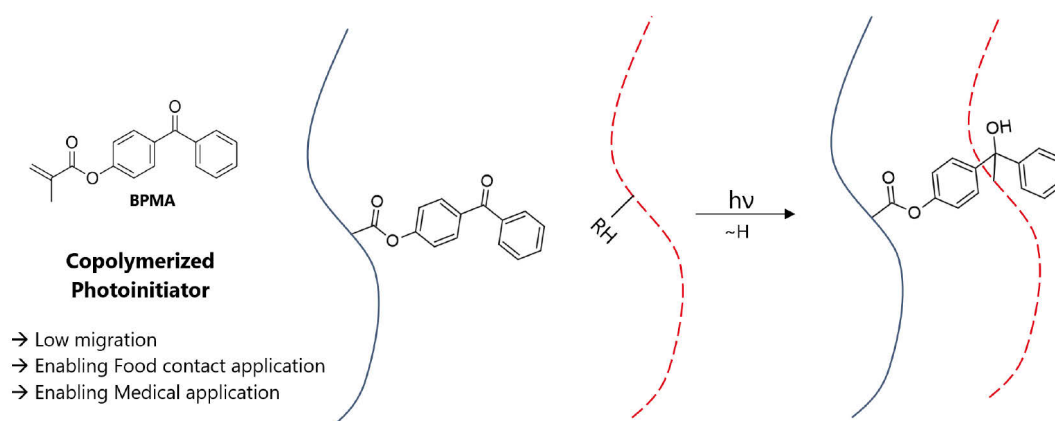


Figure 9: Network formation of copolymerized BPMA after UV irradiation

Due to the copolymerized photoinitiator, curing reactions take place very rapidly as the photoinitiator is already linked to one of the polymer chains and only needs to find a second chain.⁷ A freely moving Norrish Type II photoinitiator however needs to find a polymer chain for hydrogen radical abstraction after UV excitation first and then the polymer chain with a free radical can find a different one (same chain possible as well) to build up the polymer network. Regarding the curing speed, the photoinitiator amount has a direct impact onto it but there is a certain limitation often caused by missing photobleaching effects leading to uncured deeper layers.^{1,19,23-25} However, as

the photoinitiator is copolymerized into the backbone in the polymerization step, the curing speed cannot be increased noteworthy by a formulation step where a freely moving photoinitiator is added. This is connected to the fact, that the network formation of a free moving Norrish Type II photoinitiator does not proceed rapidly as will be demonstrated later in this work. Following that, the polymer-depending curing speed of the PSA is already pre-determined during the copolymerization step of the PSA polymer as the photoinitiator is also copolymerized here. Even though the polymerizable Norrish Type II photoinitiators show several advantages, there is a major limitation of commercial availability as the BPMA is the only commercially available type.^{12,13} Generally free radical UV curing technology can be stated as a robust and fast curing methodology. However, in some cases oxygen inhibition might cause some issues with uncured PSA surfaces. As already addressed before, mercury pressure bulbs overcame this issue by the fact that generated ozone was quenching the oxygen radicals and with that improving surface curing.^{19,20} In case of LED technology, especially UVA LEDs, there is no generation of ozone at all and with that the oxygen radicals are not quenched. Besides methods like increasing photoinitiator concentrations or using nitrogen blankets to reduce oxygen in the atmosphere where the curing takes place, there are some synergists which help to stay at a high reactive radical species.^{19,20} The most popular synergists are amine synergists, as they not only can form reactive peroxy radicals with oxygen but also donate a hydrogen radical for the Norrish Type II mechanism as the neighbored hydrogen to amines often is easily abstractable.^{19,20}

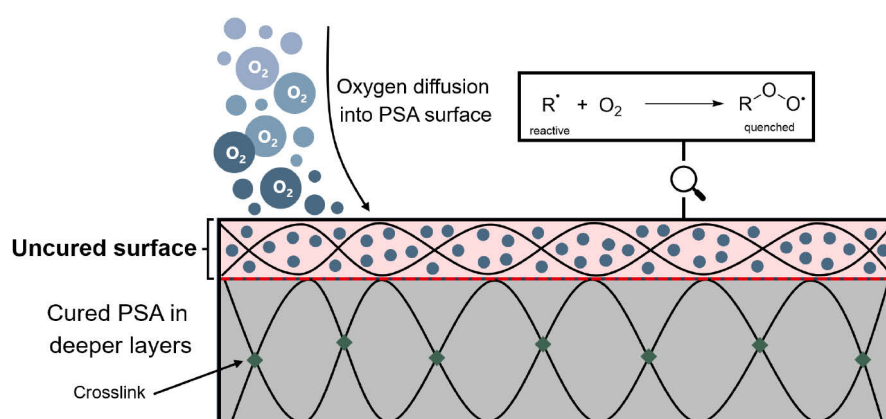
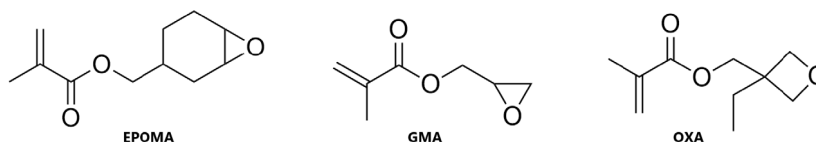


Figure 10: Oxygen inhibition effect onto PSA surface

2.5 UV crosslinking of acrylic hotmelts: Cationic

Besides UV induced free radical crosslinking of acrylic PSA it is also possible to build up a polymer network via a cationic curing mechanism. In combination with the hotmelt application it is essential to stick to a temperature stable reaction mechanism and with a temperature stable monomer selection. Consequently, even though vinyl ethers show a high reactivity in cationic polymerization they are not suitable for a hotmelt application as their reactivity is too high.^{16,26–30} In addition to that, it is not possible to copolymerize acrylic vinyl ethers in a free radical solution polymerization without gelation occurring as some of the vinyl ether groups will already react in this step and form an undesirable network.^{8,10} As a result, epoxy groups with an acrylic functionality are used, e.g. cycloaliphatic epoxy methacrylate EPOMA (see Scheme 3).



Scheme 3: Cationic curable acrylate – epoxy / oxetane hybrid monomers

They can be copolymerized in a first step with other acrylics in a free radical solution polymerization without any gelation occurring as the epoxy groups remain stable in this reaction mechanisms. Thereby it is possible to synthesize an acrylic hotmelt polymer with epoxy groups in the side chain which can be crosslinked with suitable photoinitiators (see Figure 11).^{16,26–30}

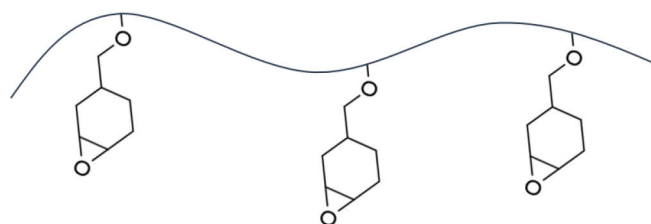


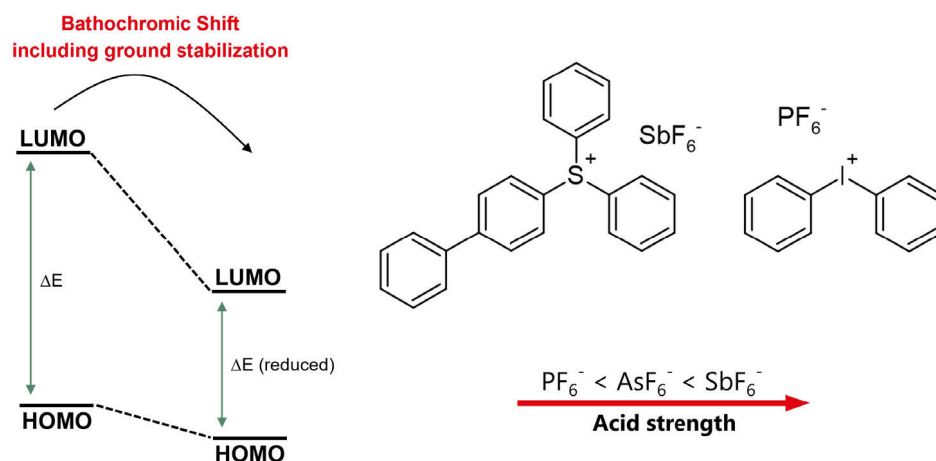
Figure 11: Simplified polymer structure of cationic curable acrylic hotmelt

As shown in Scheme 3 and Figure 11, cycloaliphatic epoxy acrylic monomers are the best choice for a fast-curing reaction induced by UV light. These types of epoxies show rapid curing induced by a super acid without a required post-curing by temperature.^{16,26–30}

Due to the steric hindrance of the cycloaliphatic ring, it is unlikely to happen that the proton which starts the cationic crosslinking is simply complexed by the oxygen of the monomer.²⁶⁻³⁰ In contrast to that monomers like glycidyl methacrylate (GMA) tend to complex the proton first instead of a direct electrophilic attack of the proton onto the epoxy oxygen.²⁶⁻³⁰ This complex can be opened by post curing at elevated temperatures for several minutes, however, this process is not fast enough for belt coater applications in the industry.²⁶⁻³⁰ In addition to that, GMA based epoxies show higher reactivity towards ring opening reactions by contaminations like carboxylic acids and amines. Thereby, the stability of the polymer would be worse compared to the polymer with cycloaliphatic epoxy groups in the side chain.³¹ Another monomer class which is suitable for cationic curing acrylic hotmelts are oxetane derivatives.^{28,32,33} They are also available with an acrylic functionality and can be copolymerized without interfering with radicals on the oxetane side. Yet a polymer with oxetanes being the only cationic curing functionality in the side chain shows slow curing at the beginning as oxetanes have a rather long induction period at the start.^{28,32,33} However, once the induction period is over oxetanes show rather rapid curing with high conversions.^{28,32,33} The induction period can be overcome by reaction heat which is produced during the curing reaction but again this process alone is too slow as curing needs to be done in less than a second. A synergetic effect can be seen when cycloaliphatic epoxies are combined with oxetanes.^{28,32,33} The rapid initial curing reaction of the cycloaliphatic epoxy groups produces enough reaction heat to overcome the induction period of the oxetane curing reaction. Thereby, the oxetanes react fast from the beginning, pushing the overall conversion rate by even more reaction heat and reactive species.^{28,32,33}

Besides the type of epoxy monomer, the cationic photoinitiator has a big influence on the curing speed, conversion and stability of the overall product. There are several different cationic photoinitiators which have been developed by different research groups in the past.³⁴⁻³⁶ Many of them have been commercialized as this type of photoinduced curing reaction was a new alternative to the well-known radical curing reaction while having some advantages like no sensitivity to oxygen. Cationic photoinitiators based on an onium salt became very popular after James Crivello invented them in the 1970s. These salts consist of either an Iodonium cation or a Sulfonium cation (Scheme 4).³⁶ Those cations are combined with an anion which can be

metal based or metal free. Both type of onium salt show high reactivity when excited by the desired wavelength and together with the anion a super acid is formed which starts the cationic curing reaction of epoxies.



Scheme 4: Impact of increased π stabilization; common Onium salts

Generally, the UV/VIS absorption can be controlled by the design of the onium cation as its main characteristic is to define the stability in excited state, ground state and overall stability e.g. temperature stability.³⁷ With increasing stability of the onium cation at its excited state e.g. via multiple π - or mesomeric systems it is possible to shift the absorption to higher wavelengths. The energy gap between HOMO and LUMO is reduced and with that longer wavelengths can be used in order to bring the cationic photoinitiator in its excited singlet state from which several different reaction paths are possible.³⁷ Given the times when those salts have been developed, they were equipped with a strong absorption in the UVC region because of popularity of standard mercury bulbs at that time.³⁶ However, the absorption of sulfonium salts shows a worth mentionable tail towards the UVB and UVA region. Nevertheless, they are not very efficient with UVA LEDs as the absorption is only very small in the 365nm region even though it needs to be said that a low absorption is not consequently connected to low reactivity as proven by several groups in the past.³⁸ Some groups have modified the onium salts in the last years by synthesizing different cation structures, but most of them are still not commercially available.^{25,39}

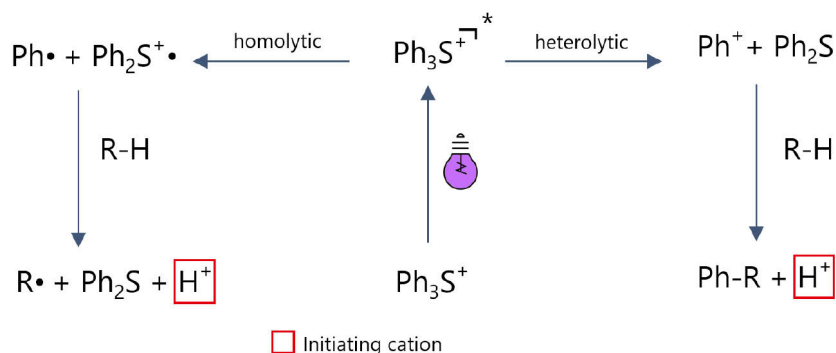
Comparing Sulfonium salts to Iodonium salts, not only the UV absorption differs as Iodonium salts often tend to show only absorption in the UVC region but also their reactivity to form the proton which later starts the cationic polymerization. Since the Iodine-Carbon bond shows a higher reactivity towards electrons than the Sulfur-Carbon bond, the proton yield of Iodonium salts might be higher under the same reaction conditions.²⁷ As a result, it is easier to sensitize Iodonium salts than sulfonium salts, which will be explained in a different chapter further below.⁴⁰ The drawback of the higher reactivity of the Iodonium cations is a lacking temperature stability which however is essential for acrylic hotmelt adhesives.⁴¹ This is the reason, why many thermoacid generators are based on Iodonium salts and not triaryl sulfonium salts.

In contrast to the cation, the anion defines the acid strength of the formed proton.³⁷ The more stable the formed anion after excitation, the stronger the produced acid as the strength of protonic acids are directly dependent on the belonging anion which is formed.⁴² Stability of the anion increases with the size of the whole anion where the negative load can be dissipated. As atoms of the 5th main group of the periodic table are popular, the strength of the acid increase from $P < As < Sb$.³⁶ In the past anions based on antimony or phosphate have become popular as antimony is less toxic than arsen and has a higher reactivity.⁴³ Phosphate based anions however have the advantage that they are metal free and less harmful than antimony-based salts however they have a far lower acid strength compared to antimony-based anions as the overall anion is smaller and often they are connected to bad solubility in common monomers and solvents.³⁴ Both, phosphate and antimony-based anions are hexafluoro anions. When irradiation takes place, a proton is released by the reaction path of the onium cation forming e.g. hexafluoro antimony acid or hexafluoro phosphoric acid.⁴¹

Once irradiated and excited there are two different reaction paths for both types of onium salts (Scheme 5).⁴⁴ One path is a homolytic separation and the other path is a heterolytic separation.⁴⁴ In the homolytic path the onium salt cation is split into two radicals resulting in one free radical (often aryl) and one radical cation due to the cationic state at the beginning. The radical cation further reacts with a donor group which splits a hydrogen radical apart and donates an electron to the radical cation. Thereby the radical cation is quenched, a new donor radical and the proton is formed.

The proton can initiate the cationic polymerization together with the hexafluoro-anion forming a super acid.^{41,44} The role of the donor molecule can be taken over by another onium salt molecule or a sidechain of the polymer (e.g. 2-EHA).^{8,10}

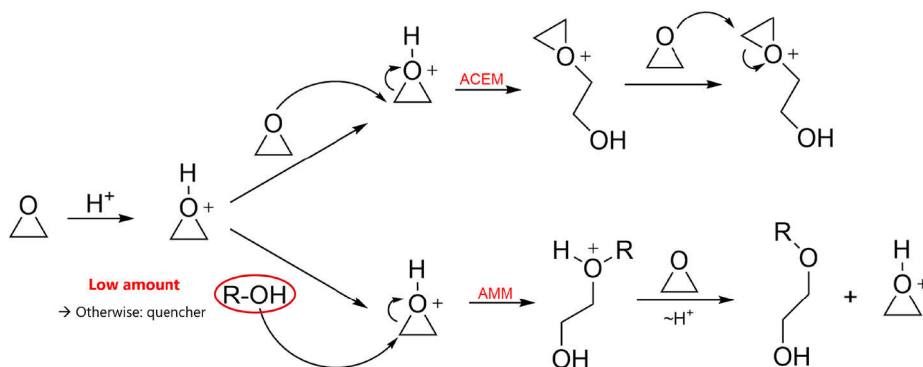
In the heterolytic path the onium salt is split into a cation (often aryl) and a non-loaded counter molecule. The formed cation (e.g. aryl cation) reacts with a donor group as well, resulting in the formation of a proton again. Which reaction path is favored depends on the type of onium salt, the type of excited state (triplet or singlet) and the matrix around it like solvent effects. Matrix effects are described as in cage or out of cage reactions in which the polymer matrix acts as cage around the activated photoinitiator species. Different reactions are possible, depending on if the reactive species are still “inside” the cage and might react with each other or get in contact with a hydrogen donor “outside” of the cage. It needs to be said that the reaction “inside” the cage still can result in the generation of a proton.^{41,44,45}



Scheme 5: Reaction mechanism of onium salts (here sulfonium salt) after irradiation; anion left out

Once the super acid has been generated, the proton can initiate the cationic crosslinking of polymer chains. Depending on the polymer design, the monomer choice and the matrix around, there are two different reaction paths the cationic polymerization can take place (Scheme 6).^{46–49} One of them is the activated chain end mechanism (ACEM). Here the proton, which is formed by the super acid, attacks the oxygen of the epoxy group in an electrophilic reaction mechanism. Due to the formed oxirane cation the neighboring carbon is activated and attacked by an oxygen of a new epoxy monomer. This opens the first epoxy ring and a new oxirane cation is formed. By that mechanism it is always the chain end which is activated and attacked by a new

monomer.⁴⁶⁻⁴⁹ The nucleophilic attack of the new epoxy oxygen can take place on both sides of the activated oxirane cation. The preferred reaction route depends on possible side groups on that carbon.⁴⁶⁻⁴⁹ As an example, the formation of a secondary alcohol would be preferred compared to the formation of a primary alcohol in most cases.



Scheme 6: Mechanism of ACEM and AMM on the example of ethylene oxide

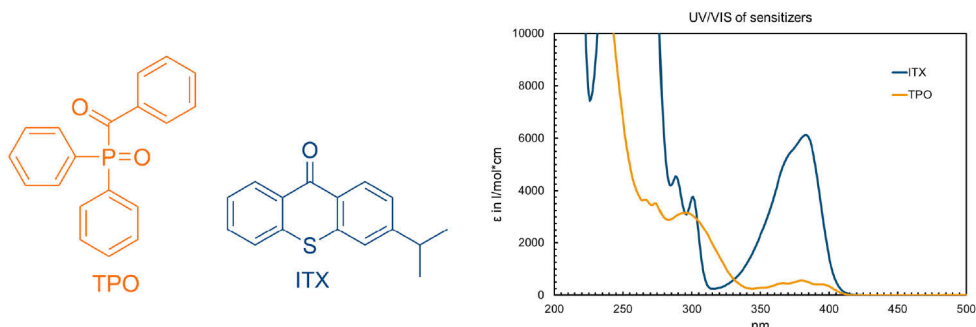
The activated monomer mechanism (AMM) works different to that and happens in a combination with a hydroxy functionality.⁴⁶⁻⁴⁹ Those hydroxy functionalities might already be inside the polymer due to polymer design, occur randomly by humidity, or addition of hydroxy species after polymerization of the polyacrylic in a separate formulation step. In this case the formed proton again attacks a first epoxy group in an electrophilic reaction, however, the formed oxirane cation does not react with a new epoxy group but with a hydroxy functionality. The hydroxy group opens the activated epoxy ring and the proton is transferred to a new epoxy monomer.⁴⁶⁻⁴⁹ On which side the alcohol attacks the activated oxirane group, is again subject to possible side groups and steric hindrance.⁴⁶⁻⁴⁹ As with the activated chain end mechanism the formation of a secondary alcohol would be preferred. Due to the continuous transfer of protons the activation centrum is always carried over to a new reaction side and does not all the time remain on one growing molecule contrary to the activated chain end mechanisms.⁴⁶⁻⁴⁹ Of course, this assumes that there are no termination reactions happening due to e.g. moisture. In case of possible ring opening polymerizations due to the characteristics of the monomer both reaction paths compete to each other.⁴⁶⁻⁴⁹ However, if the hydroxy concentration increases during progressing reaction the activated monomer mechanism is favored since the probability for its occurrence is

increasing.⁴⁶⁻⁴⁹ A reason for increasing hydroxy content can be humidity or water residues inside the polymer. Generally, the activated monomer mechanism is known to be faster than the activated chain end mechanism as its activation energy is lower.⁴⁶⁻⁴⁹ This is the reason why a slight amount of water residue inside the cationic curing polymer can be helpful for a better and faster curing reaction.⁴⁸ Nevertheless, if the water content increases further termination reactions prevail.

As already stated at the beginning, the crosslinking is based on a cationic mechanism and following that it is not sensitive to oxygen. However, it needs to be considered that during the formation of the protons and the reaction path of the onium salts radicals play a fundamental role.^{36,41,44} If those radicals are quenched the proton yield is lowered. Besides that, acrylic PSAs like in Figure 11 cured by a cationic cured mechanism are known to show rapid curing even when used at thicker layers. Since the onium salt based photoinitiators are not only absorbing in the UVC region but also in UVB and slightly in the UVA region and show certain dark curing behavior, it is also possible to cure thicker films compared to PSAs cured with a free radical mechanism.⁵⁰ In addition to that the formed adhesives often dispose of high adhesion on different substrates due to the polyether which is formed during the curing reaction. Those polyether structures allow ionic adhesion interactions with polar surfaces even though it is not possible to use acrylic acid as monomer and lead to an increase of chemical resistance of the adhesive for non-polar substances.^{2,3,6} The combination of advantages, especially the possibility to cure thicker films leads to an increasing interest in such PSAs for different applications even though the cationic curing adhesives are more expensive. However, such PSAs cannot be used within all applications relevant for the packaging industry as the onium salt and the reaction products are not fixed to the polymer backbone. These photoinitiators tend to show noticeable migration making applications like medical or food contact impossible without modification of the cation.¹³ Until the day of this thesis a polymerizable cationic photoinitiator has not been published. Needless to say, that this is quite challenging as the onium salts can be triggered by other radicals and an onium salt with an acrylic functionality could be triggered by the initiators used to polymerize the acrylic monomers to get to the uncured polymer stage which would result in gelation during the polymerization.⁵¹

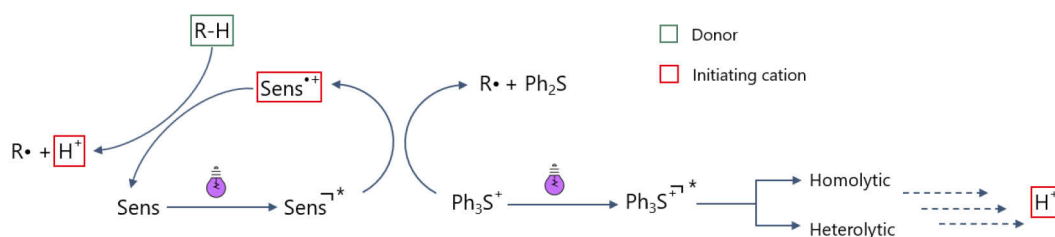
2.6 Sensitizers for onium salts

As already mentioned above many of the commercially available cationic photoinitiators based on Onium salts absorb in the UVC region. Some of them show a tailing absorption even towards the UVA region. However, this does not allow rapid UVA LED curing, even though it is worth mention that the level of absorption is not identical to the number of active species (here protons) generated.⁵² The number of active protons is highly depending on the type of onium salt, its decay mechanism and the matrix around which defines the occurrence of any termination reactions, e.g. by moisture.^{16,26,27} Nevertheless, a high absorption level at the desired wavelength leads to a more efficient system as energy transfer is easier compared to a very low absorption.²⁴ Besides the research about the investigation of novel onium salts which show a better absorption pattern in the UVA region and even at higher wavelengths by modifying the cationic part of the Oniumsalt, many research groups have been working on combining two photoinitiator systems with each other to improve the overall proton yield.⁵³ These molecules, called sensitizers, show a better absorption in the desired wavelength region and form a reaction mechanism together with the onium salt. Sensitizers are often a Norrish Type I or Norrish Type II photoinitiator, but it is also possible to use other species provided they can trigger the onium salt.^{54,55} The reaction mechanism of Onium salts shown in the previous chapter cannot only be initiated by the desired wavelength but also by energy transfer or transfer of an electron. Thereby, it is possible to initiate the reaction mechanism even though the Onium salt was not irradiated with the right wavelength or no light at all.⁵⁶ Consequently, the sensitizer must be able to donate either energy or an electron (or both) to the onium species to start the reaction mechanism and the split of the Oniumsalt. As energy transfer is only possible if the energy level of the excited sensitizer is higher than the highest energy state of the Oniumsalt, this synergy effect of cationic photoinitiator and sensitizer often is connected to the transfer of an electron, especially in case of Sulfoniumsalts. In case of a Norrish photoinitiator this electron can be generated after the proper wavelength absorption.⁵⁷ In its excited state the Norrish photoinitiator can either form a free radical (Norrish Type I) or donate a free electron (Norrish Type II).



Scheme 7: Example of possible sensitizers for Oniumsalts and their UV/VIS Absorption

This electron or radical splits the Sulfonium-Carbon bond or Iodonium-Carbon bond.^{16,53-58} The active species of the sensitizer, e.g. radical cation in case of Norrish Type II photoinitiators is also able to react with an epoxy group to start a cationic polymerization in form of an electrophilic attack onto the epoxy oxygen.^{16,53-58} Instead of directly starting the cationic polymerization, the sensitizer radical cation can also be regenerated to its original state by transferring its earlier received electron onto a hydrogen donor group.^{16,53-58} This can either be a third component which easily abstracts a hydrogen radical, or it can also be a monomer inside the monomer composition, e.g. a hydrogen positioned at a tertiary carbon which is easily abstractable.^{59,60} By that reaction path, a proton is generated which can start the cationic polymerization. Due to the regeneration of the original sensitizer molecule, the same sensitizer can take part in another reaction cycle again (compare Scheme 8).^{16,53-58} This leads to the fact that only a small amount of sensitizer is necessary as one sensitizer molecule can start several Onium species without getting consumed in theory.

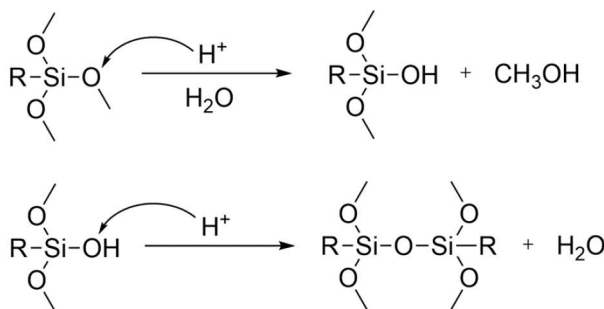


Scheme 8: Sensitizer effect onto Oniumsalt; example with Sulfoniumsalt

In case of a Sulfoniumsalt-sensitizer combination which is cured with an UVA LED where the Sulfoniumsalt itself also shows a tiny absorption in the UVA region and can be initiated by that wavelength both reaction paths are possible. The Sulfoniumsalt can either react with the excited sensitizer molecule as shown in Scheme 8 on the left side, or it can also directly be excited by the wavelength and react in either a homolytic or heterolytic path with another donor molecule again (Scheme 8, right side) as already explained in Scheme 5 in detail.^{16,53-58} Of course, if the Oniumsalt does not absorb in the wavelength region of the used light source at all, the direct excitation of the Oniumsalt does not occur at all. As stated in the chapter above, generally it is easier to initiate the Iodonium-Carbon bond by the transfer of an electron compared to the Sulfonium-Carbon bond. As a result, when comparing Oniumsalts with each other, it is easier to sensitize Iodoniumsalts than Sulfoniumsalts.^{27,58} However, this often leads to a reduced temperature stability of Iodoniumsalts as other species like impurities inside a polymer matrix might also be able to form a radical or electron which is suitable to initiate the reaction mechanism at elevated temperatures as Iodonium salts are easily sensitized by variety of electron donors.^{16,53,55} By the right choice of sensitizer, Oniumsalts can be used to initiate a cationic photopolymerization even in the visible light or NIR region as several groups have shown.^{16-18,61,62} This creates new curing technologies and allows curing of thicker samples compared to UVC curing which especially assisted in UV cured 3D printing technology in the past. However, it needs to be considered that choosing a sensitizer which absorbs in the visible light region will also lead to instabilities of the product at day light requiring special packaging. For UVA LED cured hotmelt based acrylic PSAs it is important to take the temperature stability into account again. Not only the Oniumsalt but also the sensitizer needs to dispose of temperature stability at the application temperature for several hours. Consequently, the radical or electron generation of the used sensitizer should not be initiated by elevated temperatures and only by the right wavelength.

2.7 Silanes in cationic curing PSA

The combination of silane curing technology with cationic UV curing leads to a combination of several advantages, not only because both polymers need to be protected against moisture in an uncured stage.⁶³ Silanes are commercially available with a wide variety of modifications regarding their chemical composition. For instance, there are acrylic versions which could directly be copolymerized together with other acrylics but there are also epoxy modified versions which could be added in a simple formulation step.^{64–66} Many of those epoxy silanes show very high boiling points and low volatility which enables the usage in UV curable hotmelt PSA technology as they do not evaporate during the coating process. There are also oligomeric versions on the market already. Normally silanes need to be cured over 24 to 48h as the abstraction process of the exit group and the following condensation reaction takes place rather slow.⁶⁷ Of course, there are possibilities to catalyze those reactions by certain metal or non-metal-based catalysts, however, the reaction speed still would not come close to the required curing speed of an acrylic PSA as explained in chapter 2.1 above.⁶⁸ When taking the technology behind cationic curing PSA into account it stands out that they mainly run via a photo generated superacid with a very reactive proton. As described by other groups before, strong acids can catalyze the silane reaction as well provided there are some water molecules present during the reaction which can also be fulfilled by humidity.^{69,70} This leads to the conclusion, that the catalysis via a photoacid is very elegant as it not only leads to a UV induced fast abstraction of the exit group but also promotes a fast condensation reaction of silanols and epoxies.^{71–73}



Scheme 9: Photoacid triggering silane curing (simplified)

As can be seen in Scheme 9, the proton triggered silane curing reactions leads to the formation of new chemical species which could take part in several reactions since the silanes are multifunctional and of hybrid moiety. Depending on the raw material the silane is capable of taking part in a simple silane – silane crosslinking reaction as it already has been copolymerized or it is able to act as monomeric or oligomeric crosslinker with higher mobility. But not only the silane and its crosslinking reactions are of interest but also the leaving groups are attractive for cationic polymerization of epoxies. In standard silicone chemistry it is popular to have acid or amine derivatives as leaving group instead of standard alcohol to reduce the VOC level of silicones but here, during the cationic polymerization, it is especially the alcohol leaving group which is interesting and can influence the reaction mechanism of epoxies.

As explained, the curing reaction of epoxies can follow two different reaction paths depending on the monomer characteristics and also the surrounding matrix. In the absence of water and other hydroxy containing species an activated chain end mechanism (ACEM) is favored. However, the introduction of small amounts of hydroxy functionalities can shift this mechanism towards an activated monomer mechanism (AMM) increasing the polymerization speed (curing speed) noticeably without leading to a complete termination of the overall curing reaction. Certainly, this could also be achieved by the introduction of a hydroxy based acrylate into the polymer main chain, however, this hydroxy acrylate would also affect the radical copolymerization by noticeable transfer reactions leading to a change in molecular weight distribution and instabilities could occur due to unwanted crosslinking of polymer chains inside the reactor. An addition of an alcohol like a polyol after the polymerization reaction being used to make sure that the alcohol does not interfere with the radical copolymerization would fix this problem, however, besides solubility issues due to different polarity, instabilities at higher temperatures when heating up the hotmelt are likely to occur.

Silanes have the advantage that prior to any occurring separation and starting reaction they (almost) do not have any free hydroxy functionalities which could cause those issues and the release of hydroxy species can be triggered by the UV irradiation with the LED as the photoacid only then generates the protons provided that the photoacid is temperature stable itself.^{71–73}

3. Motivation and aims

In the context of global warming, not only consumers but particularly the industry is increasingly focused on more sustainable and environmentally friendly processes. The foundations of UV-curable adhesives based on hot melt adhesives are already established on a process that is more sustainable compared to other technologies. However, even seemingly sustainable processes and technologies offer opportunities for further improvement and reduction of the ecological footprint.

The advanced development of LED technology in the UV emission spectrum presents new possibilities for light curing compared to the previous use of mercury vapor lamps. By substituting mercury vapor lamps, significant energy and overall cost savings can be achieved, while the total CO₂ consumption per kilogram of adhesive used will also decrease, leading to a more sustainable process.

The aim of this work is to evaluate the LED curability of existing UV adhesive systems in terms of their curing efficiency. Furthermore, opportunities will be explored to enhance these adhesive systems for LED curing, thereby creating efficient curing kinetics. This will involve not only the investigation of different curing systems, such as cationic and free radical systems, but also a comprehensive study of various photoinitiators and their combinations also with regard to thermal stability which is essential for hotmelts. Given the potential for application across diverse industries, such as packaging, automotive, and electronics, the focus will particularly be on commercially available photoinitiator systems. Additionally, the adhesive systems will be examined for potentially newly developed properties resulting from LED curing, which will be further improved through various formulation steps.

4. Results and discussion

4.1 Cationic UV curable PSA

As shown in Figure 12, the polymerization was carried out in ethylacetate as solvent to ensure moderate transfer reactions with the solvent leading to a broader molecular mass distribution to not only form cohesive base strength but also keeping the desired adhesion strength for PSA applications.^{1,2,8} The fact that the polymerization was carried out as 43% total solid (TS) process in combination with 0.37 mol% AIBN leads to a molecular mass of approx. 120.000 Da as can be seen in figure 13. The combination of Methylacrylate as hard monomer and 2-EHA as soft monomer results in a glass transition temperature of -25°C also allowing applications near the freezing point without losing too much tack.

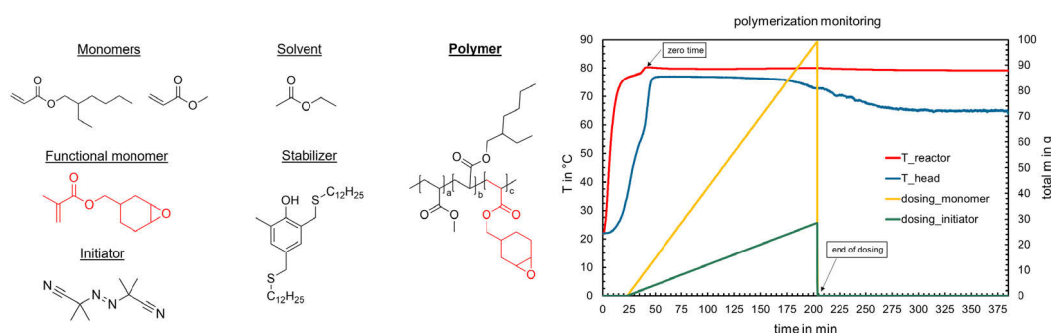


Figure 12: Polymer design of cationic curable PSA; polymerization monitoring

The reason an Azo based initiator was used is based on the fact that these types of initiators tend to favor the reaction path with monomers instead of hydrogen radical abstraction reactions on the polymer side chain which would be followed by a more branched polymer chain.⁷⁴ This polymer chain might have the same molecular weight however increases hotmelt viscosity because of increased entanglement which is not always beneficial because of processing reasons.⁷⁵ After the formulation has been done and the solvent has been removed this epoxy group can be crosslinked via a photoacid as explained in chapter 2.5 above.^{29,30}

A monomer which stands out is the epoxy acrylic monomer EPOMA. This monomer can be copolymerized with other acrylics without reacting via the epoxy group. As explained in chapter 2.5, cycloaliphatic epoxy monomers are more favorable for cationic curing processes while keeping temperature stability at a high level since reactions with suitable nucleophiles like amines are not favored. This leads to more stable polymer chains during processing and an increased shelf life.^{26,28}

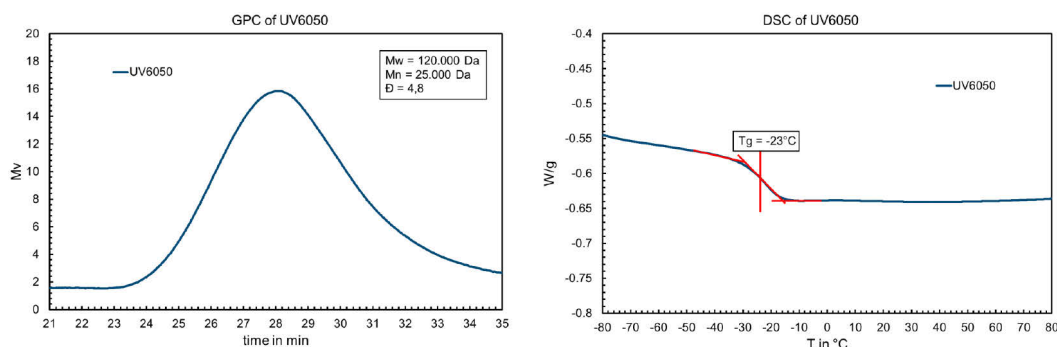


Figure 13: GPC of cationic curing PSA (standard: Polystyrene); DSC measurement

It sticks out that this monomer is a methacrylic type instead of an acrylic type than the other two monomers. Regarding the copolymerization of acrylic monomers this combination is not the best, however, the acrylic version of the EPOMA is much more expensive than the methacrylic version and therefore exceeding any price border in packaging industry. To promote a statistical copolymer a semi feed batch process is used as it was already explained above. Due to the continuous dosing of the same monomer composition the formation of a statistical copolymer is promoted as there are only a few monomers of EPOMA at once in a high radical concentration leading to its consumption without the formation of an own homopolymer or block inside a copolymer.⁷⁶ Nevertheless, the monomer composition of all three monomers has been analyzed by GC MS. During the whole polymerization time samples have been taken and rapidly quenched by phenothiazine in order to stop any ongoing radical reaction. All samples have been analyzed regarding their composition at every time stamp. If one of the monomers showed a tendency to form more like an own homopolymer this could be seen in an initial consumption of that monomer right at the beginning or at the end. In case of a steady consumption equal to the other monomers it can be expected that a statistical copolymer is formed during the polymerization. As can be seen in Figure 14

(left), the monomer is consumed relatively steady over the entire reaction time. At the beginning of the polymerization the consumption of all monomers is quite rapid as the radical concentration is high and low viscosity allows high mobility of active species inside the matrix. After 180 minutes the delays are stopped as the function of consumption changes its behavior by means of an initial drop. This can be explained by the fact that the number of monomer molecules and initiator molecules decreases as no further dosing takes place. Once this change in polymerization process control has taken place the consumption curve gets back to a steadier state. Most importantly it can be seen in Figure 14 on the right-hand side that the monomer composition at almost every sample point does not drastically change irregularly. In fact, it might be possible that during the first 70 minutes the EPOMA is slightly preferably incorporated into the polymer, however, this might be connected to measurement inaccuracies. The monomer concentration process over time would be completely different if the EPOMA was not built in statistically if its reactivity was fundamentally different compared to the other two monomers. This would lead to a drastic change in monomer composition inside the sample. Also, with the addition of the DSC analysis where only one T_g can be seen a statistical copolymer can be expected.⁷⁷

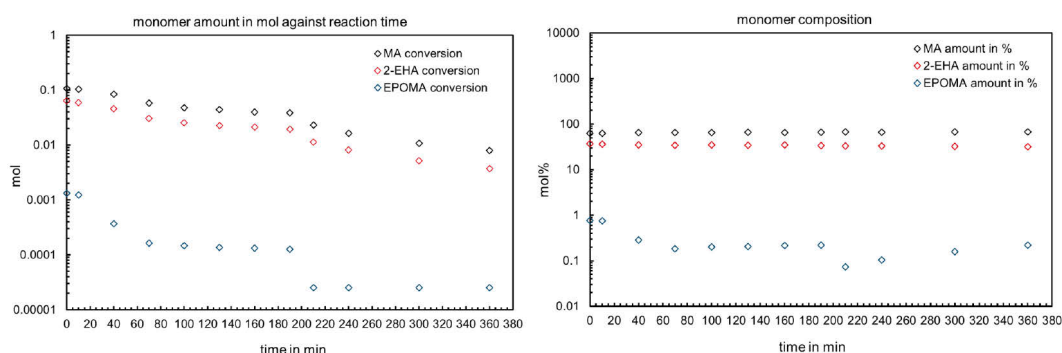
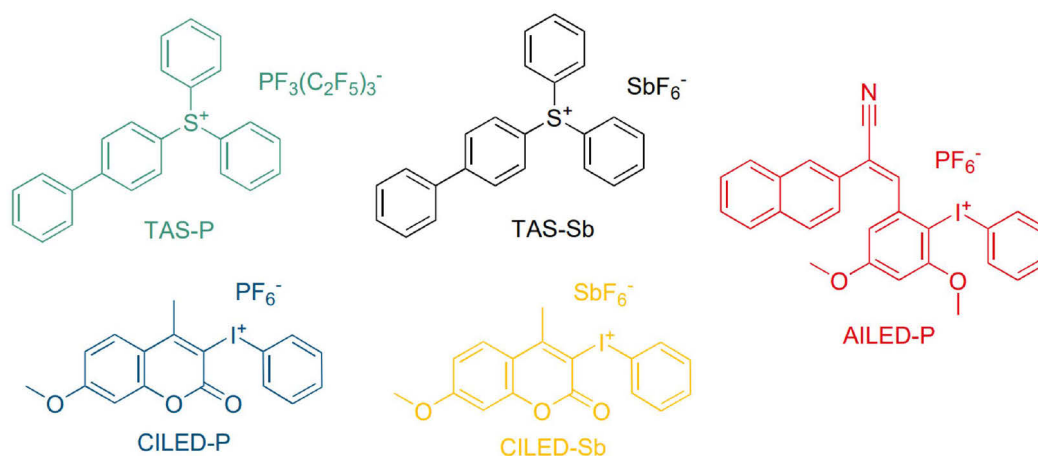


Figure 14: Monomer consumption over time; monomer composition over time

In combination with the measured molecular weight from the GPC data it can be calculated that approx. 7 epoxy groups per polymer chain can be expected. Of course, this must be seen statistically as well, as there might be chains having a different amount of epoxy groups and because of the broad molecular weight distribution shorter polymer chains might have less epoxy and longer chains might have more epoxy in their respective composition.

4.2 Cationic curing: photoinitiator possibilities

To ensure rapid curing of the cationic curing PSA while keeping the temperature stability at the desired level it makes sense to select the right photoinitiator first. When the optimum photoinitiator (composition) is found, other parameters like the polymer design or epoxy amount can be adapted. Taking the industrial availability into account, the cationic photoinitiator which enables the best LED curing needs to be commercially available. This is the reason why novel LED curing cationic photoinitiators published by different research groups in the past months cannot be screened here.⁷⁸ Even if they showed outstanding performance regarding the curing reaction and stability it would not be possible to commercialize such a product in the next 2 to 5 years. After investigating the latest literature carefully, the following photoinitiators have been selected to be benchmarked against each other. They have been compared in the same molar amount and also the same base polymer from chapter 3.1 has been used.



Scheme 10: Potential cationic photoinitiators for LED curing PSA; commercially available

All photoinitiators shown in Scheme 10 can absorb photons from 365nm (see Figure 15) which is the wavelength of the LED used for curing the PSA. Two sulfonium salt based cationic photoinitiators with the same cation structure were chosen whereas the anion is of different structure. This leads to a similar wavelength absorption pattern while the reaction in a cationic polymerization might be different as the anion determines

acid strength and mobility of the acid inside the polymer matrix.⁷⁹ The TAS-Sb has been used in a standard cationic curing product cured by mercury bulbs in the past, however, as this structure is containing antimony, it would be of high interest to achieve a heavy metal free formulation in the future, if possible. In addition to that, three different Iodonium salts are investigated as well where two of them again share the same cation while having a different anion. As the cation of CILED-P and CILED-Sb are based on coumarin, their UV/VIS absorption spectrum shows outstanding absorption in the 365nm area. This applies also for the third Iodonium salt AILED-P which is an Onium salt still being in the late R&D phase of UVA absorbing Iodonium salts.

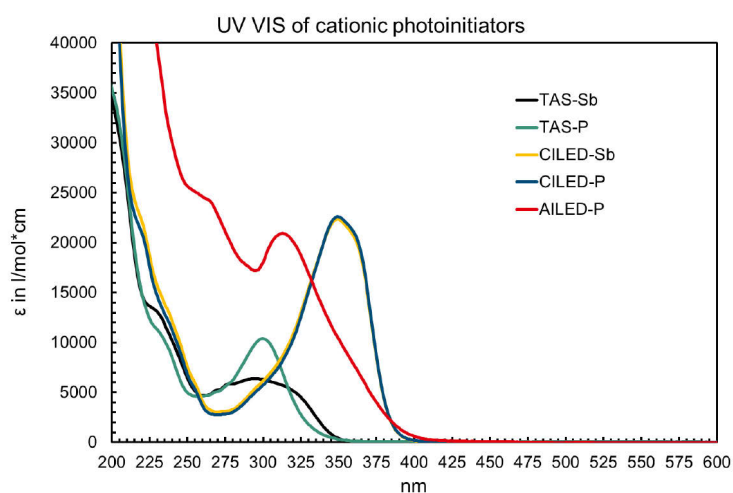


Figure 15: UV/VIS absorption spectrum of investigated cationic photoinitiators for 365nm LED curing.

Regarding the UV/VIS absorption of cationic photoinitiators it must be noticed that a high absorption at the desired wavelength is not inevitably the most important factor regarding the photoinitiator reactivity. Wavelength absorption at the desired wavelength cannot proportionally connected to reactivity as already demonstrated by other research groups before as intermediate reactive species might not only chose the reaction path which results in the formation of a proton required for the cationic polymerization but may also result in a termination reaction.^{38,52} In addition to that, the acid strength and the mobility of the acid inside the matrix is crucial for a rapid curing reaction.⁸⁰

The base polymer was formulated with 1.92×10^{-5} mol/g (hotmelt) of cationic photoinitiator and mixed in solution for 24h on a rolling bank. Temperature stability and performance have been checked separately from each other to be able to investigate the combination of performance and potential temperature instabilities independently from each other. In detail this means that coatings for performance and rheological behavior tests were made from material in solution while the same wet material has been put into a rotary evaporator to strip the solvent off and achieve the hotmelt stage. Using this hotmelt material the temperature stability of the polymer composition has been verified.

In order to investigate the potential curing kinetic of each photoinitiator in the same base polymer 100gsm (80 μ m) free films of each sample with different cationic photoinitiators in the same molar amount have been made for UV rheology. Two different methodologies have been chosen, permanent irradiation and an initial flash of the 365nm LED for 1.5s. This allows the prediction of any dark curing behavior of a certain cationic photoinitiators and would indicate if there are any differences with regard to the dark curing behavior depending on the photoinitiator. It must be noticed that a light impulse of 1.5s is much closer to the later production process where a belt is running underneath a LED at high speed. Consequently, the time frame for a certain part of the coating to be set under irradiation is rather limited.

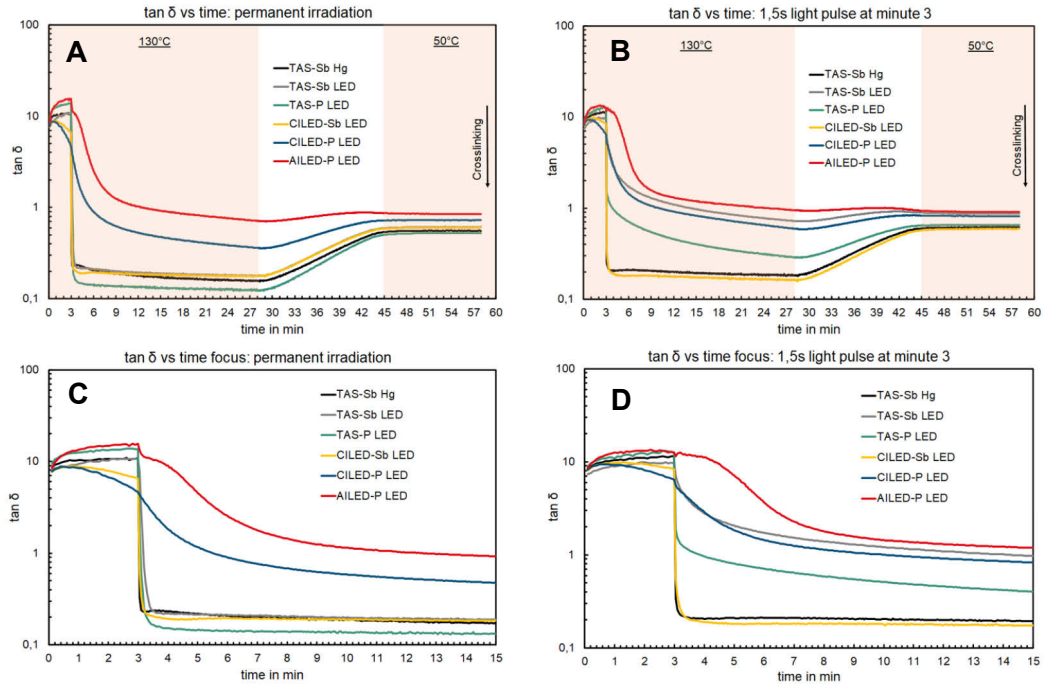


Figure 16: UV rheology of different cationic photoinitiators in the same base polymer

Again, to be as close as possible to a later hotmelt application process where the adhesive coating is at elevated temperatures while being irradiated and following the Arrhenius equation, the temperature has a fundamental impact onto the cationic polymerization, especially because of better acid mobility inside the polymer matrix due to lower viscosity, coatings have been cured at 130°C.²¹ To ensure polymer sample relaxation after the test has been started under the applied force given by the set parameters, a 3-minute sample conditioning time has been implemented. Exactly at minute 3 the LED is either turned on permanently for the whole measurement time or flashed for 1.5s. To be able to measure differences in the crosslinking structure the sample was cooled down to 50°C after some time as the rubbery plateau can be expected at this temperature ($T_g = -22^\circ\text{C}$). As can be seen in figure 16, the curing behavior fundamentally depends on the cationic photoinitiator. First, the cationic photoinitiators CILED-P and AILED-P did not perform well in both tests, the impulse test and the permanent irradiation. In both cases the decrease in $\tan \delta$ appears very slow, no matter if the irradiation is permanent or pulsed. As it is very important for an adhesive coating to cure as fast as possible this is insufficient for an efficient curing

product. It is also important that the highest degree of elasticity, meaning the lowest value of $\tan \delta$, is achieved as fast as possible. A photoinitiator composition which would show a high dark curing potential however reaching its final plateau of a low $\tan \delta$ very slowly and delayed over several hours would lead to potential problems with its reproducibility, as in the meantime termination reactions e.g., due to high humidity level at that day, might occur and leading to an insufficient curing degree compared to a day with lower level of humidity. This behavior can also be observed when investigating the same uncured sample. Regarding the AILED-P it is not clear if this behavior is caused by the anion or the cation, however, in case of the CILED-P it appears that this curing behavior is strongly connected to the phosphate-based anion moiety. The reason for this is the much better performing CILED-Sb photoinitiator which shares the same cation as the CILED-P. However, the CILED-Sb having an anion on Antimony base leading to an increased acid strength.²⁹ The CILED-Sb photoinitiator shows a rapid curing profile being completely comparable to the antimony cured TAS-Sb reference shown in black in Figure 16.

In case of LED curing with the TAS-Sb Photoinitiator, the behavior depends on the methodology of measurement. It shows rapid curing when permanent irradiation is chosen whereas the curing gets much slower when an irradiation pulse is used. As this irradiation pulse, as already explained, is much closer to the later production process it is fundamental for a photoinitiator to show rapid curing even when only flashed by the LED for 1.5s. However, the fact that there is curing at all with LED irradiated TAS-Sb again proves the point that wavelength absorbance is not the only factor affecting the overall curing kinetics. Interestingly the TAS-P sharing the same cation as TAS-Sb however having a modified phosphate-based anion shows a better curing performance in both, permanent irradiation and 1.5s irradiation pulse compared to the TAS-Sb. As the absorption characteristic is the same for both photoinitiators the difference in curing behavior is connected to the anion again. Here it can be expected that due to the modified phosphate anion the acid strength is increased compared to standard phosphate-based anion like with the CILED-P and the AILED-P. Due to the fact that the organic substituents lead to an increased anion side it can be argued that the acid strength is higher compared to standard phosphate anions as the anion size decides over its stability due to higher charge distribution and with that the later acid

strength.³⁶ It might also be the case that the organic substituent modification leads to an increased mobility inside the organic polymer matrix, however, this needs to be verified complementarily. This behavior is quite interesting as for environmental aspects it is of huge interest to run with a formulation free of heavy metals. Nevertheless, it is worth to mention that especially in these times perfluorinated substances do not fulfill the aspect of modern sustainability approaches. However, since a strong acid is needed for the cationic polymerization and crosslinking of polymer chains, there is no commercially available alternative now in which the cationic photoinitiator is not completely perfluorinated on the anion side.

To investigate the performance of each sample, free film coatings of each sample coming from solution have been made. Again, this ensures that a potential unwanted long term temperature instability and possible gelation can be observed separately from the performance and curing characteristics. The coatings have been made with an Elcometer coater with a thickness of 40µm, which is equal to 50g of adhesive per square meter (50gsm) and the solvent was evaporated for three minutes at 110°C. After the curing with 3.850mJ UVA dose (365nm LED) the coatings have been transferred to etched PET foil and left for conditioning for 24h. The performance, particularly SAFT and 180° Peel on steel, has been investigated. As can be seen in Table 1, the performance shows complementary results regarding the UV rheology test. As expected, the samples with CILED-P and AILED-P do not show the desired level of adhesive performance as the kinetics measured with UV rheology already indicated an insufficient degree of curing. Besides that, the CILED-Sb based sample shows comparable performance regarding the TAS-Sb Hg cured reference except that the peel value is higher. This might be connected to a not completely cured sample through the whole thickness as the side of the adhesive not being exposed to the light source was stuck onto the steel substrate for testing.

Table 1: Performance results; measured on steel. AF failure mode is favored.

PI-System / UV source	SAFT in °C	180° Peel in N/25mm
TAS-Sb Hg 50mJ; UVC	>200	21 (AF)
TAS-Sb LED 3850mJ	>200	35 (CF)
TAS-P LED 3850mJ	>200	20 (AF)
CILED-Sb LED 3850mJ	>200	33 (CF)
CILED-P LED 3850mJ	51 (CF)	30 (CF)
AILED-P 3850mJ	81 (CF)	36 (CF)

There are several potential reasons like an unwanted termination reaction which might explain why this occurred even though the UV rheology indicated a very well cured sample. Regarding the TAS-Sb (LED cured) and the TAS-P the performance underlines the UV rheology investigation. Even though the TAS-Sb LED curing did not show great curing kinetics it seems to be enough to at least reach a sufficient cohesion even though the sample is not completely cured as the high peel value indicates again. The improved curing profile from UV rheology with the TAS-P can be observed here as well, in comparison with the TAS-Sb as the sample shows completely comparable performance to the mercury cured reference where also the peel performance is in line. Generally, it needs to be said that a higher peel value is often favored, depending on the application, however the failure mode has a big influence on the later application. In several applications a cohesive failure mode in peel tests is not desired as it is the case with these adhesives here. Consequently, a lower peel value in the 20 N/25mm range with an adhesion failure mode is often favored compared to a peel value in the 30 N/25mm range with cohesive failure mode. In case of the samples with TAS-Sb and CILED-Sb a higher UVA dose would be required to get to the desired peel level which would slow down the speed of the belt coater in an industrial process again.

The temperature sweep test of all samples indicates in a similar direction as UV rheology and performance tests have already shown. In Figure 17 it can be seen that the samples including CILED-P and AILED-P as cationic photoinitiator show the highest level of $\tan \delta$ and with that the lowest level of curing. Even though both samples did not

perform well especially in the cohesion performance test, a certain amount of crosslinking can be seen in the DMA as $\tan \delta$ is below the sol gel crossing point of $\tan \delta = 1$ and even with increasing temperatures $\tan \delta$ does not increase rapidly, which would indicate a melting process. This underlines the fact which could be seen in UV rheology for these samples, that there is a certain degree of curing however this is not enough for a well and cured product in a certain amount of time. Regarding both tested sulfonium based cationic photoinitiators TAS-Sb and TAS-P both show a proper degree of crosslinking and a higher crosslinking level as AILED-P and CILED-P. Again, as already visible in the UV rheology test the phosphate based TAS-P outperforms the TAS-Sb when LED cured and the LED cured TAS-P sample even reaches the level of crosslinking the Hg cured TAS-Sb reference sets as benchmark. The change of the anion from phosphate based to antimony based in case of the CILED photoinitiator range leads to a better curing performance as it could already be noticed in the tests before, however, this photoinitiator does not achieve the curing level of the benchmark.

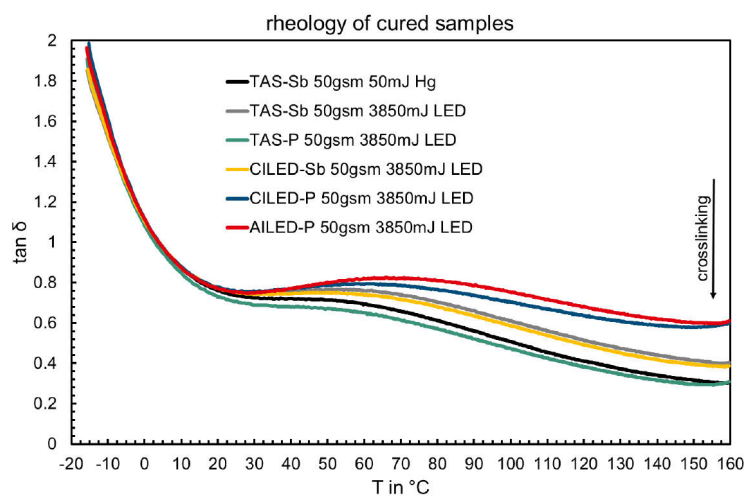


Figure 17: DMA of cured adhesive samples.

Interestingly it can be seen in the DMA that for a good cohesive performance of the PSA it is not enough for the sample and its curing behavior to just get over the sol gel point but a noticeably level below that. Without that further curing level, the polymer network on the one hand side is strong enough to withstand a melting process as the storage modulus is higher, on the other hand side the storage modulus is still not high enough to withstand a high level of shear force as the elastic parts of the polymer are

still too low and / or too weak for this force. As already mentioned in an earlier chapter, the temperature stability of each sample has been investigated in separation of the investigation of performance and curing kinetics. All samples have been formulated as explained above, however, the solvent (Ethylacetate) has been removed under reduced pressure and elevated temperatures up to 120°C to achieve the 100% solid hotmelt. During the solvent stripping process via rotary evaporator, it could be noticed that all Iodonium salt containing samples (CILED-P, CILED-Sb, AILED-P) did not get through the solvent removal step without gelation occurring. Following that, it was not possible to measure a 24h hotmelt stability of those samples and the Iodonium salt containing samples are not suitable for a stable UV curable hotmelt which could be safely commercialized.

Bearing that in mind, it is necessary to look back to the performance and curing kinetics of those samples. As the UV rheology has been measured at 130°C the degree of curing and also its speed cannot only be connected to a well working photoinitiation process anymore but also to a temperature induced curing which is definitely not desired in these products. Both Sulfonium based cationic photoinitiators, TAS-Sb and TAS-P however got through the solvent removal step without gelation occurring and also showed excellent temperature stability over 24h at 130°C in a Brookfield viscosimeter. For both samples the increase in viscosity was below 15% over 24h which enables an application in a commercial hotmelt. Besides the stability, the factor of cost is important to notice here as well. All performed tests indicated that the TAS-P is an outstanding photoinitiator to be used in these kind of adhesives, enabling not only a stable product and rapid curing under a 365nm LED but also leading to a product free of heavy metals like antimony. However, the TAS-P photoinitiator cost per kg is more than 50 times the cost of the TAS-Sb which would lead to a later doubling of the overall adhesive price. As it would not be possible to commercialize such a product because of the high product price, it has been decided to stick to the TAS-Sb photoinitiator even though the curing speed is lower than that of the TAS-P. From a scientific perspective however the TAS-P is by far the better solution.

4.3 Sensitizers for improved LED curing

Once the best fitting cationic photoinitiator for the UV hotmelt adhesive system has been found there is still room for improvement regarding the efficiency of the photoinitiator system with a focus on curing efficiency and speed of curing. As the speed of curing is fundamental for the industrial process and a key factor for saving energy and leading to a more sustainable adhesive and coating process it is necessary to design the curing system as efficient as possible. Basically, it might work to simply improve the amount of cationic photoinitiator, however, besides increasing costs this could lead to connected problems due to surface curing effects.²³⁻²⁵ Increasing the photoinitiator amount more and more would imply that the surface of the PSA on which the first photons occur during the irradiation gets cured more rapidly. In case of a photoinitiator, where its byproducts formed due to the irradiation triggered reaction are absorbing at the same wavelength as the non-reacted photoinitiator molecules, this leads to limited penetration depth of the photons.²³⁻²⁵ The PSA on the one hand side would have a well cured surface, however, the deeper structures which are especially responsible for cohesion formation would remain undercured resulting in an overall bad performance.

Another way to improve the photoinitiator system is to introduce a sensitizer to the adhesive.^{16,53,56,57} When choosing potential sensitizers, it was again important to focus on the respective cost incurred and the commercial availability since the UV LED hotmelt PSA is expected to run commercially in the packaging industry in the future. With that in mind, the market and literature has been screened in view of the required wavelength absorption and the desired stability under standard environments inside a building. This leads to the fact that no sensitizer was chosen which has a noticeably higher absorption inside the visible light area or even above that.^{61,62} The following sensitizers were chosen and tested in a combined reaction path with TAS-Sb as cationic photoinitiator.

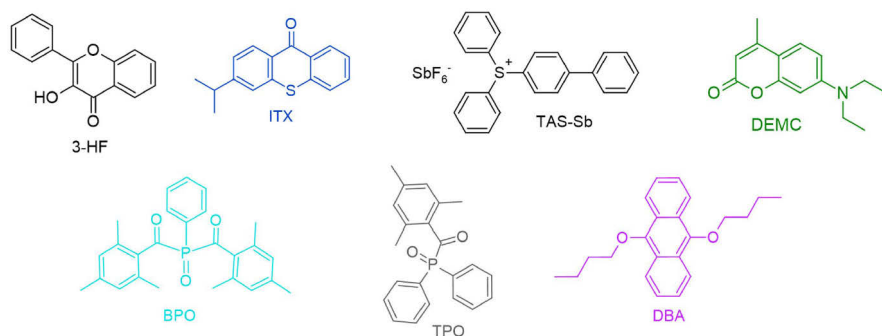


Figure 18: Structures of potential sensitizers for LED curing with TAS-Sb

As can be seen in Figure 18 most of the chosen sensitizers are free radical photoinitiators themselves which either follow a Norrish Type I or Type II reaction path. All of them fulfill the needed absorption pattern with an absorption at 365nm however having no excessive absorption in the visible region, as can be seen in Figure 19.

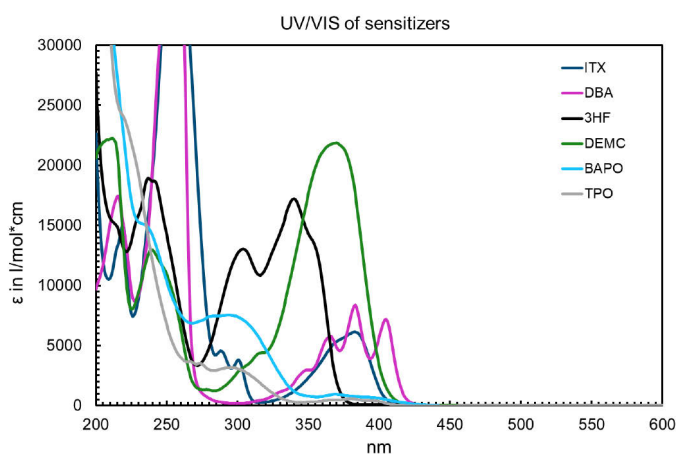


Figure 19: UV/VIS absorption spectrum of potential sensitizers for LED curable hotmelt PSA

As well as the UV/VIS absorption and the commercial availability it is important to verify temperature stability of all photoinitiators as it was already necessary with the cationic photoinitiators. This results in the fact that any potential positive effect of the new introduced sensitizer to the adhesive system needs to be investigated if this is an undesired temperature driven effect or a synergistic effect of the sensitizer and the cationic photoinitiator aimed for.

To investigate the influence on the curing efficiency and a potential in curing speed, UV rheology was measured for all samples. A molar excess of two regarding the cationic photoinitiator TAS-Sb was used so the sensitizer amount was always double the molar amount of cationic photoinitiator to remain comparable. The base polymer was kept the same for all samples and it is the same base polymer which has already been used for the photoinitiator investigation. Also the coating process was kept the same; all samples have been made from solution and the solvent was evaporated in coated stage. With that, any potential temperature curing effect was not triggered that much as it would have been in a solvent stripping process. Again, this does not allow any conclusion regarding the temperature stability of the hotmelt as this needs to be tested separately. All samples have been irradiated with the 365nm LED and compared to the mercury cured reference as well as the LED cured sample with only TAS-Sb in it.

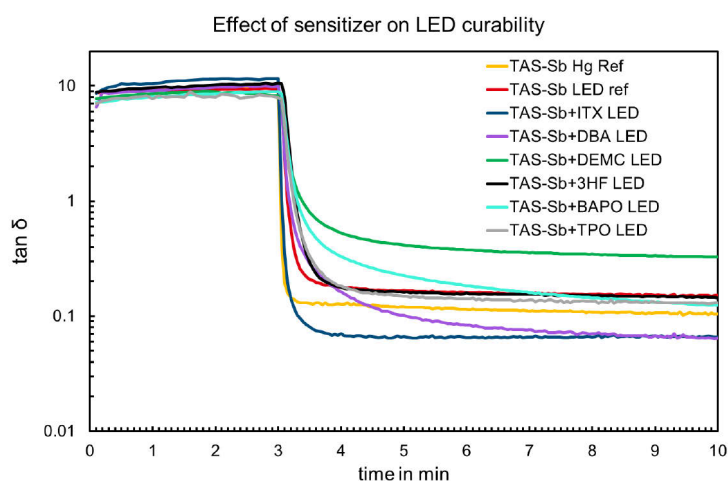


Figure 20: UV rheology of sensitized and non-sensitized PSA samples

In Figure 20 it can clearly be noticed that the introduction of a sensitizer has a direct influence on the overall curing behavior of the sample even though the cationic photoinitiator and the base polymer were kept the same. First, the combination of TAS-Sb with BPO and the combination of TAS-Sb with DEMC made the system worse than it has been before. The speed of curing generally decreases for both samples compared to the TAS-Sb LED reference and the final plateau of $\tan \delta$ is higher than the value for the LED reference sample in case of the DEMC sample. This results in either an even lower belt speed which would be needed or an uncured product for the DEMC

sensitized sample. When using 3HF or TPO as sensitizer, the curing gets slowed down as well even if it is not that bad as with the BPO and DEMC, but the investigation shows that both sensitizers are not beneficial for the system to improve the curing speed. An interesting behavior can be seen when using DBA as sensitizer as it first appears that the system is hindered in curing as well, however, the final plateau of $\tan \delta$ is lower than that of the LED reference which indicates a better cured adhesive compared to the TAS-Sb LED reference. Nevertheless, as already stated earlier, the initial network formation right after the LED is switched on is very important for a reliable product. The DBA sensitized sample might work perfectly well in most cases, however, if there is an unwanted termination reaction of the cationic polymerization e.g., because of temporarily very high relative humidity, the system might only get to an insufficient curing degree e.g., $\tan \delta$ level at minute 3.5.⁷⁵ This would lead to poor reproducibility and therefore demonstrates why it is important to reach the final plateau of $\tan \delta$ with its connected good adhesive performance as fast as possible even though dark curing reactions are occurring.

The only sensitizer which sticks out is ITX. Introducing ITX to the adhesive system increases the 365nm LED curability fundamentally. The initial network formation right after the LED is switched on appears very rapidly and the final $\tan \delta$ outperforms the TAS-Sb LED reference completely. The final level of curing is even higher than that of the TAS-Sb mercury cured reference. This leads to the fact that ITX is the best sensitizer for TAS-Sb out of all the tested sensitizers. Why ITX performs better than the other sensitizers may have different reasons which cannot be completely confirmed as they have not been investigated. On the one hand side, solubility plays an important role again as well as the reactivity of the sensitizer as well. On the other hand, the reaction path of an active sensitizer species decides if the TAS-Sb can form a proton or not.⁶⁴ It might be that even though a sensitizer shows a very good absorption at the desired wavelength that the yield of intermediate active species is very low or even if it is high and the sensitizer itself is very efficient regarding its active species / photon ratio, the formed intermediates may not take the needed reaction path with the TAS-Sb e.g., by different quenching reactions.^{41,81}

A similar trend can be seen in the DMA investigation of cured PSA samples. As can be seen in Figure 21, the addition of ITX to a sample cured with 2850mJ UVA dose led to the best crosslinked polymer of all sensitized samples. The ITX sample even outperforms the mercury reference sample, however, it was observed that reducing the dose further led to an initial jump to poor cohesion. It could not be clarified why only a slight reduction in UV dose led to this effect, but this effect was already known for cationic curing PSAs cured with mercury bulbs. Besides the ITX, other sensitizers managed to reach a well cured stage as well, according to the DMA, like the DBA sensitizer or the BAPO. However, when taking the DMA and the UV rheology into account it can clearly be demonstrated that ITX works best as sensitizer with regard to curing speed and final curing level.

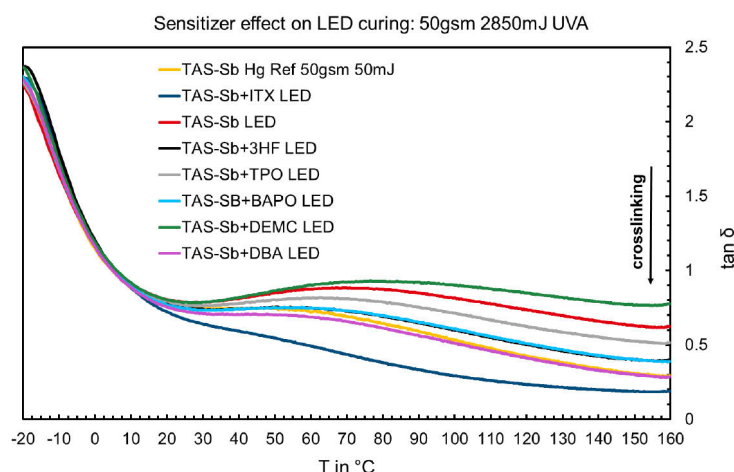


Figure 21: Impact of sensitizer addition onto the DMA of cured adhesive samples

Interestingly it can be noticed that DBA was able to reach a similar curing level like ITX in the UV rheology in Figure 20, however, a noticeable difference in the DMA of cured samples can be demonstrated. The ITX sample shows a higher level of crosslinking than the DBA sample. This underlines the fact that the initial curing responsiveness during the first seconds is very important and later occurring decrease in $\tan \delta$ might not happen reproducibly and is more depending on potential termination reactions occurring or not.

As ITX showed the best sensitizer effect in the DMA and the UV rheology, it has been decided to continue with further tests, like performance tests of adhesives and gel content measurements only with ITX as sensitizer. However, before verifying the UV rheology and the DMA investigations with performance tests, the amount of ITX has been varied to check if it is supportive for the system to increase the molar amount of ITX or if it can be decreased to save costs. In addition to that the temperature effect onto the curing kinetics has been investigated.

For the concentration row, two additional samples have been prepared, one with a molar amount ratio of ITX / TAS-Sb 1:1 and one with a molar amount ratio of ITX / TAS-Sb 4:1. Both have been compared to the sample from the sensitizer screening investigation which had a molar amount ratio of ITX / TAS-Sb 2:1. As can be seen in Figure 22 (A), the increase of the molar amount of ITX to a ratio of 4:1 regarding the TAS-Sb amount did not improve the LED curability further but made it worse again. The same conclusion can be made with lowering the ITX amount by 50% to a molar ratio of 1:1. Both alternatives, increasing and decreasing the ITX amount, will have their respective limitations because a certain amount of ITX molecules is needed to produce enough active species which can react with the TAS-Sb, however, increasing the ITX amount excessive might lead to problems like surface effects again or increase the probability for termination reactions of active ITX intermediates.⁸² The rheology data shows that a molar ratio of ITX / TAS-Sb of 2:1 provides the best results with regard to the curing speed and overall efficiency.

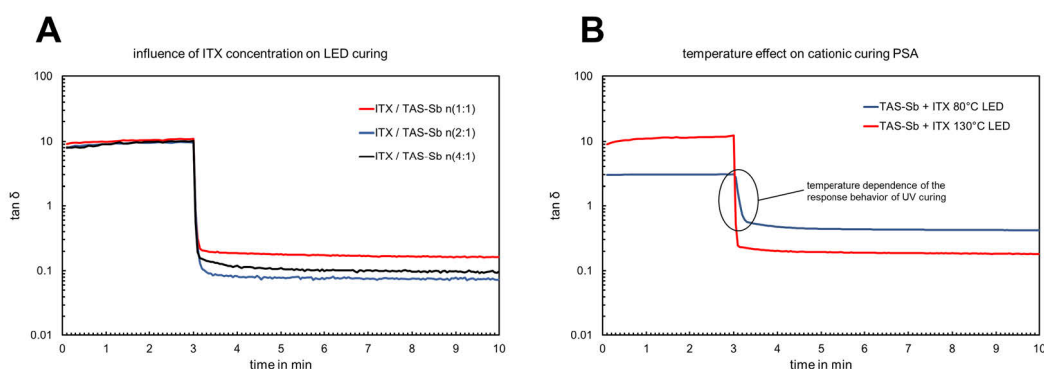


Figure 22: Impact of ITX amount on LED curing efficiency

After finding the sensitizer working best with TAS-Sb and investigating the right amount of sensitizer regarding the amount of cationic photoinitiator, the adhesive performance has been analyzed. As before the coatings have been made from solution in order to verify temperature stability separately. All samples have been tested according to the previous chapter. In addition to the performance the gel value has been determined using soxhlet extraction with Ethylacetate over 5h.⁸³

Table 2: Impact of ITX on adhesive performance and gel value

PI-System / UV source	SAFT in °C	180° Peel in N/25mm	Gel in %
TAS-Sb Hg 50mJ; UVC	>200	21 (AF)	49
TAS-Sb LED 2850mJ	80 (CF)	35 (CF)	32
TAS-Sb LED 5500mJ	>200	22 (AF)	51
TAS-Sb + ITX LED 2850mJ	>200	24 (AF)	67

Table 2 shows, that the positive impact of ITX is not only visible when using UV rheology and DMA, but also has a noticeable impact onto the adhesive performance and the gel amount. When comparing the LED cured samples with each other the implementation of ITX saved 50% of the UVA dose to gain the same performance level as for the LED reference without ITX. Without ITX as sensitizer a satisfactory performance with both SAFT and peel in line with the mercury reference sample 5500mJ of UVA dose were needed whereas the addition of ITX to the same system reduced that dose to 2850mJ while keeping the performance close to the desired level. Curing an ITX free sample with only 2850mJ lead to an uncured adhesive sample with bad cohesion and adhesion. The same pattern can be seen in gel content levels. Without ITX and by using only 2850mJ of UVA dose the gel level only reached 32%, whereas the addition of ITX increased the gel value to 67%.

Finally, this underlines how important it is to investigate and compare different samples with each other and with complementary methods as one or two methods on their own might not show the full verity about the system even though the base polymer and other additives are 99% the same. The investigation shows how sensitive these materials are regarding their speed of curing, potential termination reactions

and resulting performance values even though they are cured by a cationic polymerization.

Besides the investigation of curing kinetics, performance values and rheology it is important to not disregard the temperature stability of the hotmelt with TAS-Sb and ITX as this is a key fact for the product to work. For this test the formulated base polymer was put in rotary evaporator to remove the solvent under reduced pressure and elevated temperature. The achieved hotmelt was measured for 24h in a Brookfield viscosimeter to realize any change in viscosity at 120°C. During the measurement the viscosity only increased by 10% which is a good result for cationic curing hotmelts.

Apart from the importance of hotmelt temperature stability, cationic polymerizations are known for being very temperature sensitive regarding their kinetics but also a lower viscous polymer matrix will lead to higher proton mobility.⁸⁴ In most cases higher temperatures lead to faster polymerizations and following that quicker crosslinking reaction in case of the PSAs in this work. Bearing that in mind there will be always a problem in using LEDs compared to mercury bulbs as the mercury bulbs produce a lot of heat due to side production of infrared irradiation on their own and as a result heating the probe actively.⁸⁵ Even though this is something which is positive about LED technology as a lot of energy is saved since more electrical energy is put into UV irradiation instead of IR irradiation, this leads to potential difficulties by using LEDs for curing.

In fact, using LED technology also produces a certain amount of heat, however, way less than a standard mercury bulb produces. Taking this into consideration, the general temperature sensitivity of the cationic PSA system has been evaluated to better understand the temperature dependency of the PSA curing and as a result being able to formulate consequences for the polymer design. Even though low viscosity systems or even room temperature coatable systems might be very interesting at first glance, they might not be curable in the required time frame as the temperature e.g., room temperature, is too low to improve the curing kinetics to the needed level.⁸⁶ This would result in a minimum temperature for which any cationic curing UV PSA hotmelt could only be coated with in order to ensure a fast curing reaction while not using excessive amounts of epoxy or cationic photoinitiator. To investigate the temperature sensitivity

of the curing reaction again UV rheology was measured for the same polymer at different temperatures.

As expected, when investigating the identical polymer in UV rheology at different temperatures, a temperature dependent curing profile can be seen as shown in Figure 22 (B). When increasing the temperature from 80°C to 130°C the polymer shows an advanced curing reaction with a faster decrease in $\tan \delta$ and with that a higher degree of curing at the same time. This is very interesting for the PSAs as it clearly could be seen before that especially this part of the UV rheology measurement has a fundamental impact onto the later performance of the adhesive. The final $\tan \delta$ plateau is very different as well but here it needs to be taken into account that due to the difference in temperature the plateau values of $\tan \delta$ cannot be directly compared to each other. This can be explained by the time temperature superposition as a change in temperature would be connected to a change in frequency and with that both samples are not completely measured the same way anymore.⁸⁷

However, even if this is applied onto the initial increase, the speed of curing would be identical and there would be just an offset between the curves showing the same slope which cannot be determined for Figure 22 as there is not only an offset but a change in the slope of the graph. This shows that there is a temperature dependency during the curing and with that a difference in the later adhesive and performance cannot be excluded. Generally, this demonstrates that between all the factors for developing UV hotmelts e.g., performance, viscosity, price, etc., also the application temperature cannot be chosen too low as this would have a negative influence onto the curing rate of the polymer. This contrasts with the general idea of designing cationic UV hotmelts with the viscosity being as low as possible to save energy during the heating process as those polymers would not be fast curing anymore without increasing the photoinitiator or epoxy amount drastically which, however, would then lead to other problems again as explained in chapter 2.5 above.

4.4 Optimization of cationic curing

After the perfect fitting cationic photoinitiator/sensitizer combination has been found, the polymer system already shows an advanced 365nm LED curability compared to the initial starting reference which only contained TAS-Sb. Even though the needed UVA dose could already be halved by the addition of ITX there might be room of improvement to speed up the LED curing even further. As the needed UVA dose for curing is directly connected to the belt speed on an industrial coater it is essential to lower the needed UVA dose to an absolute minimum while keeping the desired performance. This allows also saving even more energy because the required heating time for the same amount of adhesive can be lowered in case the coating process is faster.

There are several different approaches how the system could be improved further. One of them would be to increase the photoinitiator amount, which might lead to difficulties when curing thicker coatings, as explained in chapter 2.4 above.⁸² Another one could be to increase the initial molecular weight of the base polymer. This would however not be connected to the UV curing process and have a direct negative influence onto the later hotmelt viscosity as it would tremendously increase with increasing molecular weight. An approach which does not highly affect the viscosity and through-cure ability that much, would be to increase the polymerization degree of the cationic polymerization of epoxy groups. As the cationic polymerization can follow a direct dependency on the initiator / monomer ratio, the polymerization degree could either be increased by lowering the initiator amount or by increasing the epoxy monomer amount.^{44,88}

A higher degree of cationic polymerization is expected to either lead to a further crosslinked polymer cured with the same dose compared to the reference or to a curing with less UVA dose in order to get to a similar curing level which the reference achieved, however, with a higher UVA dose. Basically, the degree of cationic polymerization can be increased by either lowering the acid amount (initiator amount) or increasing the epoxy monomer amount. Theoretically one single proton would result in a maximized cationic polymerization degree, however, this far away from reality.

Again, potential side reactions consume a certain amount of acid and further reduction of the cationic photoinitiator might not result in the desired outcome.^{89,90}

Besides the initiator concentration which might not have a large effect onto the polymerization degree, the monomer concentration plays a fundamental role which is also easier to control since the concentration range of the epoxy monomer is higher than the concentration of cationic photoinitiator.⁸⁸⁻⁹¹ A change in epoxy monomer instead a small change in cationic photoinitiator amount can be expected to be more reliable. As part of this adhesive, the monomer for cationic polymerization is copolymerized during the initial base polymer polymerization as an acrylic epoxy hybrid monomer in a radical copolymerization. An increase of the epoxy monomer amount could either be achieved by using a reactive diluent with epoxy functionalities or by increasing the amount of EPOMA in the base polymer production. The addition of an epoxy reactive diluent could finally also lead to a softer adhesive in case of non-reacted epoxy residues which would dilute the polymer matrix again. Following that, the addition would lead to a better curing performance, however, the final adhesive could have worse performance values than before. Taking that into consideration, the amount of EPOMA in the acrylic base polymer has been increased so there is no possibility of dilution even for non-reacted epoxy monomers as they are fixed to the polymer backbone. During the first investigation the focus was put onto UV rheology and the curing kinetics again. After determination of curing kinetics, an impact on adhesive rheology and performance but also stability was considered. New base polymers with more EPOMA have been copolymerized and formulated with the same TAS-Sb and ITX amount as the reference.

As expected, increasing the amount of EPOMA in the base polymer led to a faster curing reaction of the formulated adhesive which can be seen in Figure 23. Even increasing the EPOMA amount only by 25% lead to a noticeable impact onto the curing kinetics and a faster initial decrease in $\tan \delta$. However, to be able to outperform the initial decrease of $\tan \delta$ of the mercury cured reference it was necessary to double the amount of EPOMA. Besides the positive impact onto the initial curing behavior, the final level of $\tan \delta$ is impacted as well, indicating a more elastic product compared to the standard references. The elasticity of the samples with +50% and + 100% EPOMA even

reached certain values where the chosen methodology and setup of the UV rheology gets to its limits as the measured values start scattering. Here it would be necessary to change the frequency in order to measure smoother curves again.⁸⁷

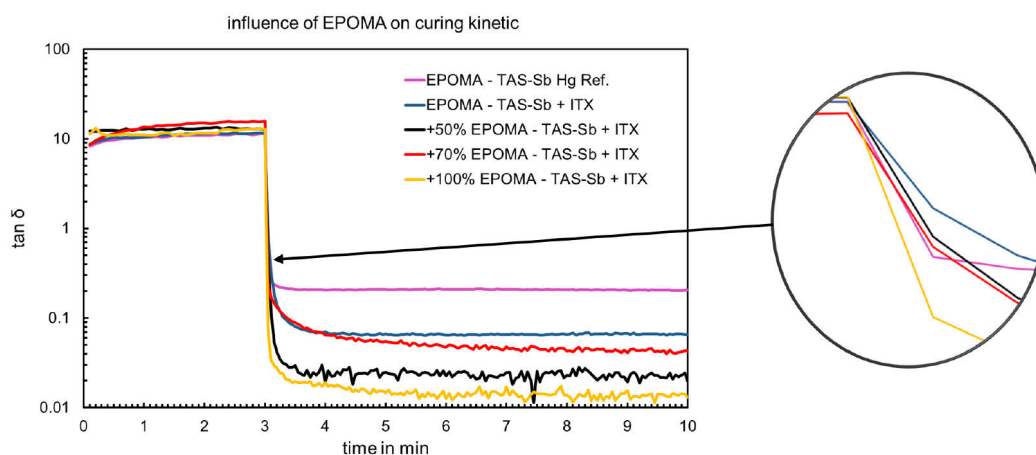


Figure 23: Influence of EPOMA increase onto curing kinetics; cured with LED

Nevertheless, as learned in previous investigations, the final plateau of $\tan \delta$ might not be reached due to potential termination reactions right after the curing process. In this case the adhesive would not be as elastic as indicated by UV rheology. Combined with the initial idea to be able to cure as fast as possible it was continued with the 100% EPOMA version regarding the DMA measurement and adhesive performance investigation. Increasing the EPOMA amount further might be even more beneficial, however, the high price of the EPOMA would again lead to a very high adhesive price which would not be suitable for the packaging industry. In addition to that, increasing the EPOMA amount excessively might increase temperature instability problems as the overall reactivity of the adhesive increases which follows also by the possibility being miss-triggered by environmental influences.

When comparing the +100% EPOMA adhesive with the reference adhesive in the DMA complementary to the UV rheology, the positive effect onto the adhesive curing can be recognized. As can be seen in Figure 24, it is also possible to cure a higher coat weight of 100gsm with a lower UVA dose than a 50gsm coating with the standard amount of EPOMA. Whereupon, the +100% EPOMA version can be cured with a lower dose while reaching a higher elastic state at higher temperatures.

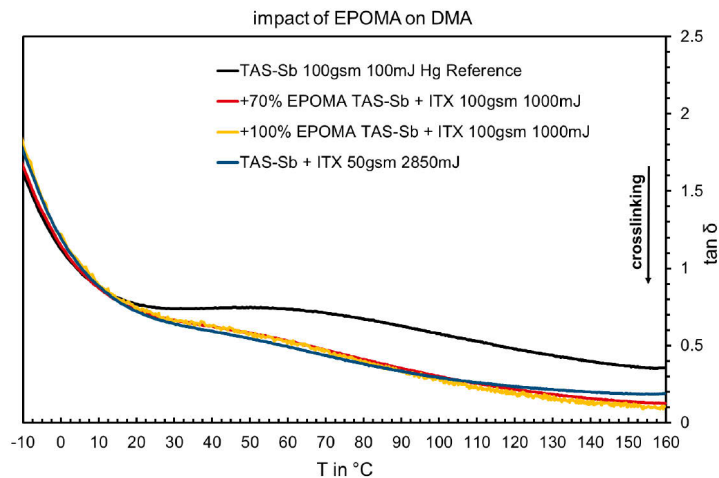


Figure 24: DMA of EPOMA modified adhesive compared to references.

Besides the positive impact onto the adhesive curing speed, it must be noticed that a difference in the polymer network after the curing can be expected. But it was not possible to lower the curing dose of the +100% EPOMA sample to get back to the reference DMA level. As a result, the EPOMA modified version will be more elastic at temperatures above room temperature than all reference samples including the TAS-Sb + ITX sample. This might be reasoned with higher temperature resistance and even increased chemical resistance because of a reduced swelling behavior due to a denser network, however, this will also influence peel values at higher temperatures.^{92,93} This does not affect all applications but needs to be kept in mind when using the adhesive within applications which require a higher peel value at elevated temperatures.

When investigating the influence of the EPOMA modification onto the adhesive performance a gain in curing speed and better curability of higher coat weights can be confirmed. The increase of EPOMA lead to a reduction of the needed UVA dose for the same coat weights and as a result, allows faster belt speeds and further energy reduction. As the DMA already indicated, the measured peel values are slightly lower than of the reference samples. It was not possible to get to higher peel values by reducing the UVA dose further as this would lead to bad cohesion again. Again, this shows that increasing the curing speed by raising the EPOMA amount allows to cure at lower dose, however, reduces adhesion slightly due to a denser polymer network and reduced viscous parts in viscoelasticity. Interestingly the more elastic behavior could

not be connected to an increased gel amount with the respective network size, as can be seen in Table 3. Both samples, the sample TAS-Sb - ITX and the epoxy modified sample with the identical photoinitiator composition reached the same gel amount. Here it can be assumed that the change in viscoelastic behavior might be reasoned with a change in mesh size and molecular weight between crosslinks instead of an increased network size.⁹⁴

Table 3: Impact of EPOMA modification onto adhesive performance

sample	SAFT in °C	180° Peel in N/25mm	Gel in %
TAS-Sb Hg 50mJ; UVC	>200	21 (AF)	49
TAS-Sb + ITX LED 50gsm 2850mJ	>200	24 (AF)	67
TAS-Sb + ITX + 100% EPOMA LED 100gsm 1000mJ	>200	18 (AF)	66

As cohesion and chemical resistance are connected to gel amount and network density because of swelling effects, the new sample can be expected to have a higher level of cohesion and chemical resistance which is very beneficial for certain applications.⁹² After increasing the curing speed by adjusting the EPOMA amount and the connected investigation of DMA and performance values, the temperature stability needs to be verified as it is fundamental for a later product. The temperature stability test has been executed over 24h at 120°C and 130°C in a Brookfield viscosimeter again. It was found out, that the hotmelt viscosity increases 40% at 120°C over 24 and 250% at 130°C over 24h which is not acceptable for both values. As already mentioned earlier above, increasing speed of curing and epoxy amount is expected to have a negative influence onto temperature stability.

Given that, it has been decided to reduce the EPOMA amount to the maximum value where the temperature stability was regained. This status has been found at +70% EPOMA. Here the 24h temperature stability remained at <5% viscosity increase over 24h at 120°C and <20% viscosity increase over 24h at 130°C which is in line with the standard reference cured with mercury bulbs. The investigation of curing speed still showed a very positive effect. Regarding the performance, the needed UVA dose for a well cured 100gsm sample needed to be increased from 1000mJ to 1500mJ, however,

still showing a rapid curing and fundamental decrease in UVA dose compared to the starting point where only a 50gsm coating was curable with 5000mJ for the mercury version or 2850mJ for the ITX modified version at only 50gsm. In summary, it was possible to reduce the needed UVA dose to $\frac{1}{4}$ of the initial UVA dose by not only implementing the ITX but also increasing the EPOMA amount by 70%. This allows to cure the adhesive at faster belt speeds or reduced LED power which is directly related to save energy during the curing process and leads to a more sustainable adhesive taking into consideration, that no mercury containing bulbs are needed for the curing.

4.5 Upscaling of LED curable cationic PSA

After the initial adhesive cured with mercury bulbs has been optimized with regard to its LED curability by using a sensitizer to the photoinitiator system to increase the absorption at 365nm and as a result increase the photoinitiator efficiency combined with a higher epoxy value of the polyacrylic, the final LED prototype (LED mod) has been upscaled in a 10l reactor. The recipe for the polymerization and the later formulation step has been kept the same only the total amount of product has been increased. During the upscaling step in the 10l reactor no problems occurred and the relative viscosity of the polymer including the hotmelt viscosity after the solvent stripping process was comparable to the values achieved in the lab development. The polymerization in the 10l reactor was done three times to gain approx. 3.5kg of LED curable hotmelt adhesive. By using that amount of hotmelt it was possible to run first coating trials on an industrial coater setup as it will be done by customers as well with a finished commercially available adhesive. As measuring the UVA dose on an industrial coater is still a large problem in the industry due to the fact that it is not possible to run measurements with UV Pucks on the machine, the UVA dose could only be calculated approximately connected to the UVA doses from the lab with the assumption that there is a linear behavior between belt speed, coating thickness and lamp power. On the industrial coater the belt speed was fixed to 10m/min and the power of the LED was varied. With the assumption of a linear behavior, it would be possible to run an adhesive showing good performance at 10m/min and 50% LED power also at 20m/min and 100% LED power without a lack in performance. This might not be

completely correct, it might also be possible that the speed needs to be adjusted slightly but at least it can be assumed that the failure is not more than 20% (based on internal experience and data sets of mercury cured products). As a standard reference, the original mercury cured adhesive was run on the industrial coater as well to investigate the LED curability and to compare it with the results found during the lab development. In Table 4 the details regarding the setup and the performance results are demonstrated. In order to save material, it has been decided to not run 100gsm coating trials, also because, the hotmelt pumps on the coater are not strong enough to pump enough adhesive for a 100gsm coating at higher speeds than 5m/min.

Table 4: Performance results of industrial coating trials compared to lab development (50gsm).

	adhesive	LED/Hg	LED power %	dose	20' peel N/25mm	24h peel N/25mm	SAFT in °C
A	Hg original	Hg	-	50mJ UVC	22 (AF)	26 (AF)	>200
B	Hg original	LED	100	-	24 (AF+Spots)	34 (CF)	>200
C	Hg original	LED	50	-	36 (CF)	37 (CF)	77 (CF)
D	Hg original	LED	Lab trial	5000mJ UVA	27 (AF+Spots)	22 (AF)	>200
E	LED mod.	LED	Lab trial	1000mJ	18 (AF)	20 (AF)	>200
F	LED mod.	LED	60	-	15 (AF)	16 (AF)	>200
G	LED mod.	LED	30	-	15 (AF)	18 (AF)	>200
H	LED mod.	LED	10	-	31 (TF)	31 (TF)	47 (CF)

As shown in Table 4, the results with the standard mercury cured product cured with LED on the industrial coater are comparable to the results found in the lab at an earlier stage. It was only possible to cure the adhesive to an acceptable performance level with 100% LED power at 10m/min. At this stage the adhesive sample (Sample B in Table 4) passed the SAFT cohesion test, however, the peel values already indicate that the sample is on the undercured side. When reducing the UVA dose by 50% for example (Sample C), it is not possible to achieve the desired performance once again. This behaves very similar to the lab development, where approx. 5000mJ UVA were needed

to get to comparable performance values (Sample D). Reducing the dose by 50% resulted in bad performance of the adhesive in adhesion and cohesion tests. When having a look at the LED mod version of the initial adhesive in the lab, this adhesive showed a curing behavior four times faster than the original adhesive cured with LED as only 1000mJ for a 50gsm coating were required and only 1500mJ for a 100gsm coating. Compared to that the non-modified reference sample was not LED curable at 100gsm. During the industrial coating trials those changes can be confirmed as only 30% LED power was needed to get to the desired performance level of adhesion and cohesion (Sample G). This already illustrates that less than one third of the dose is needed and by using this the belt speed could be tripled with 100% LED power if everything behaves linear. The research proved, that the LED coating trials of the LED modification have not been set to 50gsm but to 60gsm resulting in a 20% increased coat weight in comparison to the other references. Bearing that in mind, the industrial coating trials performed even better and a 50gsm coating can be expected to work with less power than 30% and also at an even higher belt speed than 30m/min. This results in the fact that approx. 40m/min of belt speed can be expected which would indicate a four times faster LED curing as well, which was already found in the lab. Thus, it can be said that the findings during the lab development with the introduction of ITX as sensitizer and increasing the EPOMA amount by 70% and the connected benefits in curing speed and performance levels could directly be transferred to an industrial coating trial which is typically carried out by many adhesive customers in a similar way. This shows that even though a stationary LED unit has been used for the lab developments, the results and achieved experiences are nearly completely transferable to an industrial setup which allows precise LED developments for other products as well. With the introduction of the LED mod prototype, it is not only possible to switch from mercury bulbs to modern LED technology but also to have a reliable and fast curing setup without any loss of performance, time or adhesive handling. The total cost of ownership during the coating with the LED mod prototype can be expected to be lower than the one of the mercury bulb cured products, since the energy consumption of LED bulbs is lower compared to mercury bulbs. Not to forget the longer lifetime of LEDs compared to mercury bulbs. In addition to that this type of adhesive is not relying on any futural RoHS exemptions for mercury containing bulbs anymore.

4.6 Free radical curing LED PSA

As already elaborated during an earlier chapter, apart from the cationic curing hotmelt PSA a big market share is connected to free radical curing PSA hotmelts.² Thereby the coating process is completely identical to the cationic curing hotmelt adhesives, however, the benzophenone based photoinitiator is directly copolymerized in the polymer chain during the solution polymerization enabling low migration resulting in food contact applications and medical contact applications becoming possible for such adhesives.²

Again, most of the cohesion is generated by UVC induced crosslinking via a Norrish type II mechanism of the benzophenone but as there are no epoxy groups used like in the cationic adhesives it is also possible to introduce functional monomers like acrylic acid to the copolymer. Following this, there is not only the generation of hydrogen bonds between chains leading to natural increased cohesion but also hydrogen interactions with certain polar substrates are possible leading to an increased adhesion on such substrates.^{2-4,6} In contrast to the cationic curing PSA no dark curing effects can be expected and because of the benzophenone based photoinitiator the adhesive is mostly relying on UVC irradiation. The strongly UVC based crosslinking reaction is connected to a limitation of coat weights as the shorter wavelengths cannot penetrate as deep into the polymer as it is the case with UVB and UVA irradiation of the cationic curing PSA, cured by TAS-SB.⁹⁵

For the investigation of LED curability of free radical curing adhesives, a standard grade from Henkel has been chosen. This grade is expected to reach a high cohesive level with medium peel values on standard substrates like stainless steel. This adhesive has been chosen as a reference because it is likely to be more difficult to reach a certain degree of cohesiveness with LED irradiation than achieving a PSA having a very high adhesion due to an uncured moiety and cohesive failure on the substrate.

As can be seen in Figure 25, again Ethylacetate has been used as solvent for the polymerization in order to control the reaction heat on the one hand side via the solvent reflux but also allow for transfer reactions in order to achieve a broader molecular weight distribution which is essential for a well performing PSA.² Some

differences in relation to the polymerization of the cationic curing PSA can already be observed when looking into Figure 25 which also outlines the reaction monitoring of the copolymerization.

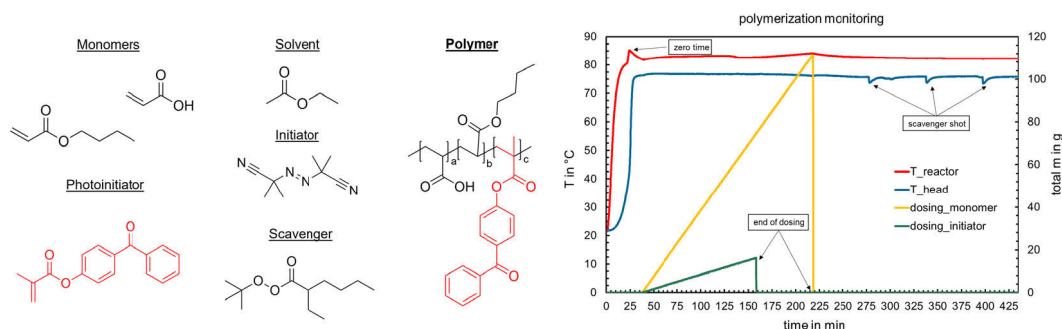


Figure 25: Polymer design of free radical curing PSA; polymerization monitoring

First the difference in the dosing time scales can be observed. The dosing step of the monomer is held for a longer time than the initiator amount. This might be controversial to the fact that a low residual monomer content is wanted, however, this reaction process allows to be able to form longer polymer chains for a short amount of time as the active radical concentration depletes while there are still new monomers dosed to the reactor.⁹ As the amount of longer polymer chains is limited by the later hotmelt viscosity the whole reaction cannot be processed in a way to form longer chains also because of lowering the adhesion then. Potential residual monomers are reduced by the peroxide scavenger shots. In Figure 25, they can easily be seen in the slightly dropping head temperature (blue curve) as one plunger stopper in the lid of the reactor head has been removed for a few seconds.

Generally, AIBN is used as initiator for the copolymerization again for the same reason as it has been used in the production of cationic curing PSA: increasing the potential to form linear polymer chains with only a low amount of branching because of viscosity reasons.^{8-10,96} When choosing the type of scavenger, it is important again to choose a scavenger which is able to reduce non reacted monomers reliably without causing branched polymer chains by hydrogen radical abstraction from the main polymer chain. The usage of POX is based on internal experience of the product and the history of the product inside Henkel, AIBN could also be used again. However, when using AIBN as a

scavenger this is directly connected to an increase in TMSN as a side product.⁹⁷ Removing TMSN in the rotary evaporator can be critical and lead to high residuals in the later adhesive. As the legal limits for TMSN need to be considered especially with food contact and medical applications, the concentration needs to be as low as possible. In fact, the trend in producing polyacrylates for those applications is starting to move away from the AIBN which has been the workhorse for free radical copolymerization over the last decades because of the TMSN.⁹⁸

Besides that, the total solid of the free radical curing adhesive with 60% is higher than that of the cationic curing polymer. Increasing the total solid often leads to problems with gelling effects and reduced process control especially with very reactive systems including bi-reactive monomers like the EPOMA.⁹⁹ The experience showed that the production of the cationic curing PSA works best at 45% TS, however, the free radical curing PSA can be polymerized at 60% TS which of course is better from the perspective of sustainability. GPC and DSC data of the free radical curing PSA are shown in Figure 26.

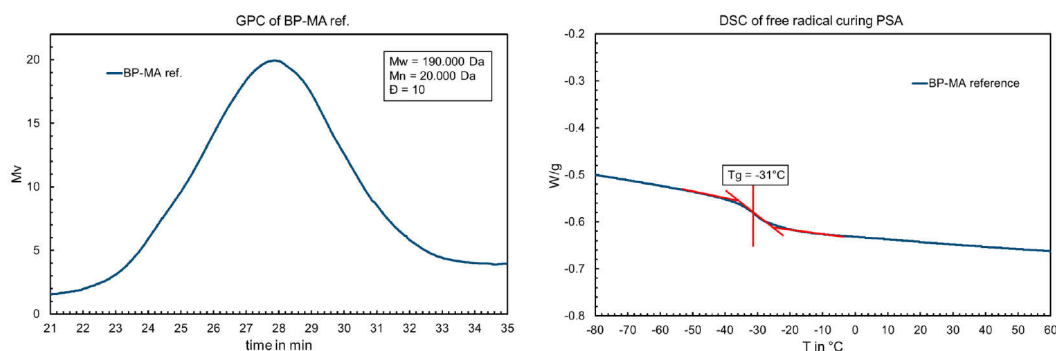


Figure 26: GPC and DSC of Hg curable reference PSA

Because of the copolymerized BPMA, the potential for curability with a 365nm LED is even more limited than the LED curability of the cationic curable PSA from earlier chapters as the BPMA does not show a sufficient absorbance in that wavelength region as can be seen in Figure 27. This leads to the fact that a change in the photoinitiator composition is unavoidable. Based on the experience from the investigations of the LED curability of the cationic curing PSA, ITX has been tested as photoinitiator in the free radical curing system as well.

The ITX showed the best performance in the cationic grade because of its sensitizing effect and in addition to that is a Norrish Type II free radical photoinitiator, so very similar to the benzophenone based photoinitiator.

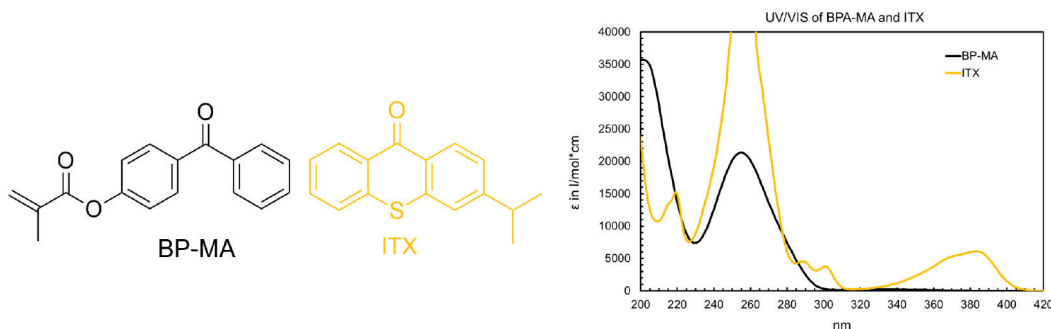


Figure 27: UV/VIS absorption spectrum of BP-MA compared to ITX.

Of course, it might also be possible to use a Norrish Type I photoinitiator but during the cationic curing PSA investigation they did not show an improvement to the curing speed even though a free radical curing mechanism without any interaction with the TAS-Sb would have been possible as well. As Norrish Type I photoinitiators disintegrate into two radicals after excitement with the right wavelength it cannot be ensured that those free radicals react in a hydrogen transfer reaction to ensure sufficient crosslinking of polymer chains and a high chance for migration exists in contrast to formulations where unsaturated systems are used and high reactivity and low migration can be expected.¹³ Here, the Norrish Type II photoinitiators show their advantage with a high favor to abstract a hydrogen radical leading to a high chance that this hydrogen radical is coming from a polymer chain and leads to a radical activated polymer chain which could take part in a crosslinking reaction with another polymer chain.⁷

As a first step the LED curability of the standard product with BP-MA has been compared to a polymer with ITX which has been formulated equimolar to the BP-MA to the base polymer which already includes the BP-MA. With that procedure it could be investigated if the ITX could either support as a sensitizer for the BP-MA or act as an own photoinitiator for the curing reaction. For the initial investigation and the curing speed determination, the UV rheology has been measured again, which can be seen in Figure 28. As well as both LED curing samples, also the mercury cured sample has been

measured for direct comparison. In Figure 28 the BP-MA based sample shows a slight responsiveness to the LED irradiation (red curve) even though the BP-MA does not show any absorbance at 365nm. It needs to be said that the curing profile which can be observed is far away from a well cured polymer which would show the needed performance values. Not to forget the rather slow curing speed and low belt speed connected to that as the sol-gel point still does not get crossed even after several minutes. The unexpected responsiveness to the 365nm LED is conveyed to be connected to the intrinsic coloring of the polymer. The free radical curing copolymer shows a not to be neglected yellow color which is expected to be connected to a generated Benzoquinone formed by the Hydroquinone-inhibitor used for stabilization of acrylic acid.¹⁰⁰ As this color generally is not wanted and there are investigations to get to a water-white product, this color cannot be seen as an advantage, especially when thinking about graphic applications of the finished adhesive.

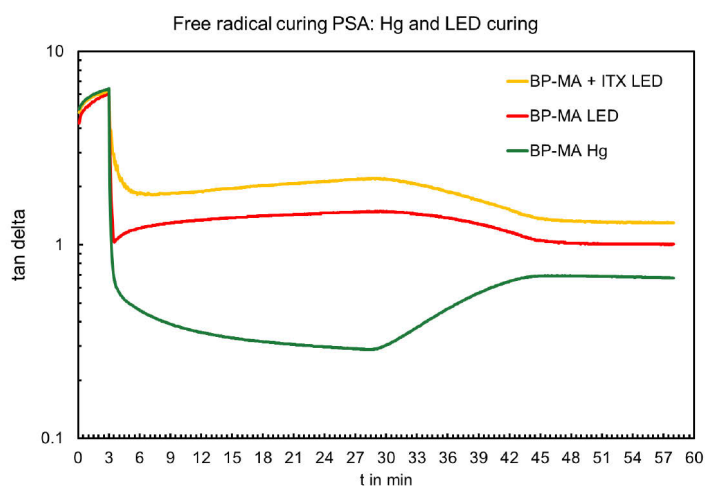
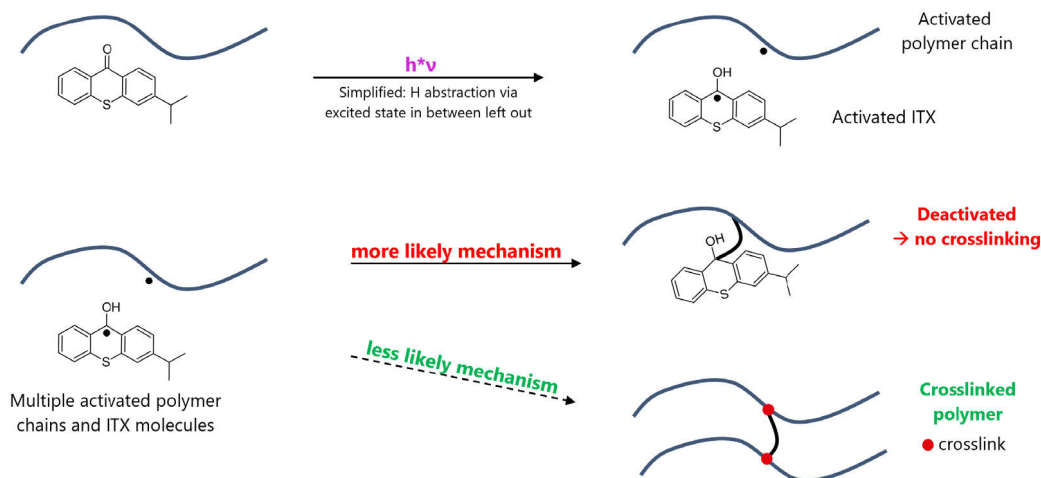


Figure 28: UV rheology of free radical curing PSA.

It could not be finally clarified why the BP-MA sample shows a slight increase in $\tan \delta$ after the first seconds. The sample has been measured several times and always showed the same curing profile whereby $\tan \delta$ first decreases and then slightly increases for a few seconds with stagnation following. Interestingly when adding an equimolar amount of ITX to the BP-MA sample, the curing speed is worse than of the LED cured sample without BP-MA (Figure 28, yellow curve). The initial decrease in $\tan \delta$ is slower and the final plateau of $\tan \delta$ is higher compared to the BP-MA LED sample

indicating a lower degree of curing. Generally, there are several potential reasons why this might be observed. In case of a potential sensitization effect (if there was one possible at all) of the ITX on the BP-MA it can be said that this cannot be seen, at least not beneficial for the curing reaction. A positive influence of the ITX onto the formation of activated chains via a hydrogen radical abstraction could not be observed either as this would increase the curing speed which could not be seen in the UV rheology. Now, it needs to be said that the ITX behaves very different to the BP-MA as the BP-MA is fixed to the backbone due to its copolymerization and the ITX can freely move around. Generally, the freely ITX should have a higher mobility inside the polymer matrix than the copolymerized BP-MA however mobility might not help here if the curing mechanism does not work as it is supposed to do. Assuming, that the BP-MA abstracts a hydrogen radical from a donor group (potentially polymer chain) after its excitement by the desired radiation, there is the formation of two activated centers.⁷ One activated position at the benzophenone itself with the radical on the original ketone carbon which is now an alcohol and one activated center at the position where originally the hydrogen was coming from. With that there is the formation of two activated positions on the polymer chain which might react with each other or with the other type of activated center, so there could potentially be the recombination of two original hydrogen positioned carbons or two benzophenone groups via the generated radical.

Taking the postulate further, that both polymer chains have the same molecular weight and length, the possibility for both chains is equal to find another recombination partner as every activated specie basically has the same mobility and reaction probability.



Scheme 11: competing mechanism when using a freely moving Norrish Type II photoinitiator

When applying this postulate on the freely moving ITX, the ITX is excited by its desired wavelength as well and abstracts a hydrogen radical from a donor group. Again, this donor group will potentially be a polymer chain.⁷ This leads to a freely moving activated ITX radical and a polymer chain with a radical on a suitable carbon because the hydrogen radical was abstracted. Clearly the ITX radical has a higher mobility inside the polymer matrix than the activated polymer chain just because of the huge difference in size and molecular weight. For a crosslinking and the formation of a cohesion to happen, it would be essential for two activated polymer chains to recombine with each other to build up a polymer network. Taking the factor of probability into account, which is mainly driven by mobility as the concentration of an activated ITX and an activated polymer chain should be identical, it is more likely to happen that an activated ITX radical will dominate the further reaction process. It could either recombine with a polymer radical or recombine with another ITX radical. Both reaction paths lead to no formation of a network and as a result no increase in cohesion. Further or longer irradiation would certainly not fix the problem as the ITX radicals which might be connected to the polymer chain now could not take part in another curing reaction again as they have been reduced to an alcohol. If the BP-MA sample is combined with the freely moving ITX, the ITX generally leads to a decrease in network formation because it basically quenches activated chains produced by the ITX

itself and the BP-MA. This leads to a worse performance in the UV rheology and with that no improvement of the overall system.

In addition to the UV rheology, the performance of all three samples has been measured as well to prove that the freely moving ITX does not support the polymer system when curing with a LED. The coatings have been done according to the procedure for the cationic curing adhesives while remaining at a thickness of 40µm (50gsm).

Table 5: Performance of free radical curing PSA; gel content

PI system / UV source	SAFT in °C	180° Peel in N/25mm	Gel in %
BP-MA Hg 50mJ	>200	18 (AF)	45
BP-MA LED 3000mJ	66 (CF)	28 (AF+CF)	30
BP-MA + ITX LED 3000mJ	32 (CF)	25 (CF)	0

As can be seen in Table 5, the performance supports the first results generated by UV rheology investigation. When switching from Hg curing to LED curing with the standard adhesive with only BP-MA inside, it can be observed that a low proportion of curing can be recognized as the adhesion shows a shared failure mode of not only adhesive failure but also cohesive failure, however, as it could be seen in the UV rheology, the curing is way too low for proper cohesion as the SAFT temperature is very low with a cohesive failure. The same can be seen in the gel values generated by soxhlet extraction with Ethylacetate. Whereas the standard adhesive cured with a mercury bulb reached 45% gel, the switch to LED irradiation with the same adhesive lowered the gel to 30%, which is acceptable but too low for a cohesive product and again might be completely gone when having a water white product due to even lower photon absorption. Introducing the freely moving ITX equimolar to the BP-MA into the same adhesive shows worse performance results as well, especially when compared to the BP-MA LED sample. This is exactly what could be seen in the UV rheology. The sample shows the lowest cohesion of all samples and a straight cohesive failure mode in peel tests. During the soxhlet extraction the complete adhesive could be solved in Ethylacetate leading to a gel content of 0%, fundamentally indicating a lack of curing.

Next all cured PSA samples have been investigated in a temperature sweep rheology measurement as well, complimentary to the measured performance. The setup was chosen identical to the setup used during the cationic PSA investigations.

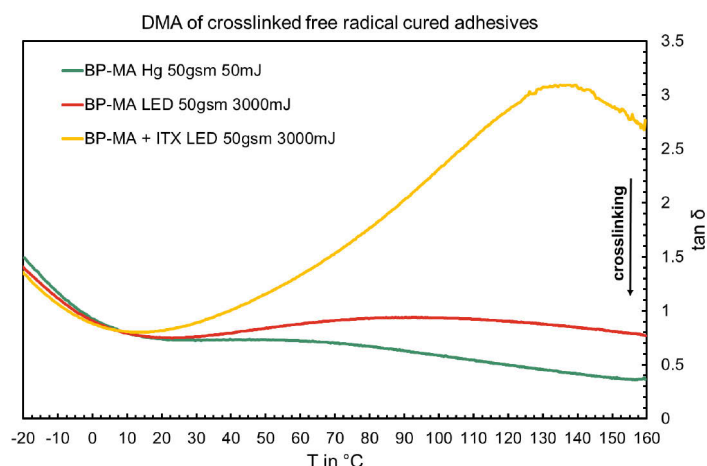


Figure 29: DMA of free radical cured PSA; temperature sweep

When comparing the samples in Figure 29 to each other a similar trend like to the former research can be noticed. The switch from mercury curing to LED curing in case of the standard sample with only BP-MA shows a reduced curing but still enables a cured product which cannot be molten anymore. The level of $\tan \delta$ stays below the sol-gel crossing point of $\tan \delta = 1$ indicating an elastic sample induced by network formation. However, this sample is not able to match the curing level of the achieved mercury cured reference sample (green curve). This could already be seen in a lower gel amount and lower cohesion in the SAFT test not to leave out the lower curing speed observed in UV rheology. What was already visible in the gel amount of the ITX formulated BP-MA sample can clearly be underlined by the DMA of the respective sample. During the temperature sweep no rubbery plateau occurs and $\tan \delta$ increases at elevated temperatures clearly indicating a melting process of the adhesive even though it has been irradiated with the LED. Again, this sample performs worse than the BP-MA LED cured sample without ITX as additive, which supports the overall investigation and the postulate of a hindered curing reaction by the mobile ITX radicals. In general, it can be said that the BP-MA sample cannot be LED cured sufficiently even though there is a curing responsiveness to the LED. However, this responsiveness is

not fast and efficient enough to produce a cohesively strong adhesive in a short time period resulting in a very inefficient curing process. The addition of ITX as additive to either sensitize the benzophenone or to advance the curing by itself has no advantage at all, on the contrary, it further slows the curing down. A copolymer made only from acrylic acid and butyl acrylate, formulated with ITX, has not been measured, as this would not have led to an overall improvement of the curing since the postulate of the ITX recombination would not be influenced positively. The fact that a freely moving Norrish Type II photoinitiator is not able to lead to an LED curable PSA even though the wavelength fits, underlines the importance of a copolymerized photoinitiator in the backbone of the polymer. This copolymerized photoinitiators not only adds advantages to the later product by reducing migration to a minimum and enabling special applications like food contact or medical applications, but it is also essential for the curing process of the overall adhesive.^{1-4,6}

Without being copolymerized, the crosslinking reaction is either slowed down tremendously or does not take place at all. The same might occur for the mercury cured BP-MA system. If the BP-MA was not copolymerized but a copolymer of acrylic acid and butyl acrylate was just formulated with the equimolar amount of benzophenone, there is a high chance that even the mercury cured system either loses curing efficiency or does not cure at all anymore. Exceeding this theory to Norrish Type I photoinitiators this could also explain why these photoinitiators cannot be expected to bring an advantage here as well and why they did not cure the cationic system via free radical mechanisms without even reacting with the TAS-Sb, which was possible. After the formation of a Norrish Type I photoinitiator radical the next step could only be a hydrogen radical abstraction as well as there must be a radical species on the polymer chains for proper crosslinking and network formation. However, even if this process takes place, again there is a competition of the activated polymer chain with a photoinitiator radical. As the Norrish Type I photoinitiator radical would be far more mobile again, compared to the activated polymer chain, the curing would be hindered as well. This highly supports the need for a copolymerizable photoinitiator which does not only take part in the solution polymerization with the respective acrylate side, but also absorbs at higher wavelengths like 365nm to enable LED curability for polymeric saturated acrylic PSA systems sufficiently.

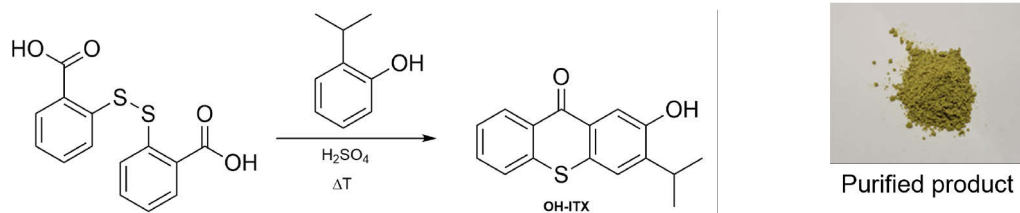
4.7 Polymerizable free radical LED photoinitiator

In order to be able to achieve an LED curable PSA which cures via a free radical crosslinking mechanism it is essential to have a polymerizable photoinitiator which could be proven in the chapter above. As there are no commercially available photoinitiators which could not only be copolymerized in a free radical solution polymerization with other acrylics but also showing a sufficient absorption at 365nm for proper LED curability it is necessary to design a new photoinitiator which fulfills these requirements. A polymerizable Norrish Type II photoinitiator would also match the potential for showing a very low migration potential and would also provide solid results comparable to the existing version based on BP-MA when speaking about the mechanism. Even though the freely moving ITX did not show sufficient curing in the chapter above, it might be a very interesting choice for modification to enable the potential being polymerized as the poor performance was mainly driven by the mechanism explained above. The absorption of ITX matches the 365nm LED wavelength perfectly and it showed high solubility in the system as experienced during earlier investigations.

To ensure that the copolymerization of the acrylics runs as smooth as possible it makes sense to move away from a methacrylate-based version to an acrylic version as this matches all the other monomers. As the production of most acrylics proceeds via the esterification of an acrylic acid derivative with a respective alcohol the commercially available ITX is not suitable for a direct modification.¹⁰¹ In a first step an alcohol functionalized ITX needs to be produced to make a later esterification possible.

The complete reaction mechanism of the thioxanthone synthesis has not been finally proven in academia yet, however, it could be confirmed that the mechanism runs via the disulfide based on thiosalicylic acid.^{102,103}

Step one



Step two

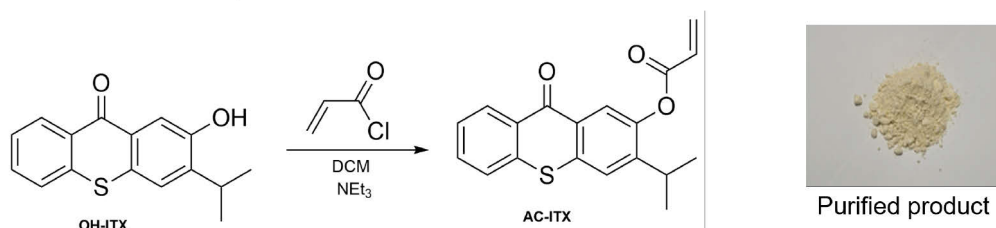


Figure 30: Overview of OH-ITX and AC-ITX; polymerizable LED photoinitiator

Based on that, the reaction has directly been started with the disulfide since it is commercially available. As a second educt the respective phenol derivative needs to be chosen. In this case in order to achieve the ITX an isopropyl phenol derivative was used. Inside the group of isopropyl phenol derivatives there are several isomers which could be used. The ortho version has been used as it is commercially available and in liquid form. This allows a smoother dosing step without any additional solvent or premixing with sulfuric acid compared to the solid derivatives. Depending on the choice of isopropyl phenol derivative the later, Acrylic ITX (AC-ITX) will have a different orientation of both the acrylic group and the isopropyl group.

It needs to be said that both steps of the synthesis have not been further optimized with regard to the yield and purity. This can mainly be explained by the fact that the priority was more put onto the synthesis of a potential working polymerizable LED photoinitiator than finding the optimum stoichiometry and reaction setup. Of course, there is a lot of optimization potential in both reactions, however, after the second step had been completed no negative impact of the 80% purity onto the second step could be observed. As the choice of Acryloyl chloride is highly depending on a water free system as much as possible there can be rather big error expected which not only

effects the yield but also the purity. Normally the esterification of alcohols with Acryloyl chloride nearly runs at 100% yield because of the high reactivity, however, this requires a completely water free and pre dried setup which has not been used for this study.¹⁰⁴ The remaining 15% impurity of the final product could be connected to 13% remaining OH-ITX (according to GC-MS) which could also be seen in the IR of the AC-ITX (Figure 31). Generally, this would have a negative influence onto a later copolymerization as the alcohol would lead to chain transfer reactions reducing the average molecular weight.⁸ However, it needs to be considered that only a very low amount of AC-ITX is used and with that approx. 100-200 ppm of alcohol can be expected as impurity. As standard commercially available acrylic monomers generally contain alcohol impurities because of the polymerization process this can be seen negligibly. When comparing the AC-ITX to the commercially available ITX in regard to their UV/VIS absorption it can be said that the modification by adding an acrylic functionality only led to a slight Bathochromic shift. This is important for the later processing of the photoinitiator and the finished adhesive as additional protection against visible light would make handling and packaging much more complicated.

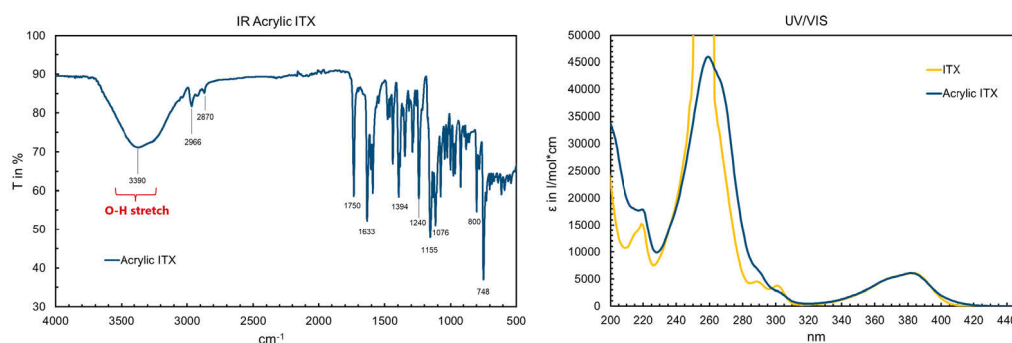


Figure 31: IR of Acrylic ITX; UV/VIS absorption spectrum compared to commercial ITX.

After the synthesis of an acrylate functionalized photoinitiator which also fulfills the absorption requirements it has been copolymerized according to the BP-MA based PSA. This means the BP-MA has been replaced equimolar by the AC-ITX, besides that everything else has been kept the same. During the polymerization no noticeable differences to the original product could be observed regarding the viscosity or glass transition temperature (Figure 32). The molecular weight distribution changed slightly due to the residual alcohol, however, did not affect the overall polymer tremendously.

Besides that, the adhesive showed up in a different yellowish color which can not only be connected to the inhibitor theory explained earlier above, but also to the fact that the AC-ITX has an absorption which reaches up to 415nm. Even though there is a tiny absorption into the visible region it could not be observed that the product acts unstable during the polymerization and the processing steps after that while operating under normal lab light, so there was no need to switch to special lab lights.

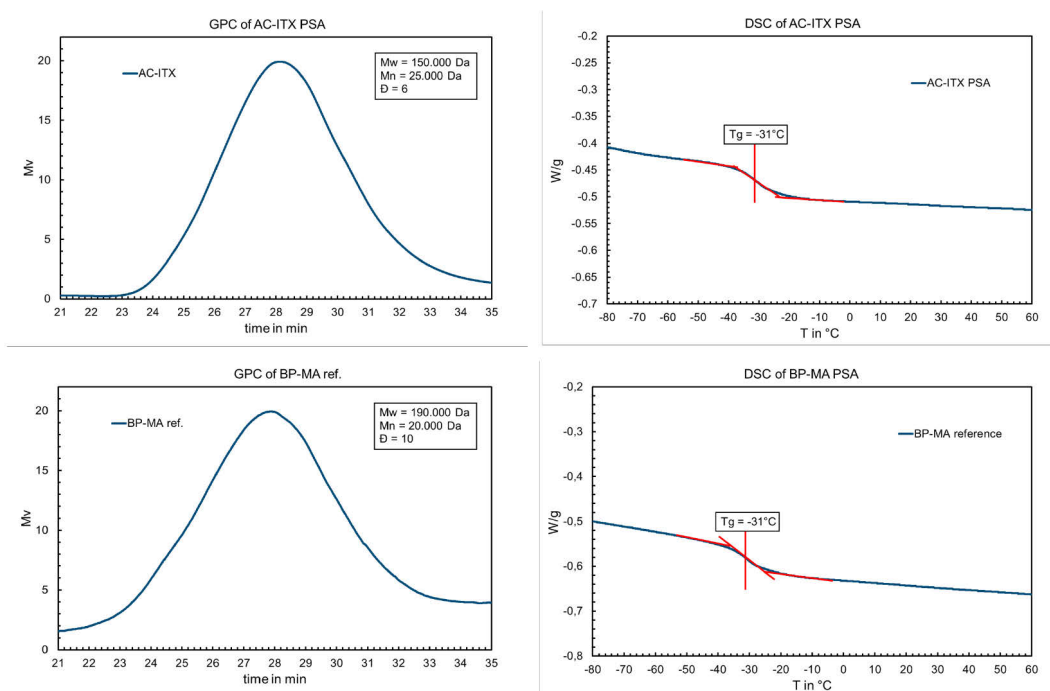


Figure 32: GPC and DSC of AC-ITX modified PSA polymer compared to Hg reference

As a first step to verify any impact onto potential improvement in LED curability, UV rheology has been measured according to the same methodology used before. As can be seen in Figure 33, the equimolar switch from BP-MA to AC-ITX has a fundamental impact on the curability with a 365nm LED. It clearly can be seen that the sample with the copolymerized ITX cures much faster than the LED cured sample of BP-MA and the modified sample with the freely moving commercially available ITX. The initial decrease in $\tan \delta$ occurs very rapidly, well below the sol gel crossover point and the final reached plateau of $\tan \delta$ when measuring at the rubbery plateau is the lowest of all LED cured samples, indicating the best crosslinking of the LED samples. Even though it appears that the AC-ITX sample even cures further than the mercury cured BP-MA reference

at the beginning, it looks like this is a reversible effect as $\tan \delta$ increases slightly again. Even after several measurements with different material, this phenomenon could still be observed and it could not be clarified why this occurs. It might be that shrinking effects play a role, but this could not be confirmed. Following that, it can already be seen that the switch from a freely moving photoinitiator (ITX) to its polymerizable version has a big influence on the curing kinetics without changing any other aspects like absorbance, type of photoinitiator mechanism and molar amount used.

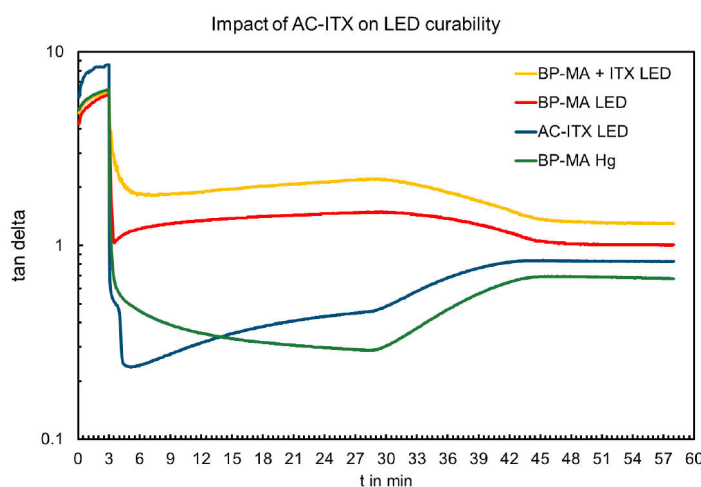


Figure 33: Impact of AC-ITX on LED curability of free radical curing PSA.

To verify if the positive impact of the AC-ITX can also be observed in the adhesive, the performance has been measured according to earlier procedures and is compared to the performance measured in Table 5 earlier above. As can be seen in Table 6, the introduction of AC-ITX to the copolymer lead to a fundamental improvement in performance as well. When using AC-ITX as copolymerized photoinitiator in an equimolar amount to BP-MA used before, the cohesion increases to a SAFT of 140°C while failing cohesively. The adhesion on steels shows a residue free adhesion failure indicating a further cured product than before. With the freely moving ITX in comparison, there was no cohesion visible as shown in the DMA in Figure 34 and 0% of gel content was found as displayed in Table 6, whereas the AC-ITX sample now has a gel content of 60%, which is even higher than the mercury reference. Here it needs to be said that the overall performance not only depends on the amount of gel produced during the crosslinking step but also on the network and its density itself, similar to

the observations achieved during the investigation of cationic curing PSA earlier above. With that it can be explained why a sample shows a worse cohesion while having a higher gel amount than a sample with lower gel amount which shows a higher cohesion level. The sample having the higher cohesion, but lower gel amount, most likely has a denser network. As mentioned before, the effect of the network and its contribution to mechanical properties might vary over the surface area as the network does not occur homogeneously regarding the mesh size and molecular weight between crosslinks for the same polymer sample.¹⁰⁵ However, as the PSA is tested on a quite wide surface area or length at the same time this potential inhomogeneity can be neglected in this case and a statistical decrease in mesh size can be expected.

Table 6: Impact of AC-ITX onto the PSA performance

PI system / UV source	SAFT in °C	180° Peel in N/25mm	Gel in %
BP-MA Hg 50mJ	>200	18 (AF)	45
BP-MA LED 3000mJ	66 (CF)	28 (AF+CF)	30
BP-MA + ITX LED 3000mJ	32 (CF)	25 (CF)	0
AC-ITX LED 3000mJ	140 (CF)	20 (AF)	60
AC-ITX (+50%) LED 3000mJ	>200	16 (AF)	60

The performance of the PSA with the newly synthesized photoinitiator shows a better LED curability than the BP-MA sample cured with LED, which underlines the fact that the absorption pattern of the ITX based photoinitiator better matches the wavelength of the LED and in addition to that supports the postulate how essential it is to have the photoinitiator copolymerized in this special case. Now, the difference between the ITX sample and the AC-ITX sample is only connected to the fact that one sample has a freely moving photoinitiator and the other has a copolymerized photoinitiator of the same chemical class. Since there is a fundamental distinction in curing kinetics and PSA performance as well, this highly supports the theory established earlier as both photoinitiators work via the same mechanism and share the same absorption. Nevertheless, the switch to an equimolar amount of AC-ITX still did not lead to the same cohesion as the mercury cured BP-MA reference when speaking about SAFT. Potentially this could be achieved by using a higher UVA dose but as established in previous studies in this study this would affect the belt speed negatively again. When

changing from mercury bulbs induced UVC irradiation to LED induced UVA irradiation with a free radical curing adhesive system, the potential for oxygen inhibition needs to be considered.^{19,20} As the UVC irradiation produces ozone as a side product this can be seen as highly efficient in reducing the oxygen inhibition. However, when using a 365nm LED this effect does not take place anymore as there is no ozone generated anymore.¹⁰⁶ In this case there are several potential ways in reducing the oxygen inhibition which is mainly a surface effect driven by the oxygen diffusion potential. One would be inclined to use a Nitrogen blanket over the coating while irradiating so there is no oxygen during the curing process, however, this is not easy to achieve and requires different machine setups in industrial coating processes. Two other alternatives in order to achieve an impact of the adhesive composition would be to increase the photoinitiator amount or to use a synergist which reduces oxygen inhibition chemically.^{19,20}

As a first step the amount of AC-ITX in the copolymer has been increased by 50% and the same curing dose was used. This sample was able to achieve the desired performance which is very similar to the mercury cured reference as shown in Table 6. The SAFT increased to the right level and the adhesion decreased slightly, indicating a further cured product also in deeper layers and not only at the surface where oxygen mainly quenches radicals.^{19,20} In this case the gel amount stayed the same, again potentially driven by the fact that the network itself got denser but did not increase in overall size which still leads to a higher elastic modulus. When comparing all samples in the DMA, this effect could also be recognized as shown in Figure 34.

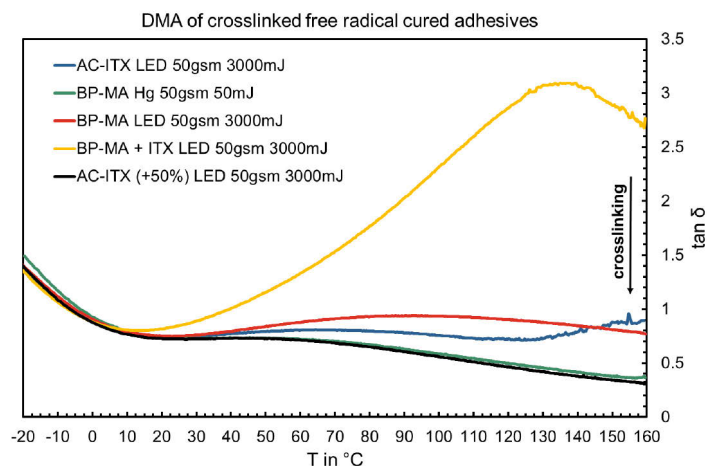


Figure 34: DMA of free radical curing PSA

Comparing the DMA samples with each other, the difference between the freely moving ITX and the copolymerized ITX is magnificent. Even using an equimolar amount of AC-ITX according to the BP-MA amount led to a high improvement in crosslinking potential with a LED, whereas the sample with the same amount of freely moving ITX did not show any curing at all. The sample with the equimolar amount of AC-ITX shows a cohesive behavior until it reaches 130-140°C. When reaching this area tan δ starts increasing again slowly which indicates the starting point of a further melting process which is completely in line with the measured SAFT value where 140°C was the maximum temperature to be achieved by this sample. At this stage the polymer chains increase their mobility tremendously and the sample fails cohesively. Increasing the AC-ITX amount by 50% while keeping the UVA dose at 3000mJ shows a completely cohesively strong PSA which does not show any similar melting process up to 200°C when the measurement of the DMA stops. In fact, this sample shows a perfect matching DMA when comparing to the mercury cured reference with BP-MA copolymerized.

4.8 Reducing oxygen inhibition of free radical PSA

Whereas increasing the photoinitiator amount has a direct influence on not only the surface curing of the adhesive but also on the degree of curing in deeper layers, the usage of synergist focuses on the oxygen inhibition mechanism itself.¹⁹ Since oxygen inhibition mainly occurs at the surface it should not have a fundamental impact on the overall performance of the adhesive but mainly on the adhesion of the side which is facing the LED. Potential synergists which could reduce oxygen inhibition are (poly)ethers, thiols, alcohols and amines.^{19,107} In this case a urethane derivative which could be copolymerized as well has been tested. This is especially important as the migration should be kept at a minimum level and it would not make sense to use a polymerizable photoinitiator, not only for being able to cure the system but also to move towards a low migration system and combining it with a freely moving synergist with a high risk of migration. As thiols and alcohols would have a fundamental influence onto the copolymerization of the adhesive and (poly)ethers can be seen as the most inefficient synergist for reducing oxygen inhibition, they have not been considered for this investigation.^{19,107}

An equimolar amount of VMOX as synergist regarding the molar amount of AC-ITX has been copolymerized together with the other monomers used earlier above (Details can be found in the experimental section). To be able to investigate the surface effect of the synergist the coating process needs to be adapted slightly. For all earlier investigations the coatings have been made as transfer coatings, where the light facing side was laminated against etched PET later. However, for measuring surface effects on the light side the coatings have been directly made on etched PET foil, cured and laminated against a silicone paper. Following that, the light facing side could be stucked onto a test substrate and differences could be investigated. To make sure that the percentage of the surface is only rather small compared to the overall adhesive thickness it makes sense to increase the coat weight to 100gsm. Now it is easier to connect a measured effect only to the surface.

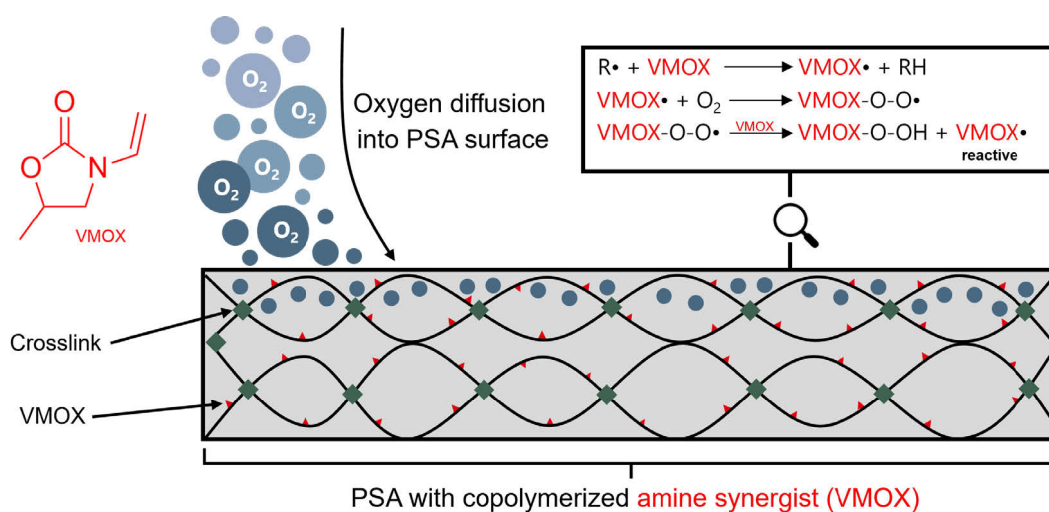


Figure 35: VMOX, used as copolymerized synergist against oxygen inhibition.

If the synergist reduces the oxygen inhibition the measured peel value and with that the adhesion of the surface should be lower compared to the reference without synergist. Occurring oxygen inhibition leads to a lower crosslinking at the surface following which the adhesion is being pushed to higher levels. It is still possible that the respective sample shows an adhesion failure, but it could also move more towards a mixture of adhesion and cohesion failure if not a complete cohesion failure. The lower curing degree of the surface can also lead to worse resistance against environmental aspects over the time in comparison to a well cured surface as the lower crosslinking density at the surface improves migration of e.g., water or solvent depending on the application of the PSA. As shown in Table 7, the implementation of VMOX as synergist to reduce oxygen inhibition led to a noticeable change in adhesion performance of the light facing surface. Both adhesives have been coated to the same thickness and the same UVA dose has been used for irradiation. When comparing the peel values with each other it stands out that the surface of the adhesive with VMOX as synergist inside is further cured than the surface of the adhesive without synergist. The peel adhesion could nearly be halved by an equimolar amount of VMOX as synergist regarding the photoinitiator amount. While the effect of the VMOX on surface curing characteristics shows an outstanding difference, a possible impact on cohesion as well cannot be displayed by the performance tests alone. This can be explained by the fact that both

samples reached the maximum SAFT and the gel content is comparable. However, it is still possible that one of the gels has a higher crosslinking density than the other one.

Table 7: Impact of VMOX on surface curing; 100gsm coatings

Adhesive / curing	SAFT in °C	180° peel in N/25mm	Gel in %
AC-ITX LED 3000mJ	>200	24 (AF)	58
AC-ITX + VMOX LED 3000mJ	>200	14 (AF)	54

To further understand the impact of the VMOX on the whole adhesive system and not only with regard to the surface, a DMA of both samples has been executed (Figure 36). When comparing both samples in a temperature sweep no noticeable difference can be seen which supports the fact that the impact of VMOX only occurs at the surface facing the irradiation, which was expected for a synergist to reduce oxygen inhibition. Oxygen inhibition only occurs at the very top of the coating which makes only a few percent of the overall thickness.^{19,107} As the adhesive is coated and irradiated at 100-130°C due to the hotmelt application process, this further limits the solubility of oxygen inside the adhesive, supporting the fact that only the top layer is affected.¹⁰⁸ This process is enough to have a fundamental impact onto the adhesion of the adhesive as the top layer has a higher chain mobility and can form a stronger bond to the surface via different adhesion theorems.

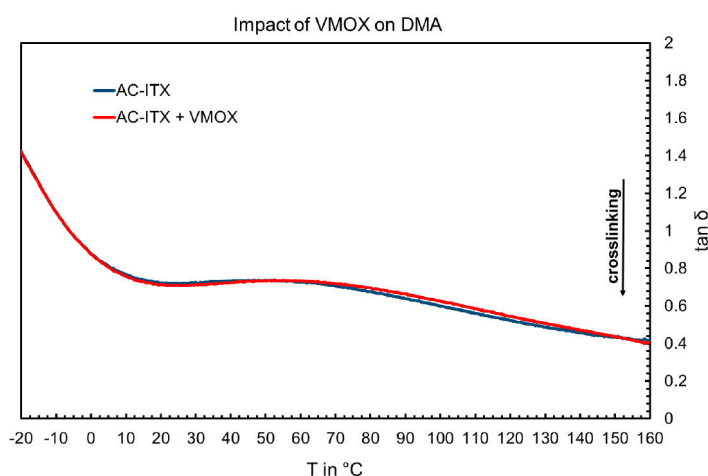


Figure 36: Impact of VMOX as synergist on DMA

However, when testing the whole adhesive over the complete cross section via DMA, the percentage of the top layer is very low in comparison to the rest of the adhesive. This explains why the effect of VMOX cannot be seen in the DMA and a consequence cannot be seen in the cohesion of the PSA as well, but only in adhesion tests of the light facing surface. Bearing that in mind, the addition of VMOX cannot be seen as a curing enhancer but only as a surface effecting synergist which especially plays an important role when having adhesives of high thickness and in case the light facing side is bond to the later substrate. With the combination of an increased AC-ITX amount and VMOX as synergist to reduce oxygen inhibition it is possible to produce a LED curable adhesive based on a free radical curing mechanism. With the learnings generated during the tests with the cationic LED curing PSA on an industrial pilot coater, belt speeds of approx. 20m/min for a 50gsm coating can be expected. This is comparable to mercury curable UV PSA, in fact while the switch to LED technology saves energy and reduces the total cost of ownership. Since the AC-ITX can be copolymerized like the BP-MA an adhesive with low migration characteristics can be expected, where food contact and medical applications are certainly possible after adequate testing has been done. The potential of upscaling the AC-ITX to an industrial scale to achieve commercial availability can be judged as very promising as both steps of the organic synthesis are already established in the industry, especially for thioxanthone suppliers and acrylic monomer suppliers. To enable a LED curable hotmelt PSA which shows the needed performance, especially cohesion generation in a short time scale and it also has the potential to fulfill low migration standards, the investigations and tests have shown that it is essential to stick to a copolymerizable photoinitiator. Even when leaving the low migration potential aside, the comparison of ITX versus AC-ITX has shown that from the perspective of the curing mechanism a freely moving photoinitiator rather tends to harm the curing instead of leading to an acceptable curing level. The postulate of curing mechanism established during the investigation could be supported by switching to a copolymerized photoinitiator. A simple addition of a LED suitable photoinitiator, irrespective if it is a Norrish Type I or Norrish Type II photoinitiator, did not achieve the status of an LED curable hotmelt. These kind of photoinitiators are expected to only work with unsaturated, monomeric to oligomeric systems where acrylic groups can be cured.

However, this type of curing cannot be used with a hotmelt system due to temperature instability. In a hotmelt system in which comparable high viscous polymer chains need to be networked via hydrogen radical abstraction reactions, the addition of such a photoinitiator potentially only works up to the step where the hydrogen radical is abstracted but after that the high mobility of the freely moving photoinitiator radical predominates the following reaction steps. Following that, the chance for a recombination of two activated polymer chains is rather low and the network formation either takes place very slow or not at all. Both cases are not acceptable as fast curing is essential for an industrial coating process where the time scale of irradiation is <1 s. With the copolymerization of AC-ITX the same reactivity and absorption like with the ITX can be expected, however, in this case there is no competition between a fast-moving photoinitiator radical and a less mobile polymer radical. After the activation of AC-ITX by the LED only AC-ITX radicals and polymer chain radicals generated by a hydrogen abstraction process are generated. Both types of radicals are located on a polymer chain, so no matter which recombination is favored, the following reaction will lead to a crosslinking reaction and network formation. Now it is possible to achieve a high cohesive PSA even when the time scale of irradiation is very low.

4.9 Migration study on AC-ITX

Switching from a freely moving ITX to a copolymerized ITX via the implementation of AC-ITX enables a LED curable PSA with an outstanding adhesive performance completely comparable to the mercury bulb cured reference adhesive. Since the new photoinitiator is copolymerized, not only the curing mechanism is promoted, but also a lower tendency regarding migration of the photoinitiator is expected. To investigate if this can be proven, migration studies on this system have been done, compared to a system with an equimolar amount of commercial ITX which can move around freely inside the polymer matrix according to the amount used earlier in this thesis (AC-ITX = 0.5w%). Of course, in the end the reference system will be an uncured adhesive but from the perspective of photoinitiator reactivity with photons, they can be seen

identical as there is no fundamental difference in the thioxanthone structure of ITX and AC-ITX.

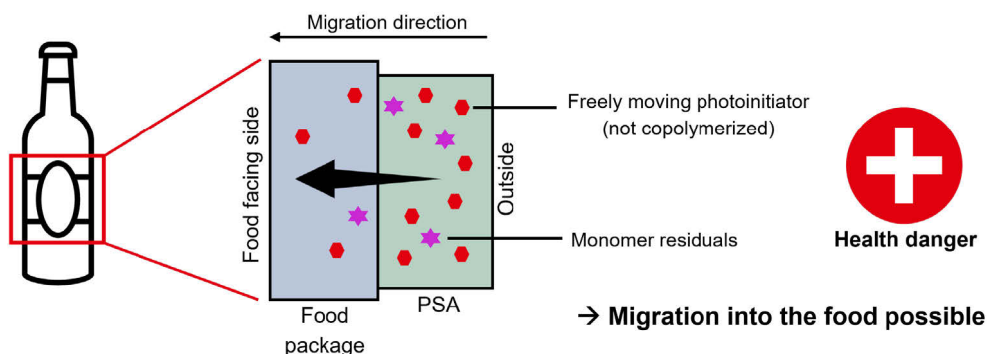


Figure 37: Possible migration process for photoinitiator and monomer residuals in food packaging

The test conditions have been used according to EU regulatory standards.¹⁰⁹ As can be seen in Table 8, five different scenarios have been simulated. In detail, 3% Acetic acid and 10% Ethanol as test solution simulate the contact to hydrophilic food or drinks.¹⁰⁹ Furthermore, 95% Ethanol solution simulates the contact to lipophilic food and Tenax, a polymer with defined pores made of Poly(2,6-diphenylphenylene oxide), which simulates the contact to dry food.¹⁰⁹ In addition to that the NaCl solution is used as indicator for migration to skin which explains why this test is conducted at 37°C.¹¹⁰

Table 8: Migration test conditions and results

sample	condition	ITX in $\mu\text{g}/\text{dm}^2$	OH ITX in $\mu\text{g}/\text{dm}^2$	AC-ITX in $\mu\text{g}/\text{dm}^2$
Adhesive with free ITX (equimolar to AC-ITX)	3% Acetic acid 10 d, 60°C	<0.5	-	-
	10% Ethanol 10 d, 60°C	1.7	-	-
	95% Ethanol 10 d, 60°C	3400	-	-
	Tenax 10 d, 60°C	2000	-	-
	0,9% NaCl 72 h, 37°C	<0.5	-	-
Adhesive with AC-ITX (0.5w%)	3% Acetic acid 10 d, 60°C	-	<0.5	<0.5
	10% Ethanol 10 d, 60°C	-	<0.5	<0.5
	95% Ethanol 10 d, 60°C	-	240	<0.5
	Tenax 10 d, 60°C	-	3	<0.5
	0,9% NaCl 72 h, 37°C	-	<0.5	<0.5

When comparing both adhesive systems with each other, it turns out that the migration behavior for each sample is completely different. The copolymerized photoinitiator AC-ITX was not found in any of the test solutions, supporting the fact that this monomer shows high reactivity in the solution copolymerization with other acrylics which could already be seen during the performance test during which this molecule led to a fundamental change. As outlined further above, this type of photoinitiator should show low migration which could be proven in this migration studies through a variety of different test conditions. However, the OH-ITX impurity was found in two test solutions (95% Ethanol and Tenax) after 10 days at 60°C. Of course, this cannot be recognized as positive but first the amount which was found is rather low and second, it needs to be considered that an improved synthesis process for the synthesis of AC-ITX would lead to a much purer AC-ITX without OH-ITX, whereas in the AC-ITX used in this investigation 15% of OH-ITX was found as demonstrated earlier above. The migration study shows that contrary to expectations, the OH-ITX did not fully take part in the solution polymerization although for being an alcohol it could theoretically act as a chain transfer agent.⁸ Improving the synthesis with a purer product could be done by using fresher Acryloyl chloride, working as water free as possible and improving the process of product purification after the synthesis, e.g., by chromatography. Comparing the test results to the standard which contains an equimolar amount of ITX with regard to the AC-ITX, as expected the migration is much worse. Especially in a 95% Ethanol and Tenax solution, simulating the contact to lipophilic food and dry food, a high amount of ITX has been found with up to 3400 µg/dm². Since the limited value of the maximum allowed ITX amount where ITX is stated as harmless is legally set to 50 µg/kg of food, this value can easily be exceeded.¹¹¹ Therefore, this type of PSA, even if it showed sufficient performance, could not be used in food contact applications as it would not have been legally allowed. Even though both systems did not show a migration tendency in sodium solution, the usage of the ITX system in medical applications with skin contact still should not be considered. This is connected to the fact that lipophilic cremes could theoretically get in contact with the PSA on the skin and dissolve ITX out of it. Especially medical applications should only be taken into consideration if overall general substance migration is very low.

Finally, this test underlines once again how important it is to have a copolymerized photoinitiator not only from the perspective of curing kinetics and adhesive performance but also from perspective of safety in essential application areas for the packaging industry like food contact or medical applications. The implementation of AC-ITX enables a safer PSA which not only shows high LED curability but also low migration tendency. Since the photoinitiator material used in this migration test is coming from an unoptimized lab synthesis, the migration tendency of a photoinitiator coming from a well optimized synthesis in industrial scale can be expected even lower, since impurities are minimized, which were responsible for the observed migration in the AC-ITX sample and not the AC-ITX.

4.10 Silane promoted cationic curing PSA

In a best-case scenario, the implementation of silanes leads to a much faster curing reaction of cationic PSA without changing the epoxy functionality by adding more EPOMA. The increased curing speed could be used to lower the viscosity of the overall PSA polymer, for instance by a reactive diluent, and to enable the application of the hotmelt at a lower temperature which would also save energy during the industrial coating process. This would enable a completely new PSA type to which new applications might be possible.

Different silanes which are commercially available have been chosen and will be benchmarked against each other. Their influence on curing speed, temperature stability and adhesive performance will be investigated. The silanes are shown in Figure 38.

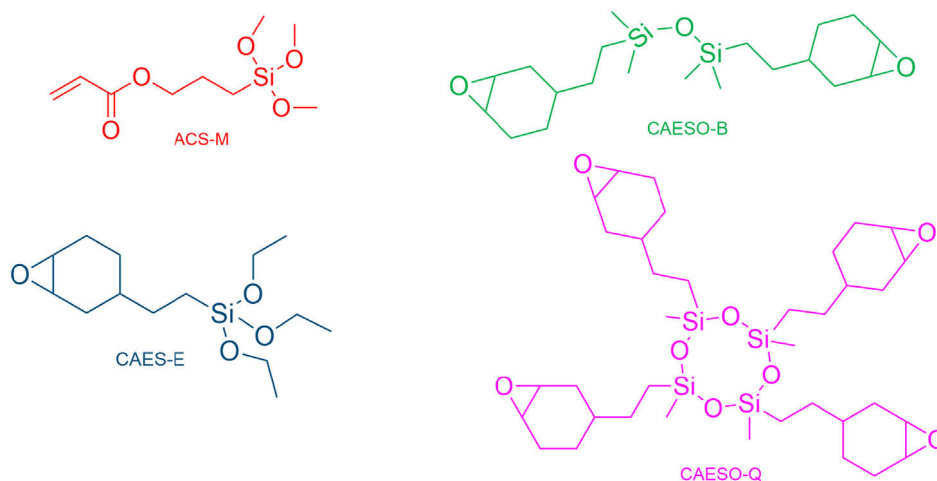


Figure 38: Overview of investigated silanes and siloxanes

As can be seen in Figure 38, different types of species are being tested. The ACS-M will be copolymerized together with other acrylics for the synthesis of cationic curing PSA. Worth to mention it is based on a trimethoxy silane which are known for being the fastest curing silanes as not only the length of the spacer but also the size and amount of potential leaving groups influence the silane curing rate.^{112,113} CAES-E however is based on a triethoxy silane, here it needs to be said that there is also a trimethoxy version commercially available, but as this substance is listed as CMR substance it is not possible to use it for PSA applications without major drawbacks. The remaining CAESO-B and CAESO-Q are not directly comparable silanes to the other two species as they are siloxane based and can only act as mobile epoxy crosslinker but not as latent hydroxy functionality producer via the alcohol separation as there is no possibility for an alcohol abstraction.

In order to be able to compare the different silanes and siloxanes with each other, they have been used in an equimolar amount as the EPOMA in chapter 3.1 of this thesis and also with a focus on the functionality. The amount of EPOMA in the cationic curing polymer was kept the same and e.g., an equimolar amount of ACS-M has been copolymerized as well. In case of both siloxanes the molar amount has been calculated with focus on the epoxy amount. Here the same amount of cycloaliphatic epoxy has been compared to each other (details can be found in the experimental part). During the implementation of ACS-M into the solution copolymerization of cationic PSA no

anomalies have been observed. The other tested silanes showed excellent solubility inside the cationic curing polymer. Of course, all epoxy silanes have only been tested in an ACS-M free cationic curing polymer which only consist of MA, 2-EHA and EPOMA. As the impact onto the curing speed is of main interest in order to modify the PSA further, UV rheology was taken as first test method as any impact onto the curing kinetics would be directly visible here.

All samples have been added with the same amount of TAS-Sb as cationic photoinitiator and ITX as sensitizer for better curability with a 365nm LED, which are also in line to earlier investigations in this research. All samples have been tested according to the test method explained earlier above. The coatings have been made from a solution again to check temperature stability of all formulations separately.

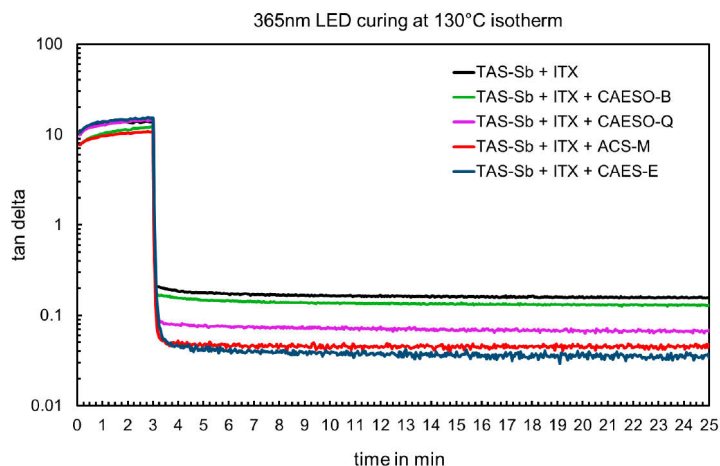


Figure 39: UV rheology of silane modified PSA compared to reference

As can be seen in Figure 39, the addition of silane-based components has a direct influence onto the curing kinetics of cationic curing PSA. Compared to the reference shown in black, most of the added species improved the curing speed. Only the addition of the bifunctional siloxane CAESO-B did not lead to a fundamental change in the curing speed. The quarter functional CAESO-Q, compared to CAESO-B, showed a bigger influence and led to faster curing even though the overall epoxy amount was kept the same in both samples. The level of $\tan \delta$ the CAESO-Q reaches in the same amount of time compared to CAESO-B is much lower, indicating a higher degree of crosslinking.

Needless to say, that the quarter functional siloxane can much better act as a crosslinker and build up a bigger network faster because of the higher functionality. This could explain why the increase in elastic modulus happens faster compared to the bifunctional siloxane. Following that, the overall decrease in $\tan \delta$ occurs much faster. The silane additives which can abstract an alcohol as leaving group after the reaction with the proton produced by the photoacid show the biggest influence onto the curing kinetics of all PSA samples. Here the observed curing takes place very rapidly and the difference to the non-modified version displayed in black in Figure 39 is extremely. This can be explained by the fact that the silanes not only act as crosslinker but also the generated hydroxy groups are able to move the reaction mechanism to an AMM leading to a faster curing rate due to transfer reactions in a controlled amount. The silanes can take advantage of humidity inside the surrounding air by starting a further crosslinking reaction and separating a controlled amount of alcohol. Without silanes the humidity could be seen as a black box, as a small amount of water still would move the reaction to an AMM, but a higher amount would terminate any further reaction. Of course, the silane modified PSA would also be terminated in its crosslinking reaction when a very high water level is reached but in contrast to the non-silane modified version there is another crosslinking possibility generated when an acceptable amount of water is present.

Since the bifunctional siloxane CAESO-B did not show a fundamental impact onto the curing kinetics it has been sorted out from further investigations. From all the other samples the solvent has been removed in a rotary evaporator under reduced pressure at 120°C to investigate any temperature stability issues before moving on with the investigation. It was found that the samples with CAES-E and CAESO-Q remained stable during the stripping process and also no noticeable change in hotmelt viscosity has been found over 24h at 120°C. However, the sample containing the copolymerized ACS-M did get through the solvent stripping process, however, this sample showed rapid gelation occurring during the 24h stability test at 120°C in a Brookfield viscosimeter. Also several new trials failed and the samples remained unstable. It might be based on the fact that the ACS-M is based on a trimethoxy based silane having the highest reactivity of silane species, compared to the triethoxy based CAES-O, leading to a fast reaction with humidity and starting a crosslinking reaction of polymer chains.

Even though there are commercially available versions of the acrylic silane based on a triethoxy modification, the raw material price is much higher than the one of the ACS-M, exceeding the possible price range for packaging applications.

As a next step, the PSA has been further modified with a reactive diluent to reduce viscosity but stay at a high reaction level and with that a high degree of curing. Since the viscosity of the system should be lowered without the drawback of reactivity, the addition of a tackifier in the required amount would certainly lead to the desired viscosity, however, the overall cohesion would decrease as the tackifier does not take part in a crosslinking reaction and loosens the entanglements of polymer chains. In contrast to that the addition of oligomeric epoxy components would not only reduce the overall viscosity but such components would also be able to take part in a later crosslinking reaction induced by UV and the epoxy reactive diluent would also benefit from the silane components. There are hundreds of different epoxy oligomers on the market, some of them based on fossil feedstock but also some based on natural feedstock.^{114,115} As commercial availability is a key fact again, the commercially available natural based epoxies have been compared to three epoxies based on a fossil feed stock.

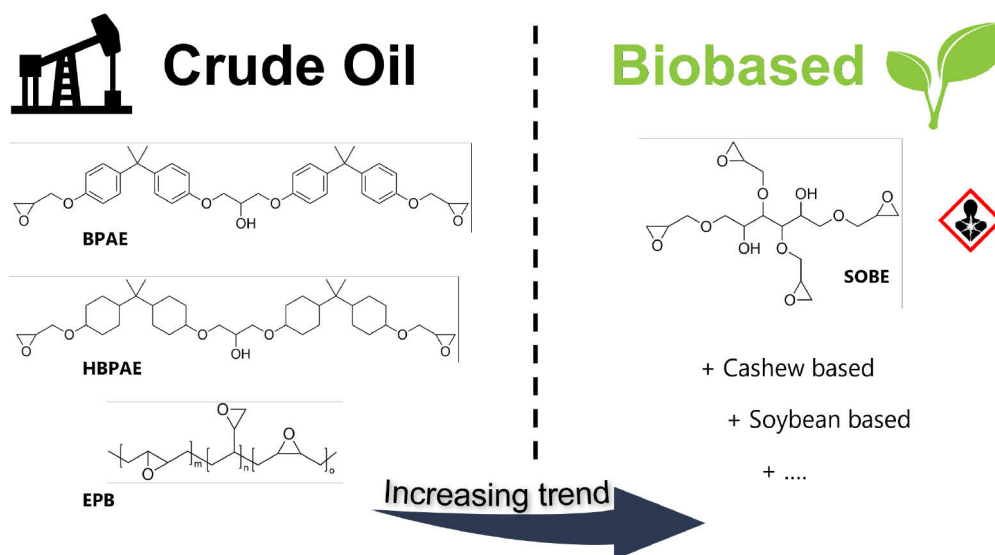


Figure 40: Overview of potential epoxy reactive diluents and their origin

As can be seen in Figure 40, there are two main classes of commercially available biobased epoxy reactive diluents, one of them based on sorbitol and the other product class based on cashew nuts.^{116,117} The first compatibility test resulted in the fact that the epoxy resins based on cashew nuts showed very poor solubility inside the acrylic polymer matrix which led to a direct exclusion from further developments. The sorbitol-based epoxy showed very good compatibility inside the acrylic PSA, however, due to manufacturing process of the epoxy impurities of toluene can be found inside the product leading to a CMR classification by the suppliers. Until the day of this thesis, there were no CMR free epoxy versions based on sorbitol commercially available on the market. As the labeling of a reactive diluent is crucial for the complete hotmelt labeling, a CMR classification unfortunately leads to a direct elimination from further investigations as well. This leads to the fact that the epoxy reactive diluent was chosen from fossil feed stock as there was no bio-based alternative. The fossil based BPAE based on Bisphenol A and the partly epoxidized polybutadiene EPB showed excellent compatibility inside the acrylic polymer, whereas the hydrogenated HBPAE showed bad compatibility inside the matrix. The Bisphenol A content in BPAE was determined at 20ppm, epichlorohydrin could not be detected. In order to significantly decrease the viscosity of the PSA hotmelt 15w% of epoxy reactive diluent have been added to the hotmelt PSA containing CAESO-Q and CAES-E. Both silane-siloxane components will now be combined to get the most out of the curing speed. Indeed, the CAES-E showed the best impact onto the system, however, it is expected that increasing the amount excessively would lead to a reduction in curing speed as the hydroxy number gets too high leading to far too many termination reactions and it is likely to influence the VOC of the overall adhesive negatively as not all the separated ethanol can be expected to take part in the AMM. The photoinitiator system has been kept the same as before, TAS-Sb has been used as cationic photoinitiator and ITX as LED sensitizer. The amount of photoinitiator and sensitizer has not been changed compared to other chapters above. Both samples have been coated to 80µm (100gsm), irradiated with a 365nm LED and the performance has been measured according to the test procedures which are described in detail further above. The results are displayed in Table 9 below.

Table 9: Performance results of epoxy-silane modified PSA against reference

sample	Curing dose in mJ	SAFT in °C	180° peel in N/25mm on steel
Hg reference	100 (UVC)	>200	20 (AF)
LED reference	3000	70 (CF)	30 (CF)
BPAE	3000	>200	23 (AF)
EPB	3000	82 (AF+TF)	17 (AF)

First, Table 9 displays, that the newly modified PSAs have much higher cohesion than the non-modified LED cured adhesive cured with the same UVA dose. On the one hand this underlines the fact that the addition of silane and siloxane components increases the curing speed, level of curing and with that the cohesion of the adhesive but on the other hand it can also be seen that the addition of an epoxy reactive diluent did not lead to a complete drop in cohesion again. However, when screening the EPB modified sample, it shows out that this sample behaves rather overcured than undercured as it fails the cohesion test with an adhesion failure at 82°C instead of reaching 200°C like the BPAE modified sample. The EPB sample has been tested several times again, however, the same failure pattern could be observed all the time.

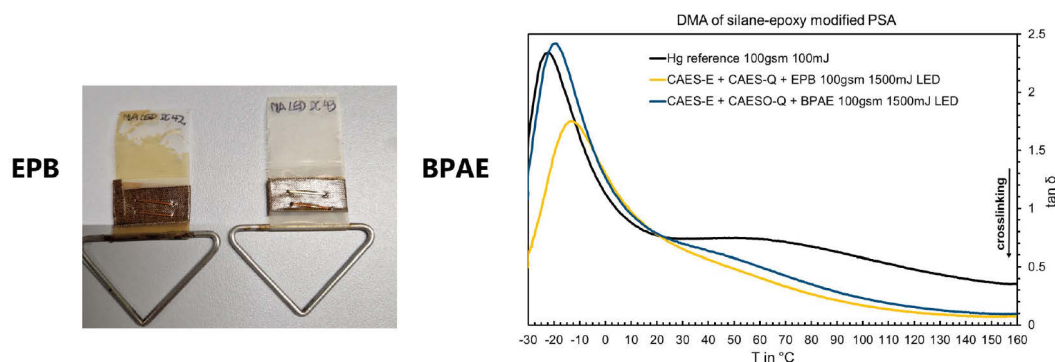


Figure 41: SAFT samples after the test

Besides that, the sample containing EPB changed its color from transparent to yellow during the test as can be seen in Figure 41. Combined with the observed overcuring it seems that the sample aged rapidly during the increased temperature. This can be explained by the fact that the EPB is only partly epoxidized and the remaining double bonds are not hydrogenated leading to the fact that temperature driven crosslinking

of double bonds occurs. Following that, the sample crosslinks even further during the cohesion test and loses adhesion during the time. This results in the adhesion failure observed at 82°C and a yellowish sample.

As well as conspicuities within the cohesion performance test also differences in the DMA could be observed for the EPB sample as can be seen in Figure 41. It shows significantly, that even without conducting a more precise test like DSC for the T_g determination that the T_g of the EPB modified version increased even though the T_g of the used epoxy is well below room temperature. In addition to that both samples, the EPB and the BPAE sample, show a higher degree of crosslinking than the mercury cured reference sample, underlining again the fact that the addition of the epoxy reactive diluent does not weaken the system as the effect of silanes leading to an increased curing still can be recognized. Of course, it is clear that due to their higher functionality both the EPB and the BPAE can behave as crosslinker as well. Since the EPB sample shows very bad thermal ageing resistance and it increases the T_g of the whole system which limits the application are of finished PSAs, further respective investigations have been stopped and additional tests were only conducted with the BPAE silane PSA. As plastic adhesion in combination with high shear values are the main drivers of this investigation, the adhesion on Polyethylene and Polypropylene has been benchmarked against the standard cured with mercury bulbs. This is connected to the fact that this PSA also fulfills the requirements of high cohesion which does not count for the LED cured TAS-Sb sample without curing the EPOMA modification with the same UVA dose. It becomes clear, that the modification of the PSA by using silane technology and BPAE as reactive diluents fundamentally changes the adhesion performance on PP as can be seen in Table 10.

Table 10: Performance on LSE surfaces; peel measured at 180°

sample	Curing dose in mJ	peel in N/25mm on PP	peel in N/25mm on PE
Hg reference	100 (UVC)	3 (AF + 100% Zip)	7 (AF + 25% Zip)
BPAE	3000	15 (AF + 20% Zip)	7 (AF + 25% Zip)

Whereas the mercury cured PSA shows very poor adhesion on PP with mainly zipping effects during the test, the new modification with silanes and BPAE shows reduced

zipping effects and much higher values. A fundamental change in peel values on PE could not be observed. It must be said that the biggest influence onto the adhesion performance is expected to be connected to the epoxy resin as it takes 15w% of the overall polymer. The amount of silane used inside the sample is not expected to have a major influence onto the peel performance and in addition to that no positive influence of silane technology onto LSE surfaces is expected from, leaving potential small changes in surface energy out. Since the DMA did not show differences regarding the viscoelastic behavior at room temperature where the peel test was executed, the change in peel behavior could be connected to a change in surface wetting and with that interaction of the PSA with the LSE surface. It needs to be said that still “zipping” effects occurred even though the occurring percentage was lower.

Generally Zipping effects, often called “Stick-Slip-Effects” can be explained by the fact that the crack at the peeling line during the test moves faster through the adhesive layer than the test arm (here Zwick arm) moves.¹¹⁸ This results in oscillating forces as the test arm catches up with the crack and the process could potentially repeat. This phenomenon occurs especially in borderline cases when testing PSA on LSE surfaces where the PSA potentially could stick from its viscoelastic characteristics, however, not perfect fitting surface energies add another factor to it.¹¹⁹ There are several theories about why this phenomenon happens and the academia is confident that it is connected to rheological behavior and because of surface effects, however, no final explanation has been elaborated so far.¹¹⁹

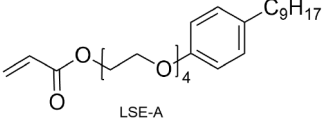
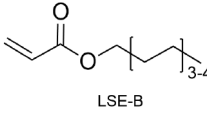
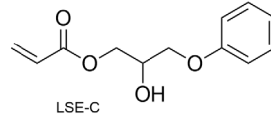
Since the incorporation of an aromatic based epoxy reactive diluent led to an increase of adhesion on PP with reduced Zipping effects, such probably due to better interaction, the weak spot for compatibility, interaction and possibly better surface wetting remains on the polyacrylate. As the epoxy reactive diluent will form an intermediate network with the epoxy groups from EPOMA, the finished adhesive can be recognized as a hybrid system consisting of a polyether with high aromatic fractions and the polyacrylate as second fraction. It is expected that the aromatic polyether fraction is responsible for better adhesion on the LSE surface. If the adhesive is wetting the LSE surface with this fraction, a good surface interaction is expected. However, in

case of wetting with the polyacrylate fraction bad wetting and bad surface interaction are expected as could be seen for the standard PSA without any epoxy or silane inside.

This postulate leads to the fact that there needs to be a change in the polyacrylate to increase the wetting and surface interaction with the plastic surface. This can either be done by losing the entanglements with a suitable tackifier or by changing the monomer composition of the polyacrylate with focus on using monomers of lower polarity. Since the incorporation of a tackifier will weaken the whole system and lead to a drop in cohesion, this method is not the preferred method with a focus on a high shear and high plastic adhesion PSA. In case of the monomer design, there are several potential monomers commercially available which are suitable as they offer low polarity and following that could potentially increase the adhesion to LSE plastics. Besides C_8 to C_{18} acrylates there are also monomers available having an aromatic side group which would match the general idea of the BPAE epoxy. It can be determined, that using aromatic structures for UV curable coatings might generally lead to negative results due to the fact that those monomers could potentially absorb the UV light and by that lower the available energy the photoinitiator would receive but this is connected to the UVC region mostly. As the PSAs in this thesis are cured with a 365nm LED, this can be neglected as the irradiation wavelength does not interfere with the own absorption of the aromatic monomers. The same can be related to the BPAE itself as well. Otherwise, the earlier tested samples which already included the BPAE epoxy would have shown a very bad cohesion and high adhesion values with cohesive failure due to incomplete curing of the PSA.

Three different monomers have been investigated with regard to their impact on adhesion on LSE plastics and also a change in cohesion was monitored. The monomers are displayed in Table 11 below. In order to keep the T_g of the finished PSA identical, the monomers have been used as partly replacement for either MA or for 2-EHA (or both).

Table 11: Overview of investigated LSE adhesion monomers

Structure			
T_g	-27°C	-66°C	7°C
Replaced monomer	MA / 2-EHA	2-EHA	MA
W%	10	5	5
M_w	448.6 g/mol	198.31 g/mol	222.24 g/mol

The monomers have been incorporated into the solution copolymerization process which was explained earlier above in chapter 3.1. No excessive amounts of the new monomers have been used in order to make sure that the adhesion on polar surfaces does not drop noticeably. In addition to that especially the monomers LSE-A and LSE-C are in the upper maximum price range for packaging PSA applications. Consequently, the monomers LSE-B and LSE-C have been used at 5w% and the entire monomer mass and the amount of LSE-A has been adjusted to 10w% due to the higher molecular weight of the monomer to enable a representative and comparable sample range. To ensure an even copolymerization with MA and 2-EHA, the monomers have been used in the initial monomer filling and in the delay monomer dosing. All other parameters like initiator, solvent and total solid were kept identical. During the polymerization process no visible changes could be observed. The final polymers have been formulated with TAS-Sb as cationic photoinitiator, ITX as LED sensitizer and the same amount of BPAE and silanes CAES-E and CAESO-Q as before. All samples have been coated separately to 80µm thick coatings and were irradiated with 3000mJ UVA irradiation coming from a 365nm LED. The cohesion and adhesion performance has been investigated to verify an impact of the respective monomer. The results of the performance tests are displayed in Table 12 below.

Table 12: Impact of LSE monomers on performance; peel measured at 180° (relative failure 5-10%)

sample	SAFT in °C	Peel in N/25mm on steel	Peel in N/25mm on PP	Peel in N/25mm on PE
LSE-A	85 (AF+CF)	23 (AF)	9 (AF + 25% Zip)	11 (AF)
LSE-B	74 (AF+CF)	25 (AF)	17 (AF)	10 (AF)
LSE-C	>200	23 (AF)	16 (AF)	9 (AF)
LED ref.	>200	23 (AF)	15 (AF + 20% Zip)	7 (AF + 25% Zip)
Hg ref.	>200	20 (AF)	3 (AF + 100% Zip)	7 (AF + 25% Zip)

As shown in Table 12, the impact of the different monomers onto the adhesion and cohesion varies. First of all, when adding the monomers LSE-A or LSE-B to the monomer composition of the copolymer the cohesion drops from the maximum reached temperature during the SAFT test to only 70-85°C with a mixed failure mode of adhesion and cohesion failure, indicating a slightly undercured sample. In case of the monomer LSE-A, the peel performance on PP decreased significantly compared to the LED reference which only contains the silanes CAES-E and CAESO-Q and BPAE as epoxy reactive diluent. At a first glance it looks like that the peel performance on PE is increased compared to the LED reference, but it needs to be considered that there is a standard deviation for every peel measurement which must be taken into account in the range of 5 to 10% of every individual measurement. Following that, the peel performance on PE does not differ that much any longer with regard to the reference and sample LSE-A.

When comparing the peel performance of the sample LSE-B with the LED reference it can be seen that the implementation of this monomer eliminated a zipping reaction on both plastic substrates which is exactly what was intended to be achieved with this monomer adaptation. Sample LSE-B shows a smooth peel behavior on PP, PE and no large drop of peel performance on steel, however, the cohesion dropped significantly, which was not intended. It is unclear why both monomers led to a decrease in cohesion but even after several additional trials the cohesion remained at a poor level. As cohesion is not only connected to the curing of the epoxy groups but also to entanglements, it could also be connected to different entanglement phenomena with very large sidechains. In case the entanglement of polymer chains is hindered by notably

large side chains the cohesion would decrease. This could also be an explanation why certain adhesion values increased for these samples.

In case of the sample LSE-C it sticks out that the cohesion remained at the maximum measurable level of 200°C in the SAFT test and there is a noticeable impact onto the adhesion values on LSE surfaces. It can be seen in Table 12 that the incorporation of monomer LSE-C into the composition led to a zipping free peel reaction on PP and PE. The absolute peel values did not increase tremendously compared to the LED reference, however, the changed monomer composition eliminated any zipping reaction reproducibly which enables applications on these plastics for this PSA. Now not only the epoxy reactive diluent has aromatic segments being able to interact with the nonpolar surface, but also the polyacrylate itself. As stated earlier above, the further addition of another aromatic specie did not harm the LED curing as the absorption does not interfere with the 365nm LED. To investigate that the improved peel performance is not connected to a change in viscoelastic behavior, the sample has been analyzed within a temperature sweep test and compared to the LED reference without adjusted monomer composition containing only the BPAE and the silane and siloxane.

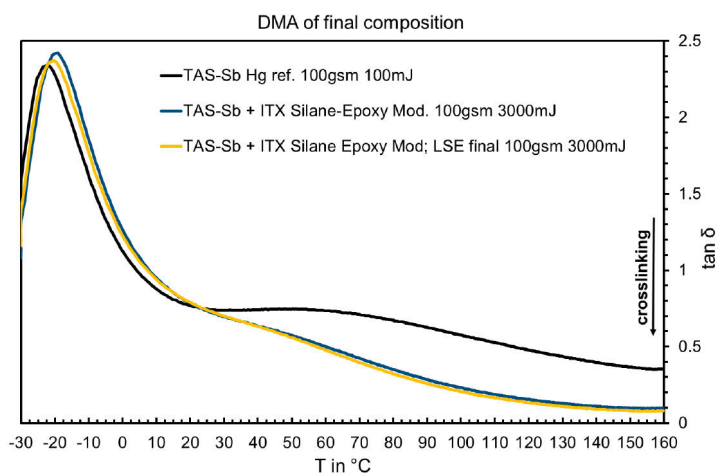


Figure 42: DMA comparison of LSE modified PSA vs LED reference and Hg reference

Figure 42 shows, that the change in the monomer composition due to the addition of monomer LSE-C to the copolymer was not related to a change in viscoelastic behavior

regarding the $\tan \delta$. The LSE-C modified version displayed in yellow fits perfectly to the LED reference displayed in blue containing only the BPAE, CAES-E and CAESO-Q. A slight deviation in the T_g area can be suspected, but as the T_g calculation of monomer compositions via the fox equation also is connected to a failure, this can be neglected. Moreover, it sticks out that the newly modified PSA shows higher cohesion at elevated temperatures compared to the mercury cured reference, whereas the difference in $\tan \delta$ at room temperature is only small. Since there is no change in $\tan \delta$ at the temperature where the peel test is executed, the change in peel behavior needs to be connected to a different reason. On the one hand the implementation of a silane, siloxane and an aromatic epoxy reactive diluent might change the surface energy of the PSA and with that its wetting characteristics but there is also the possibility that viscosity differences of the PSA at the peel test temperature lead to changes in peel behavior.

Generally, the new PSA is able to fulfill the needs for high shear applications where adhesion on LSE plastics is needed. In contrast to that, this would not be achievable with the addition of a tackifier, as the tackifier usually increases the T_g of the whole composition leading to a higher $\tan \delta$ at the application temperature which leads to an increased adhesion, not to forget the loosening of entanglements. Here the product would be able to fulfill the adhesion characteristics on plastics due to these properties, but the shear values would decrease due to lacking cohesion. In order to verify a possible change in wetting behavior and improved surface interaction, the contact angle on the cured PSA films has been measured and the surface energies have been calculated via the Owens, Wendt, Rabel and Kaelble model.¹²⁰

Table 13: Results of contact angle measurement

	PP	Hg ref.	LSE PSA final
Contact angle water in °	91.5	81.5	82.1
Contact angle Diiodomethane in °	50.3	36.9	37.2
Surface energy total in mN/m	45.4	43.9	43.6
Surface energy polar in mN/m	1.3	2.8	2.6
Surface energy nonpolar in mN/m	34.1	41.1	41

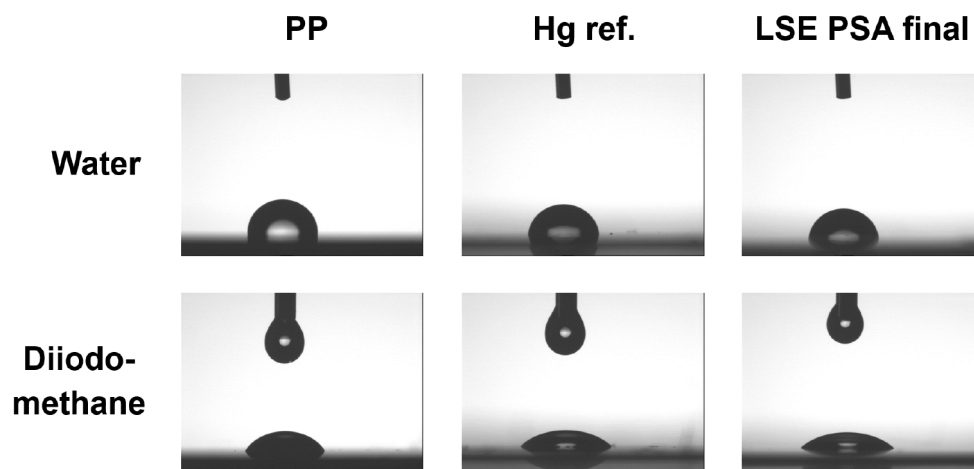


Figure 43: Contact angle measurement

As can be seen in Table 13 and Figure 43, surprisingly no fundamental change in surface energy and contact angle could be observed when comparing the LSE modified PSA sample to the Hg cured reference sample. Interestingly, the difference in peel behavior on LSE plastics cannot be connected to a change in the wetting behavior of the new PSA even though the implementation of a noticeable amount of hydrophobic aromatic structures took place. With that the reason for the improvement of peel behavior must be connected to a different factor. Provided the surface wetting by the PSA is not completely hindered and takes place, which can certainly be seen as given as there is a measured tack on the LSE plastic, the peel performance is not only depending on the surface wetting but also on energy dissipation and viscosity of the PSA. A higher energy dissipation and lower viscosity of the PSA will lead to a higher peel value as the PSA would be able to use a bigger surface area of the substrate by flowing into surface tangents. Since the DMA test already has shown that the $\tan \delta$ of both samples, the Hg reference and the final LSE PSA sample are rather similar, it makes sense to investigate the viscosity of the cured PSA at the temperature where the peel measurement takes place.

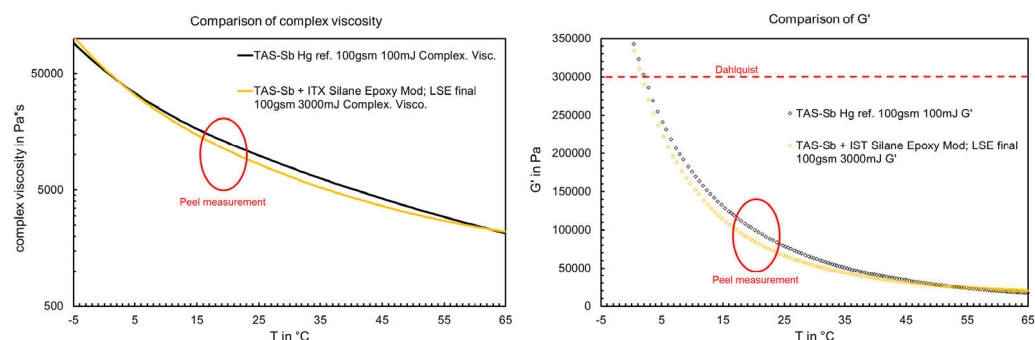


Figure 44: Viscosity effects on LSE modified PSA compared to reference

As can be seen in Figure 44, the complex viscosity and the level of G' at the temperature where the peel measurement is executed differs. The LSE modified PSA (yellow) has a lower complex viscosity and lower level of G' at the relevant temperature window between 20 to 25°C where the peel measurement is carried out than the Hg reference sample (black). Dahlquist already found out that polymers having a G' lower than 3×10^5 Pa at the application temperature and the respective frequency are showing tack and the lower the G' the higher the tack⁶. Of course, there is also a certain limitation for very low G' values but clearly the investigated PSAs in this research are above the lowest limit of G' . In addition to that, the lower complex viscosity of the LSE modified PSA allows that the PSA can flow better into the surface indentations of both the steel- and the PP surface, enabling wetting of an increased surface area and resulting in increased peel values. Again, this underlines the fact that rougher surfaces are not necessarily easier to bond with PSAs since the PSA needs to be viscous enough to use the increased area. This can be applied for a broad range of surfaces since many surfaces appear smooth at first glance, however, having a not to be neglected surface roughness as the AFM measurement of the steel- and PP substrate as shown in Figure 45. It is surprising that the PP (Sample B) surface shows a comparable rough surface even though it has been protected against scratches and has been cleaned with a special soft tissue to keep a scratch free surface. The average roughness of 59nm underlines again that even a smooth appearing surface has a certain roughness. Such roughness is a crucial factor for bonding viscoelastic PSA as it determines the surface area the PSA can use for bonding in combination with the PSA viscosity after curing took place. Compared to that, the roughness of the steel substrate (Sample A) is not

as high with an average of 28nm, however, still this has an effect onto the PSA behavior in case of very elastic PSA which cannot flow into the surface indentations.

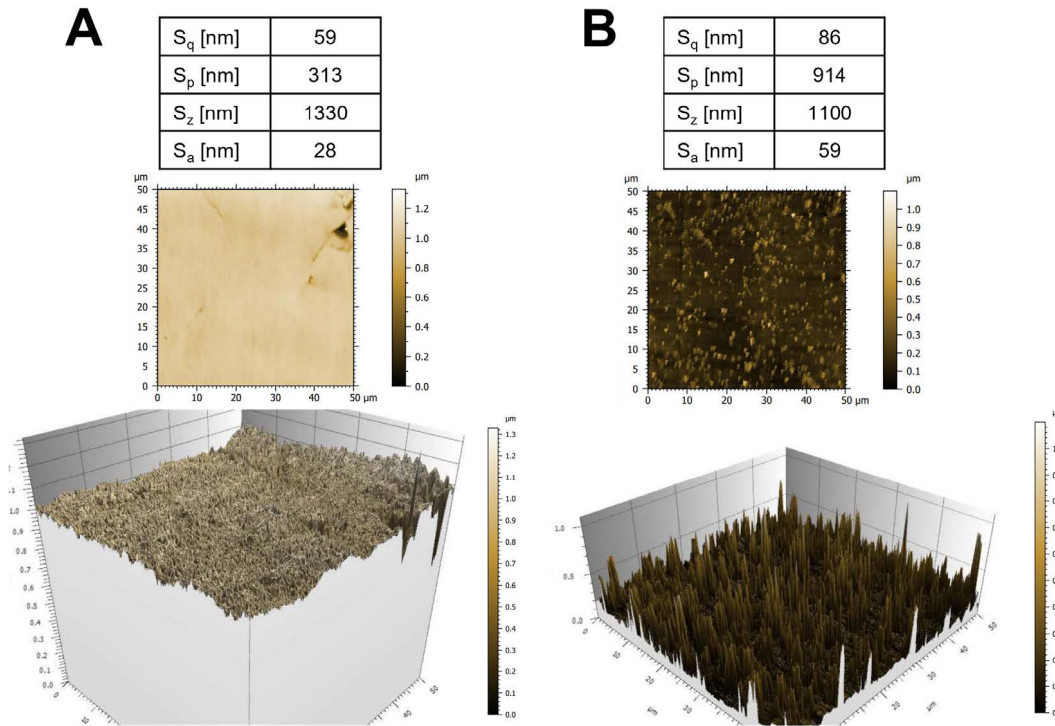


Figure 45: AFM of steel substrate (A) and PP test substrate (B)

Following that, the improved peel behavior especially on LSE substrates can mainly be connected to viscosity and rheological effects which has originally not been expected. It could be demonstrated that the change in surface energy of the PSA can be neglected, whereas the addition of the epoxy reactive diluent changed the viscoelasticity at the temperature where the peel measurement is executed. This could initially not be observed during the investigation of $\tan \delta$ only. Nevertheless, it is possible that the addition of the monomer LSE-C increased the overall compatibility of the acrylic PSA with the epoxy reactive diluent which, however, has not been further investigated during this research.

Besides PP and PE as representative plastics for LSE surfaces, the peel performance on other plastic substrates is of interest as well since several applications require high cohesion and temperature stability while keeping good adhesion to plastic substrates,

e.g., in under the hood applications in the automotive industry.¹²¹ Consequently, the peel performance on different plastic substrates of the newly modified PSA has been benchmarked against the mercury cured reference PS.

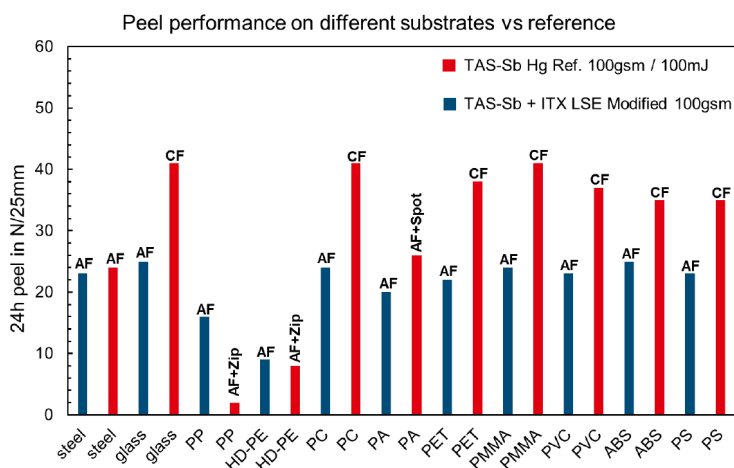


Figure 46: Peel benchmark on different plastic substrates; measured at 180° angle

The improved peel performance of the modified PSA cannot only be seen on PP and PE as shown in Figure 46. Whereas the mercury cured reference PSA shows a cohesive failure on most plastic surfaces, the modified PSA shows a residue free and zipping free adhesion behavior on all tested plastic substrates. Since the failure mode moved from cohesive failure mode to adhesion failure mode, the measured absolute peel values decreased, however, it has to be said that also in this application area an adhesion failure mode is favored in contrast to a cohesion failure mode. Even though the absolute peel values decreased for the modified version due to the failure mode switch, the values remain at a very high level between 20 and 30 N/25mm on most plastic substrates. Besides that, it is clear that all these tests have been carried out as transfer coatings. In a first step the adhesive has been coated onto a silicone release paper, irradiated and then transferred to etched PET. Consequently, the dark side of the PSA has been tested all the time which normally is the lower cured side compared to the side which was directly facing the light and is laminated against the PET foil.

As well as the overall performance data, this characteristic enables new application fields as nearly any foil or web material can be laminated onto the PSA as even the dark

side shows proper adhesion values on plastic surfaces without leaving residues behind when peeling. In case of the mercury cured reference this could only be achieved when switching to a direct coating procedure where the adhesive directly is coated onto the PET foil and then irradiated. This leads to the fact that the light side is bond to the plastic surface which of course has a higher degree of curing than the dark side of the adhesive due to cure depth effects. However, the process of direct coating drastically limits the application possibilities as it is not possible to use temperature sensitive foils or webs as they would get destroyed by the hot adhesive.

With the new modified PSA, even these applications might be partly enabled due to the fact that the viscosity of the new adhesive decreased fundamentally in contrast to the reference mercury bulb cured PSA. Through the addition of BPAE as a reactive diluent, which has a much lower viscosity than the polyacrylate itself, it was possible to reduce the viscosity by 70%.

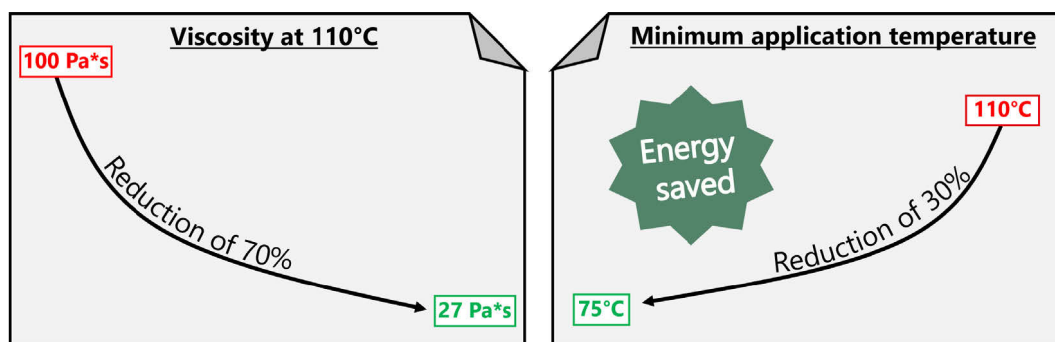


Figure 47: Comparison of non-modified and modified PSA

Since 100Pa is seen as the maximum possible application viscosity it would be possible to drop the application temperature from an originally minimum coating temperature of 110°C by 30% to a new coating temperature of 75°C. Given that it must be said that the coating temperature of a cationic curing PSA cannot be decreased to an absolute minimum because the whole curing reaction is heavily dependent on the temperature as proven in earlier chapters above. In this case it might be necessary to increase the epoxy amount on the polyacrylate backbone again in order to increase the reactivity as executed earlier above in this thesis. Due to the fact that the coating temperature is lowered tremendously, the temperature stability would also be a smaller problem while increasing the reactivity, since the whole adhesive does not need to be

temperature stable at 120°C anymore. Regarding the temperature stability the new PSA showed an outstanding temperature stability compared to the mercury bulb cured reference. The viscosity only increased 5% over 72h at 120°C in a Brookfield viscosimeter. Following that, the mercury bulbs cured reference material gelled during the test as this material is only stable for approximately 36 to 48h at 120°C.

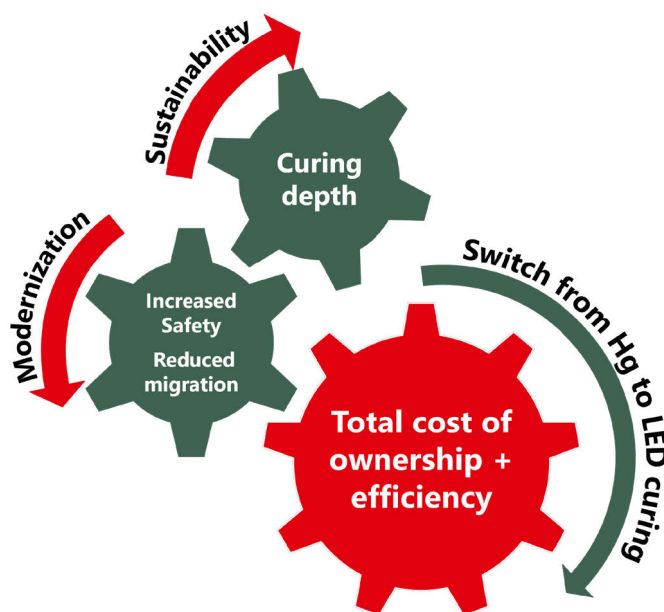
5. Conclusion and outlook

During this thesis the possibilities of the development of UV LED curable hotmelt PSA has been investigated. As can be noticed, the work has been executed with a continuously strong connection to the application of PSA and the potential within the industry regarding the probability to upscale and the cost limitation related to the resulting adhesive products. An attempt has been made to stick as close as possible to commercially available products, and if possible, to enable a quick implementation into the industry. This type of investigation has been chosen very deliberately since there is a huge pressure on the change of curing technology from mercury bulbs to LEDs within the PSA industry. As the sustainability targets not only for adhesive producers but for all companies worldwide are challenging, not only because of regulatory pressure but also due to pressure from the market, it is essential to find solutions as fast as possible while keeping an eye on costs and the possibility to implement such solutions in upscaled productions. Certainly, the investigations executed in this thesis could have been conducted with a deeper scientific and more abstract methodology, however, this would have been challenging to implement such into a cost driven industry like the packaging industry.

It needs to be considered that because of the applied pressure by sustainability, there is a run by adhesive manufacturers to fill an upcoming gap within the industry which is expected to sell millions of tons of adhesive in the future. UV LED curable hotmelts are expected to have a main market share in the upcoming years, which makes it essential to find technological solutions for the stated problem, being achievable in industrial scale while protecting broad via intellectual property (IP). Clearly, there are potentially other, more academic, solutions to achieve the desired products than the solutions displayed in this thesis, however, it is unlikely that they find their way into final products within the packaging industry. When changing the industry to e.g., aerospace or electronics, it might be the case that there is a wider price range for research purposes and more complex product solutions.

In this thesis the main curing mechanisms for UV curable hotmelt PSAs have been taken into account and their potential for LED curable hotmelt PSAs has been investigated.

First, the cationic curing technology was investigated. Here it has been observed that the present used technology indeed shows certain curability with 365nm LEDs, however, the curing takes place very slow and is limited to 50gsm coatings compared to the mercury bulb cured reference material. Different commercially available onium salts have been chosen to be investigated as replacement for the current used TAS-SB photoinitiator. Some of them were based on an Iodonium- and some were based on a Sulfonium salt. It could be determined that unfortunately all Iodonium salts did not fulfill the needs for the required temperature stability. This lead also to the fact that newly developed Iodonium salt like the CILED-P and CILED-Sb, especially developed for 365nm LEDs, could not be used since they are not stable inside a hotmelt system. The CILED-Sb showed good reactivity, which could enable an application in other LED curable adhesives, coatings, etc. beside instead of hotmelt adhesives.



Scheme 12: Driving factors making a change from mercury bulb curing to LED curing essential

As done by other groups before for different application purposes, it has been investigated if the respective Sulfonium salt TAS-Sb could be sensitized even though it is known that Sulfonium salts are not that easy to sensitize. Again, a variety of different potential photosensitizers has been investigated, some of them being Norrish Type I and some of them being Norriyh Type II photoinitiators. It was found that, contrary to

expectations gained by literature so far, it has not been the Anthracene based sensitizer which was working best but the thioxanthone based ITX. As part of the investigation it has been found that on the one hand side the perfect molar ratio is one part TAS-Sb and two parts ITX and on the other hand it has been confirmed that also the cationic curing PSA underlays a big temperature dependency during curing. Through an increase of EPOMA as epoxy functional acrylic inside the polyacrylate it was possible to remain at a high temperature stability while gaining a rapid curing profile. The new LED curable PSA shows as fast curing as its mercury reference while keeping the identical performance. The great advantages of the new technology are that by switching from mercury bulb curing to LED curing plenty of energy can be saved, toxic Ozone is circumvented and the curing technology is not connected to RoHS exceptions anymore.

As a next step, free radical curing PSAs have been investigated regarding their LED curability. These products are used in several different applications, since the copolymerized BP-MA photoinitiator leads to low migration and also enables food contact and medical applications in contrast to the cationic curing PSA. Quickly it was found, that a polyacrylate mixed with a LED suitable photoinitiator cannot be cured to the desired performance level and within the required time frame. It is expected that there is a competing reaction between a polymer chain having a radical on it and an activated photoinitiator molecule having a radical on it. Because of matrix viscosity and connected mobility of the photoinitiator and the polymer chain, it is expected that the photoinitiator molecule rather recombines with the chain and deactivates it, instead of two polymer chains recombining with each other and forming a network. Without fast network formation, the curing and the connected performance is insufficient. Since the mercury bulb cured free radical system uses a copolymerized Benzophenone which is a Norrish Type II photoinitiator and during the first step with the cationic curing investigation a positive experience has been made with the ITX, the ITX has been modified in a way that it can be copolymerized like the BP-MA. The resulting newly designed AC-ITX can be copolymerized with other acrylics. It was found out that this photoinitiator enables rapid curing of the PSA and shows the sufficient adhesive performance. As the change from mercury bulb curing to LED curing brings oxygen inhibition into play, VMOX has been copolymerized in a small amount as well in order to

enable the effect of an amine synergist together with the AC-ITX. It could be seen that the implementation of a small amount of VMOX is enough to improve the surface curing of the PSA sample without having an impact on the through cure of the sample and following that the overall viscoelastic behavior. With AC-ITX it is possible to change any existing free radical curing hotmelt PSA which has been cured with mercury bulbs before to a LED curable PSA. Since AC-ITX is copolymerized into the backbone as well, it shows very low migration, as proven in an official migration test. Following that, LED curable PSAs are achieved which still can be used in low migration applications like food- or medical applications. In addition to that it was found that with the change to a longer wavelength during curing (from UVC to UVA), there is a large potential to also cure thicker coatings with a free radical curing mechanism which was so far only achievable with cationic curing technology.

As a third step, the thesis focused on the cationic curing technology again. The experience gained during the research of the LED curable cationic PSA were implemented into a combination of LED cationic curing PSA technology and silane technology. It has been shown that silanes work well inside cationic curing UV hotmelts when they are not copolymerized as acrylic silane hybrid monomers but as cationic curable silanes or siloxanes. In this case, the hotmelt remains very stable at elevated temperatures and benefits from the silane not only as crosslinking agent but also due to the fact that the proton triggered abstraction of the alcohol from the silane shifts the curing of epoxies towards an activated monomer mechanism. This change in mechanism speeds up the PSA provided there is no excessive number of hydroxy functions. The investigation shows that both technologies have very promising synergies, as the alcohol is rapidly gained during the UV irradiation and before that it is protected by the silane, remaining soluble inside the matrix. Therefore, it was possible to achieve very rapid curing speeds of the PSA without increasing the photoinitiator or EPOMA amount by a simple formulation step while keeping high stability. This enabled the chance to add an epoxy reactive diluent which reduces the viscosity of the whole adhesive and following which saving energy during the application as it can be done at a lower application temperature. By the addition of the BPAE and the implementation of a small amount of an aromatic monomer LSE-C into the copolymer a high cohesive PSA showing medium to high adhesion on all tested

plastic substrates has been achieved, including LSE surfaces like PP and PE without any slip stick behavior. It could not be proven that the increased peel performance on PP and PE is connected to an increased compatibility of adhesive and plastic substrate via improved wetting as the contact angle did not change compared to the reference PSA. It is expected that the modified adhesive shows improved peel performance since the complex viscosity at the test temperature is lower for the modified adhesive compared to the reference material. Following that, the adhesive is able to use a bigger surface as microscopic furrows can be used better. This behavior cannot be executed with the reference adhesive since its complex viscosity is too high and therefore is impossible to flow inside the cavities on the surface during the same time period. This is also supported by the fact that the level of G' for the LSE PSA at the application temperature is lower than the G' of the Hg reference adhesive, also indicating a better wetting characteristic.

Concluding everything, the work done in this thesis could overcome an ongoing problem the PSA manufacturers within the packaging industry face, since there is more and more pressure put onto mercury bulb curing technology. Ongoing challenges being connected to the photoinitiator technology including resulting issues have been observed and solutions have been produced, being as close to commercialization as possible. Especially the research on a new copolymerizable LED photoinitiator enables new chances within the industry, not only for the PSA market but generally for low migration applications outside of the adhesive business as well. During the investigation it was found that the change from mercury bulbs to LED curing is not only related to challenges and issues but also entails new possibilities and chances for products up as well since the longer wavelength enables the sufficient curing of thicker coatings. It is clear, that the AC-ITX is not commercially available but since there is no alternative available which shows comparable performance while fulfilling migration limits, there is no other choice than designing a new photoinitiator which then finally fulfills the respective requirements. However, it is expected that the upscaling of AC-ITX is not that challenging for the industry since the synthesis of thioxanthenes, e.g. ITX, is very popular and also the esterification of an alcohol to its respective acrylate is a standard procedure.

6. Experimental part

6.1 Polymerization of cationic curable PSA

The polymerization of cationic UV curable polyacrylic PSA was done in a small 250g polymerization reactor (HTP) with a mechanical stirring unit including a reflux condenser and two automatic weight-controlled delay dosing units (Figure 48). This setup is close to a standard three neck setup however allows easier cleaning of sticky polymers and increases polymerization reproducibility because of the automatic dosing units. Those two delays were separately filled with a monomer-solvent mixture and an initiator-solvent mixture. In order to start the polymerization, 1/4th of the overall monomer mixture was put into the HTP reactor in advance including a sufficient amount of solvent, so the stirrer had enough contact to the material. The remaining 3/4th of the monomer mixture and solvent was filled into the delay flask. This so-called semi feed batch process allows excellent temperature and reaction control increasing the safety during an industrial process.⁷⁶ Via electric heating the reactor temperature was set to 95°C and once the thermometer placed in the reactor flask showed 45°C, the initial initiator shot including a small amount of solvent was put into the reactor.

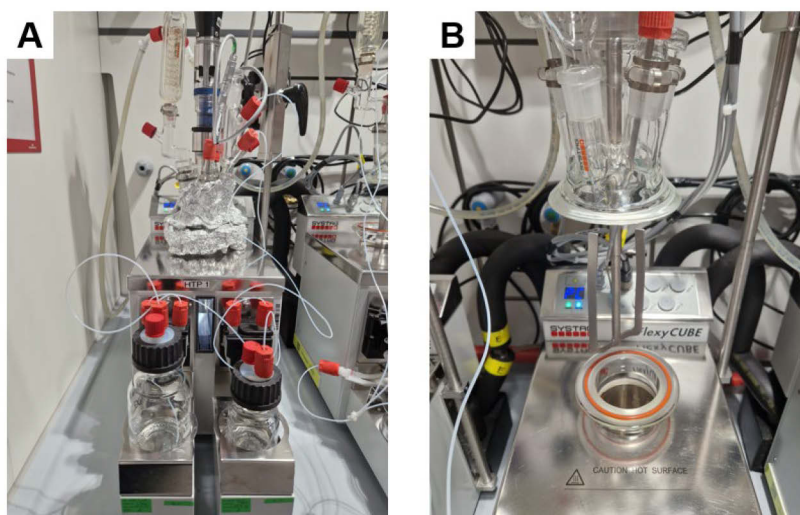


Figure 48: Running HTP reactor (A); open HTP reactor with stirring unit (B)

The remaining initiator-solvent mixture was filled into the second delay flask. 15 minutes after the reaction mixture reached reflux state, both delays were started and kept running for 180 minutes in a linear dosing process. During the whole polymerization process all relevant polymerization process parameters like head and vessel temperature were monitored. After 375 minutes of total reaction time at the boiling point of the used solvent, the reactor was cooled down to room temperature. The polymer was filled into a brown glass bottle and formulated with a stabilizer and cationic photoinitiator composition. On the next day the solvent was stripped of at 120°C and 10mbar for 6h (if needed). Table 14 shows up the detailed monomer and initiator composition.

Table 14: Monomer and solvent composition for cationic curable UV PSA

chemical	mol%	w%
Methylacrylate (hard monomer)	65.1	46.5
2-Ethylhexylacrylate (soft monomer)	33.8	51.9
EPOMA	0.68	1.1
EtOAc (solvent)	-	(57) - 43% TS
AIBN (initiator)	0.37	0.5
DTC (stabilizer)	-	(0.46) of hotmelt

In order to investigate the ability of EPOMA to copolymerize with MA and 2-EHA the absolute monomer amounts for each monomer and the monomer composition of the reaction solution has been monitored over time as displayed in figure 14. In time steps of 10 minutes samples have been taken from the reactor vessel and directly quenched with a 5% solution of phenothiazine to stop further polymerization inside the sample flask. The quenched sample was analyzed via GC in order to investigate the monomer composition compared to the initial monomer composition at the start of the reaction. All measured GC results and time steps are displayed in the table below.

Table 15: GC results of monomer conversion over time

time [min]	MA [m%]	MA [mol]	MA [mol%]	2-EHA [m%]	2-EHA [mol]	2-EHA [mol%]	EPOMA [m%]	EPOMA [mol]	EPOMA [mol%]
0	9.3	1.08E-01	62.5	11.7	6.35E-02	36.7	0.26	1.33E-03	0.77
10	8.9	1.03E-01	63.2	10.9	5.91E-02	36.1	0.24	1.22E-03	0.75
40	7.3	8.49E-02	64.9	8.4	4.56E-02	34.8	0.073	3.72E-04	0.28
70	5	5.81E-02	65.6	5.6	3.04E-02	34.3	0.032	1.63E-04	0.18
100	4.1	4.77E-02	65.0	4.7	2.55E-02	34.8	0.029	1.48E-04	0.20
130	3.8	4.42E-02	65.8	4.2	2.28E-02	34.0	0.027	1.38E-04	0.21
160	3.4	3.95E-02	65.0	3.9	2.12E-02	34.8	0.026	1.33E-04	0.22
190	3.3	3.84E-02	66.1	3.6	1.95E-02	33.7	0.025	1.27E-04	0.22
210	2	2.33E-02	67.1	2.1	1.14E-02	32.9	0.005	2.55E-05	0.07
240	1.4	1.63E-02	66.6	1.5	8.14E-03	33.3	0.005	2.55E-05	0.10
300	0.93	1.08E-02	67.6	0.95	5.15E-03	32.2	0.005	2.55E-05	0.16
360	0.68	7.91E-03	67.7	0.69	3.74E-03	32.1	0.005	2.55E-05	0.22

For the investigation of different cationic photoinitiators in order to improve the LED curability the polymer was formulated with 0.23w% (in relation to total solid mass) of TAS-SB, which was used as reference. All other cationic photoinitiators have been used in an equimolar ratio to TAS-Sb.

During the sensitizer investigation the amount of sensitizer was chosen as twice the molar amount of TAS-Sb, which later resulted coincidentally in the perfect amount. All sensitizers have been compared to each other in an equimolar amount.

The EPOMA modified polymer has been polymerized according to the earlier described procedure. Just the amount of EPOMA was increased by 70%. All other parameters displayed in Table 14 were kept the same.

6.2 Polymerization of free radical curable PSA

The polymerization was again carried out in one of the small reactors which have already been used for the polymerization of the cationic curing copolymers. As well as the cationic PSA the polymerization was carried out via a semi feed batch process.

Approximately 1/4th of the overall monomer mass was filled into the reactor as initial filling together with 80% of the solvent while stirring continuously. The mixture was heated to 95°C and an initial initiator mix of 25% of the total used initiator was filled into the reactor once it reached 45°C. A few minutes after the addition of the initial initiator shot a small exothermic peak in the reactor temperature could be noticed. This short rapid increase in temperature has been used as the reaction starting time. 15 minutes after the reaction starting time two delays have been started. One of the delays was filled with the remaining 75% of the total monomer mass and another delay was filled with the remaining 75% of the initiator solved in the remaining 20% of the solvent.

The dosing ratio of the monomer delay has been programmed in a way that the complete mass was filled into the reactor over 180 minutes while the same has been done with the initiator delay but in 120 minutes. 255 minutes after the reaction starting time a first shot of peroxide was filled into the reactor, called scavenger shot. These scavenger shots lead to a decrease in monomer residuals in the final copolymer, reducing the odor fundamental and enabling a reduced solvent stripping time later and also enable food contact and medical contact applications due to low monomer residuals.⁸ Two additional peroxide shots have been put into the reactor after another 60 minutes each. After a total reaction time of 435 minutes, the reactor was cooled to room temperature and the polymer was filled into a brown glass bottle to protect it from sunlight. On the next day the solvent was stripped of at 130°C and 10mbar for 6h (if needed). The overall monomer and solvent composition are displayed Table 16.

Table 16: Monomer and solvent composition for free radical curing PSA

chemical	mol%	w%
Acrylic acid (hard monomer)	10.7	3.8
Butylacrylate (soft monomer)	88.6	55.4
BP-MA (photoinitiator)	0.01	0.13
POX (scavenger)	0.27	0.29
EtOAc (solvent)	-	40 (60% TS)
AIBN (initiator)	0.35	0.29

The PSA synthesis with AC-ITX as novel LED photoinitiator was executed according to the earlier described procedure. First the AC-MA was used in an equimolar amount to BP-MA and later increased by 50% to 0.015mol%. For the implementation of VMOX into the PSA the polymerization process was not changed further as well. VMOX was used three times the molar amount of AC-ITX (+50% version) which results in $\approx 0.045\text{mol}\%$.

6.3 Synthesis of AC-ITX

To produce a hydroxy functionalized ITX, 5.0g 2,2'-Dithiodibenzoic acid (16.3mmol) were suspended in 50 ml of concentrated sulfuric acid (95%). Exactly 13g of 2-Isopropylphenol (95.5mmol) were added to the suspension during 10 min. During this period the mixture was heated to $\sim 50^\circ\text{C}$. The reaction mixture was then heated to 80°C where it was maintained for three hours. After three hours, the mixture was cooled down to room temperature and stirred overnight. Next, the resulting mixture was added dropwise into 500ml of boiling, deionized water. The precipitate was filtered off and washed once with 50ml of boiling water and once with 100 ml of cold water. The resulting product was dried under vacuum.^{102,103} *Yield $\approx 70\%$, appearance: green powder; purity 80% (GC-MS).*

^1H NMR (400 MHz, DMSO- d_6 , 25°C) δ (ppm) 10.18 (s, 1H), 8.43 (dd, $J = 8.2, 1.5$ Hz, 1H), 7.73 (dd, $J = 8.2, 1.4$ Hz, 1H), 7.67 (dd, $J = 8.1, 1.4$ Hz, 1H), 7.53 (d, $J = 1.4$ Hz, 1H), 7.51 (t, $J = 1.3$ Hz, 1H), 3.30 (sept, $J = 6.9$ Hz, 1H), 1.22 (d, $J = 6.9$ Hz, 6H).

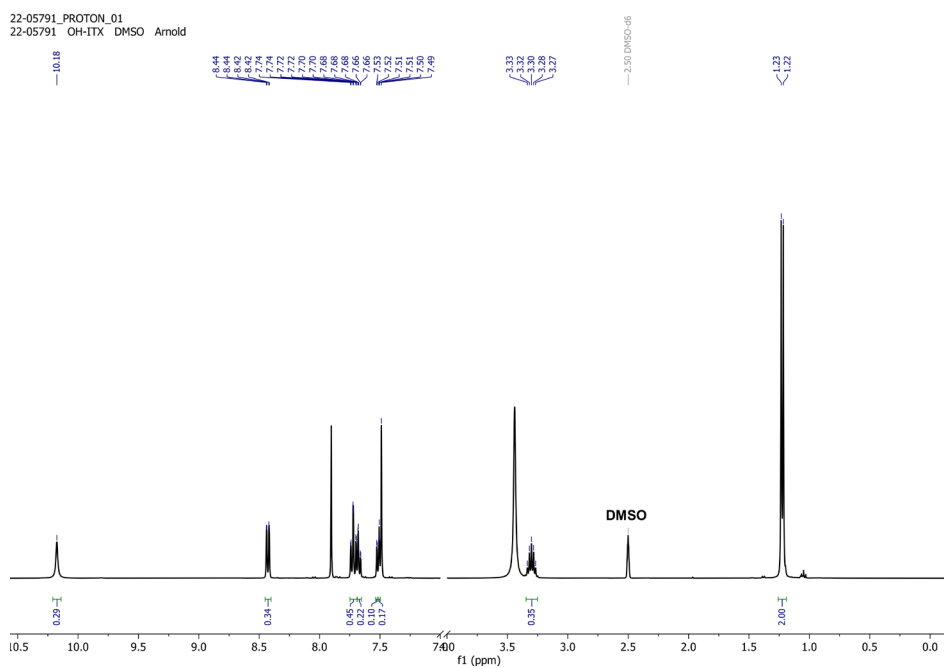


Figure 49: ^1H NMR of OH-ITX; DMSO- d_6 used as solvent

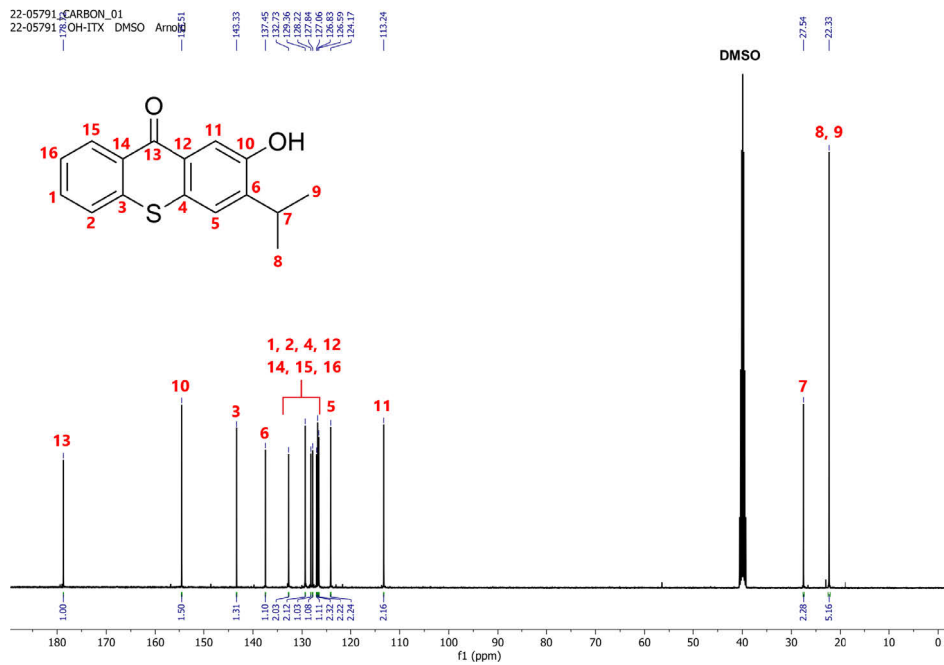


Figure 50: ^{13}C NMR of OH-ITX; DMSO- d_6 used as solvent

After the first step of the photoinitiator synthesis and the drying process of the hydroxy ITX (OH-ITX) has been completed, it has been used as educt in the second step, where 5g Hydroxy-Isopropylthioxanthone (18.5mmol) were dissolved in 200ml of dry Dichloromethane. After the addition of 4g Triethylamine (39.5mmol), the reaction mixture was cooled to 0°C under stirring and kept under Nitrogen atmosphere. Then 2ml of Acryloyl chloride (24.5mmol) were added dropwise through a septum. After stirring for 4h at 0°C, the reaction mixture was further stirred over night at room temperature. Following that, the reaction mixture was carefully washed with 50ml deionized water twice. The organic phase was concentrated on the rotavapor to ~15ml while not exceeding 40°C.

After cooling to 0°C the precipitate was filtered off and washed with Methanol. The filtered product was recrystallized from Methanol and dried under vacuum.^{102,103} *Yield* \approx 60%, *appearance: pale yellow to bright yellow powder; purity* \approx 85% (GC-MS).

¹H NMR (600 MHz, DMSO-d₆, 25°C) δ (ppm) 8.46 (d, J = 8.1 Hz, 1H), 8.14 (s, 1H), 7.91 – 7.85 (m, 2H), 7.79 (t, J = 7.6 Hz, 1H), 7.60 (t, J = 7.6 Hz, 1H), 6.63 (d, J = 17.3 Hz, 1H), 6.50 (dd, J = 17.3, 10.4 Hz, 1H), 6.24 (d, J = 10.4 Hz, 1H), 3.12 – 3.05 (m, 1H), 1.24 (d, J = 6.8 Hz, 6H).

6.4 Migration test for AC-ITX PSA

For the reference system a copolymer made of BA and Acrylic acid has been polymerized, where the ITX was added. Both polymer systems, the reference one and the AC-ITX system have been stripped in the rotary evaporator and direct coatings to 50µm etched PET foil have been made. The 100gsm (80µm) coatings have been irradiated with 3.000 mJ UVA irradiation coming from the 365nm LED and were put into migration cells after 24h of conditioning.

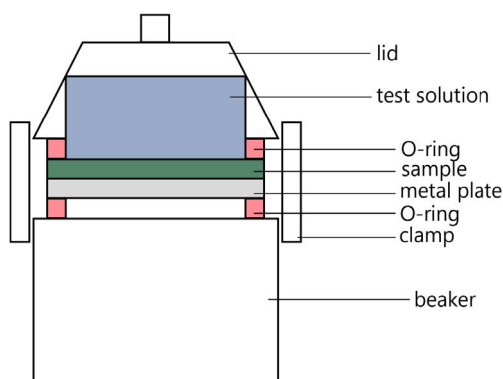


Figure 53: Migration cell for migration testing of AC-ITX modified PSA

All different migration conditions conducted during the tests are displayed in Table 17 below. After the migration test each test solution was analyzed with regard to potential migrated chemicals. As an example, the solutions, those for which the ITX reference samples were tested were analyzed regarding potential ITX content and the solutions where the AC-ITX adhesive was tested in were analyzed with regard to AC-ITX and OH-ITX as the OH ITX was determined as impurity inside the AC-ITX in earlier chapters. All solutions were analyzed via LC-MS against the standard substances.¹²²

Table 17: Test conditions for migration test and resulting simulation

Test condition	Resulting simulation
3% Acetic acid 10 d, 60°C	Contact to Hydrophilic food, especially with pH <4.5
10% Ethanol 10 d, 60°C	Contact to Hydrophilic food, drinks
95% Ethanol 10 d, 60°C	Contact to lipophilic food
Tenax 10 d, 60°C	Contact to "dry" food
0,9% NaCl 72 h, 37°C	Contact to Human skin, according to ISO 10993

6.5 Formulations for Silane promoted Cationic PSA

The investigation of silane promoted cationic PSA was started with the cationic TAS-Sb reference which is Hg bulb curable. In order to achieve better LED curability, the polymer was formulated with twice the molar amount of ITX compared to TAS-Sb. As explained in the results and discussion part, the silanes and siloxanes were used according to the EPOMA amount. In case of ACS-M it was copolymerized equimolar to EPOMA (0.68mol%) together with the other monomers according to the procedure explained in chapter 5.1.

For the other silanes and siloxanes, the exact amounts are displayed in Table 18 below. All additives have been mixed to the solved polymer and the solvent was removed after formulation according to the procedure explained in chapter 5.1, if needed.

Table 18: Amounts of formulated PSA samples; Dry Polymer mass, without solvent

Additive	Dry Polymer in g	TAS-Sb in g	ITX in g	Silane in g	Total in g
CAES-E	21.5	0.05	0.05	0.365	21.965
CAESO-B	21.5	0.05	0.05	0.242	22.742
CAESO-Q	21.5	0.05	0.05	0.233	22.733
CAESO-E+CAESO-Q	21.5	0.05	0.05	combined	22.198

For the samples with the epoxy reactive diluent 15w% according to the total solid mass have been used. The ratio of epoxy reactive diluent is not completely identical for all samples, however, as the difference is very small this influence can be neglected on the test values.

The LSE monomers have been used in a way that the T_g of the later PSA has not been influenced. In order to achieve that parts of the MA or 2-EHA have been replaced with an LSE monomer since their homopolymer T_g varied. As before, the polymerization process has not been changed further and was executed as explained in chapter 5.1. The amount of stabilizer DTC, cationic photoinitiator TAS-Sb and sensitizer ITX was kept the same as before. Exact monomer amounts which have been used are displayed in Table 19 below.

Table 19: Overview of LSE monomer modified PSA

LSE monomer	LSE in w%	MA in w%	2-EHA in w%	EPOMA in w%	AIBN in w%
LSE-A	10	54.3	34.1	1.1	0.5
LSE-B	5	46.5	46.9	1.1	0.5
LSE-C	5	41.5	51.9	1.1	0.5

In order to get to the LSE final formulated PSA sample, the samples have been prepared according to Table 18, where CAES-E and CAES-Q have been combined. However, in this case the LSE-C modified polymer has been used accordingly. As before 15w% of epoxy reactive diluent have been used according to the total solid mass.

The solvent of all samples has been removed as described earlier for cationic PSA at 120°C and 10mbar for 6h, if needed.

6.6 PSA test methods

6.6.1 Shear adhesion failure test (SAFT)

The performance of adhesives can be tested in different standardized tests. Performance of adhesives is strongly connected to adhesion and cohesion values, so most of these tests try to image one or both characteristics. One popular test for measuring cohesion performance is the shear adhesion failure temperature test (SAFT) according to GTF 6001 (Afera 5013).¹²³ During this test the adhesive is put under shear force while a defined weight pulls on it under the impact of increasing temperature. Generally, the test starts at room temperature and the temperature is increased in a constant rate, depending on the adhesive. For acrylic adhesives the temperature ramp is set to 0.5°C / minute.

The adhesive is either directly coated onto its final substrate, e.g. PET and cured, or first coated onto a silicone paper and transferred after curing. Depending on this process either the light side or the dark side of the adhesive will get in contact with the substrate (for UV cured PSA). A stripe of 2.5x7cm is cut and stuck onto a pre cleaned stainless steel plate (Ethylacetate, Acetone) in a way that the bonding area is

2.5x2.5cm². The bonding area is rolled twice with a 2kg roll to ensure the same bonding conditions for all samples. On the other side of the test stripe a hook is fixed in order to attach the desired weight for the measurement, as can be seen in Figure 54.

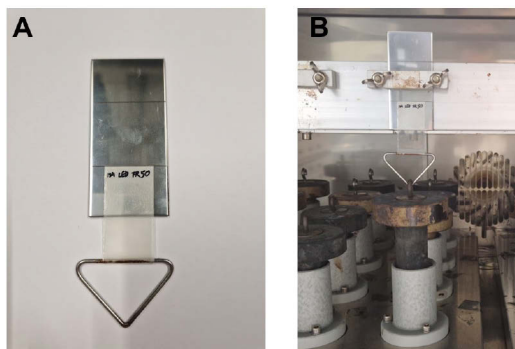


Figure 54: Prepared SAFT sample (A); SAFT sample with attached 1kg weight in the SAFT oven (B)

After a conditioning time of 30 minutes the steel plate with the bonded PSA is mounted onto a metal rack which makes sure that the steel plate is tilted backwards by 2°. This ensures that the force on the adhesive is limited to shear forces only, and no peel forces appear during the test which would otherwise influence the test results. Depending on the adhesive a 0.5 or 1kg weight is attached to the hook on the test stripe so it hangs freely. Now the weight constantly pulls on the PSA on the steel plate with shear forces. The temperature is increased with the determined temperature ramp and the temperature of failure is noticed.

PSAs with a strong cohesion might reach more than 200°C, however this is the maximum temperature which is used for these tests. If an adhesive sample fails during the test, the failure mode is considered. The SAFT allows a prediction of the cohesion level of the adhesive and with that the degree of curing for UV cured PSAs.^{124,125} However, it needs to be said that especially tackified PSAs might be cured completely but still not able to reach maximum SAFT temperature as the tackifier starts melting earlier. This leads to a sample failure at a lower temperature. If an adhesive is expected to reach up to 200°C during the test, however, fails the test at a lower temperature while showing a cohesion failure where adhesive residue is left on the steel plate and the (PET) foil, it can be determined that the elastic modulus was not high enough.^{1,2,124,125} In case of a failed test before the maximum temperature is reached showing an

adhesion failure (AF), this can be connected to an overcured adhesive having an elastic modulus which is too high. Here the adhesion is not strong enough anymore in order to enable a proper cohesion measurement with this test.

6.6.2 Peel tests

Peel values deal with adhesion strength of PSA and is one of the fundamental test methods to investigate the interaction of the adhesive with the surface. As peel strength is as important as cohesive strength to verify an adhesive for a certain application, the methodology can be extended to varying substrates, like stainless steel, glass, low surface energy substrates, etc. including different temperatures where the samples are tested. Due to the carrying temperatures it is possible to measure peel strength below room temperature as well as at elevated temperatures.

Generally, for peel tests a coating is done which again might be done as direct coating onto its final foil (e.g. PET) or it can also be done as a transfer coating where the adhesive is applied onto a silicone paper first, cured and then transferred to its final foil. Adhesive test stripes are cut to 2.5cm x 15cm and conditioned at 23°C, 50% relative humidity. The test substrate e.g. stainless steel is cleaned with solvent and conditioned at the same temperature and humidity as the adhesive stripes. After the conditioning phase the test stripes are stuck to the substrate and rolled twice with a 2kg roll at the same speed. Again, this ensures that all samples are bond with the same force. After 20 minutes of conditioning time the test stripes are pulled from the substrate and the required force is measured, as can be seen in Figure 55. The sample preparation and measurement is done according to Finat FTM1.¹²⁶

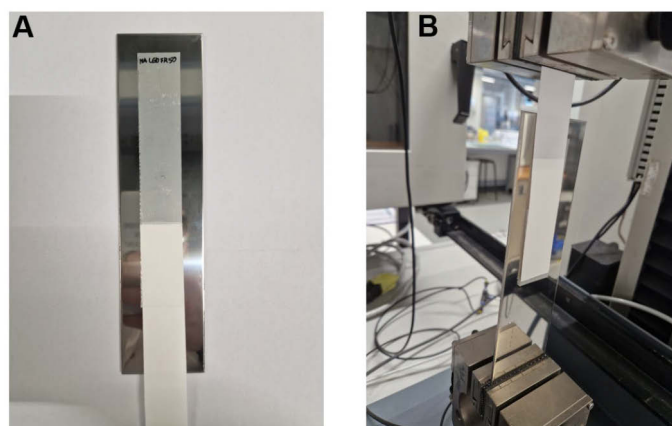


Figure 55: Prepared peel sample on steel (A); testing of peel sample at 180° angle (B)

As this force is depending on the width of the sample, this force is given in N/25mm for this example test stripe. Now there are different ways the adhesive sample can be pulled from the substrate. One of them is to pull at an angle of 90° and the more popular method is to pull at an angle of 180°. Comparing both angles, it is obvious that the force is applied at a different angle and might lead to different peel strengths which makes it important to only compare various peel values which have been measured at the same angle.^{1,11,127} From the perspective of the setup, it is easier to measure at 180° as the substrate does not need to be moved horizontally during the pulling process as it is required in relation to the 90° setup. There might be special applications where a 90° value is of greater interest, but this will not be a focus point in this chapter. When peeling the adhesive stripe from the substrate at 180° angle, different scenarios can occur which are connected to different failure modes. In case of a well crosslinked adhesive with a theoretically high molecular mass the peel failure mode will most presumably result in an adhesion failure.^{1,11,127} Thereby, the test stripe can be peeled from the substrate without leaving any adhesive residues on the substrate. In many applications this failure mode is favored during peel tests as this allows the adjustment of an already applied PSA, e.g. adhesive tape without leaving adhesive residues on the substrate. In case of an adhesive with lower crosslinking level a cohesive failure mode might occur.^{1,11,127} This leads to an adhesive residue on both, the substrate and the carrier foil.

6.6.3 UV rheology

UV rheology can be used as one of the main analytical methods to analyze the curing behavior of crosslinking reaction where the resulting material remains as sticky as in the PSA case.¹²⁸ Analyzing crosslinking of sticky products leads to the fact that sample preparation gets quite difficult for several possible analytical options as the product cannot be solved anymore or cryo sample preparation would be needed. Herewith UV rheology states out as the sample preparation is simple and subject to the setup and the methodology of measurement, different investigations can be done also with the same sample as different methodologies can be linked to each other.^{128–130} Generally, UV rheology can be seen as a combination of standard rheology with in-situ irradiation via fiber optics. The irradiation can be UV light, where different lamp options are possible, but also visible light or NIR irradiation are possible. It was already achieved to combine rheology with NIR analytics while UV irradiating in parallel.¹³¹ For analyzing PSA and their crosslinking reaction a plate-plate geometry is chosen where the lower plate is made of a quartz glass plate as this is transparent to UV light (Figure 5). The adhesive sample is applied as uncured free film onto the upper geometry and the device is run to a measurement gap of 350 μm . As chemical reactions show a direct dependency on temperature and the PSAs used in this work are hotmelt based, the test is done at 130°C which is a popular temperature for the hotmelts to be coated at. This allows to have a measurement which is as close as possible to the real production procedure.

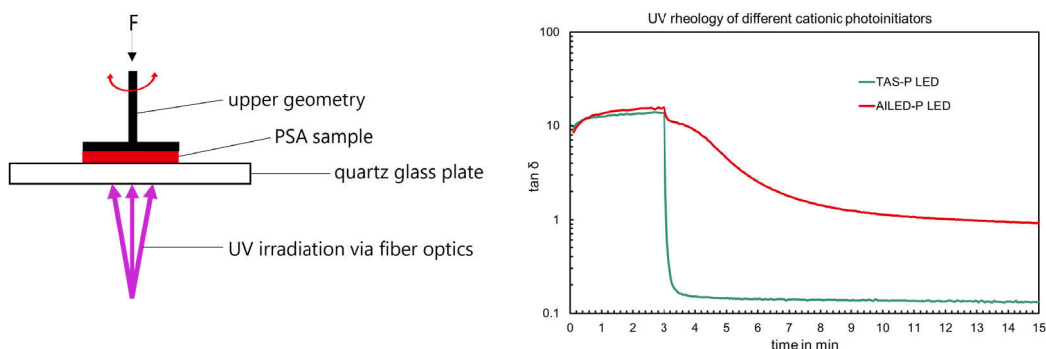


Figure 56: Setup of UV rheology measurement

A MCR2 rheometer from Anton Paar equipped with a Peltier element and a Lumatec Superlite I07 370nm LED was used to measure the curing kinetics of PSA samples. In

order to measure the curing process, the applied sample is conditioned at the elevated temperature so that the sample can adapt to the applied force achieved by 10rad/s oscillation at 1% strain. After 3 minutes of conditioning the UV source is automatically switched on and the sample is cured under ongoing oscillation test. Depending on the investigation it is possible to have the light source permanently switched on until the sample reaches a plateau regarding $\tan \delta$ or by means of another alternative to simply flash the PSA sample with a short light impulse being able to investigate any occurring dark curing reactions regarding the cationic curing technology.⁸⁶ The short light impulse would also be closer to a production setup as the coated PSA will run underneath the UV source quite quickly leading to an effective short irradiation period, possibly less than 1s.

During the crosslinking reaction the polymer changes its viscoelastic behavior as the formation of crosslinked networks leads to an increase in elasticity and loss of viscous parts. As shown by other research groups before this network appears to be inhomogeneous over the surface area with varying mesh sizes and crosslinking densities.¹⁰⁵ However, as a comparable big surface of the PSA is tested at once (often also multilayers in DMA), this effect can be neglected. The network formation results in a decreasing $\tan \delta$ during the irradiation which can be used as indicator for an ongoing crosslinking reaction.^{128–131} Depending how fast $\tan \delta$ decreases and the later plateau level, which is reached, it is possible to state the degree of crosslinking, the efficiency of the curing reaction, crosslinking speed and efficiency of photoinitiator and monomer combination.^{128–131} After the curing reaction has been monitored, it is possible to run further tests with the same cured sample without changing the setup by adding further methodologies.

6.7 Analytical methods

6.7.1 Gel permeation chromatography (GPC)

GPC measurements for all polyacrylates were done with a Waters alliance e2695 combined with Waters 2414 EI and 2489 UV detectors. The GPC was equipped with a

column oven. First a precolumn was used, which led to two main PL Gel mixed B 300mm columns (7.5mm inner diameter) equipped with 10 μ m particle size. Tetrahydrofuran was used as solvent.¹³²

6.7.2 Infrared spectroscopy (IR)

IR measurements were done with a Perkin Elmer Spectrum Two equipped with an ATR-IR unit. All samples were measured at 0.2cm/s with a resolution of 4cm⁻¹ between 4000cm⁻¹ and 450cm⁻¹ coming from a MIR laser and detected with a LiTaO₃ detector.¹³³

6.7.3 Nuclear Magnetic Resonance (NMR)

Measurements for ¹H NMR and ¹³C NMR analytics of OH-ITX and AC-ITX were done with an Agilent MR400 at a maximum field strength of 400MHz. All measurements were done with 32 scans at 25°C and samples have been solved in DMSO-d₆.¹³⁴

6.7.4 Differential scanning calorimetry (DSC)

DSC measurements were carried out using a TA DSC Q2000 V24.4 Build 116 equipped with a DSC Standard Cell RC. Approximately 50mg of cured PSA sample were placed in an Al-crucible 2.5g, lid with holes. The measurement was carried out under Nitrogen at a flow rate of 3l/h with a temperature increase of 10K/min starting at -90°C and ending at 185°C. All measurements were executed in two measurement cycles.¹³⁵

6.7.5 UV/VIS Absorption

UV/VIS absorption of photoinitiators and sensitizers was made using a Perkin Elmer Lambda850 dual beam photometer equipped with a grating monochromator and a Lead

sulfide photomultiplier. All samples have been dissolved in Acetonitrile and measured in 1cm cuvettes at 25°C.¹³⁶

6.7.6 Dynamic mechanical analysis (DMA)

DMA tests were executed with a TA Discovery HR-2 rheometer with plate-plate setup. The rheometer was connected to a Lauda Proline RP845 cooling unit. Cured samples were prepared as free films and stacked up to 1200µm thickness afterwards. A sample in 20mm diameter was applied and conditioned for 3 minutes at 160°C. After that the sample was cooled to -25°C with a temperature gradient of 2°C/min while applying an oscillation at 10rad/s, 1% strain and 2N normal force.

6.7.7 Soxhlet extraction

In order to determine the gel content of certain PSA samples, a Soxhlet extraction with 100g Ethylacetate was done over 5h at the boiling point. The cellulose capsule was dried and filled with 0.25g of cured PSA. After the extraction, the capsule containing the PSA residue was dried again and the gel content was calculated according to Equation 2.

$$g_{\%} = \frac{100 * (m_{total} - m_{capsule})}{m_{sample}}$$

Equation 1: Gel content determination

6.7.8 Atomic force microscopy (AFM)

AFM measurements of steel and PP substrate were executed with a Cantilever NCSTR-10 from Nano World in tapping mode. An area of 50µm x 50µm was analyzed after the substrates have been cleaned with Argon and the roughness parameters/ topography parameters for the respective surface areas has been determined.¹³⁷

6.8 PSA sample preparation and UV curing

PSA samples were prepared on an Elcometer 4340 applicator. The solved PSA was applied on silicone release paper using a syringe. Under a constant speed the PSA was spread evenly on the silicone paper via respective coater knife. After that the solvent was evaporated at 110°C in an Vötsch VTL 60/60 oven for 3 minutes in case of sample preparation coming from solution. After the solvent has been evaporated, the PSA samples were preheated in the same oven at the identical temperature and cured in a Loctite LED Flood Chamber equipped with an EQ CL30 365nm LED Flood. Cured PSA samples have been conditioned at room temperature and 50% rel. humidity over 24h before they were tested.

7. References

- (1) Silva, L. F. M. d., Ed. *Handbook of Adhesion Technology*; SpringerLink Bücher; Springer Berlin Heidelberg, 2011. DOI: 10.1007/978-3-642-01169-6.
- (2) Benedek, I.; Feldstein, M. M. *Technology of pressure-sensitive adhesives and products*; Handbook of Pressure-Sensitive Adhesives and Products.
- (3) Johnston, J. *Pressure sensitive adhesive Tapes: A Guide to their Function, Design, Manufacture, and Use*; Pressure Sensitive Tape Council, 2003.
- (4) Fitzgerald, D. M.; Colson, Y. L.; Grinstaff, M. W. Synthetic pressure sensitive adhesives for biomedical applications. *Progress in Polymer Science* **2023**, *142*, 101692. DOI: 10.1016/j.progpolymsci.2023.101692.
- (5) Elder, T.; Croll, A. B. Roughness tolerant pressure sensitive adhesives made of sticky crumpled sheets. *Soft matter* **2022**, *18* (40), 7866–7876. DOI: 10.1039/d2sm00858k. Published Online: Oct. 19, 2022.
- (6) Creton, C. Pressure-Sensitive Adhesives: An Introductory Course. *MRS Bull.* **2003**, *28* (6), 434–439. DOI: 10.1557/mrs2003.124.
- (7) Abu Bakar, R.; Hepburn, K. S.; Keddie, J. L.; Roth, P. J. Degradable, Ultraviolet-Crosslinked Pressure-Sensitive Adhesives Made from Thioester-Functional Acrylate Copolymers. *Angewandte Chemie (International ed. in English)* **2023**, *62* (34), e202307009. DOI: 10.1002/anie.202307009. Published Online: Jul. 13, 2023.
- (8) Elias, H.-G. Free-Radical Polymerization. In *Chemical structures and syntheses*, 1. ed., 1. reprint; Elias, H.-G., Ed.; Macromolecules / Hans-Georg Elias, Vol. 1; Wiley-VCH, 2010; pp 309–367. DOI: 10.1002/9783527627219.ch10.
- (9) Matyjaszewski, K.; Davis, T. P., Eds. *Handbook of radical polymerization*; Wiley-Interscience, 2002. DOI: 10.1002/0471220450.
- (10) Moad, G. *The chemistry of radical polymerization*, 2nd ed.; Elsevier, 2006.
- (11) Pandey, V.; Fleury, A.; Villey, R.; Creton, C.; Ciccotti, M. Linking peel and tack performances of pressure sensitive adhesives. *Soft matter* **2020**, *16* (13), 3267–3275. DOI: 10.1039/c9sm02172h.
- (12) Fouassier, J.-P. *Photoinitiators for polymer synthesis: Scope, reactivity and efficiency*; Wiley-VCH, 2012. DOI: 10.1002/9783527648245.

- (13) Liska, R. Industrial Photoinitiators: A Technical Guide . by W. Arthur Green. *ChemPhysChem* **2011**, 12 (7), 1389. DOI: 10.1002/cphc.201000542.
- (14) Understand the facts about UV-C LEDs and germicidal applications (MAGAZINE). *LEDs Magazine*, Oct 8, 2020. <https://www.ledsmagazine.com/lighting-health-wellbeing/article/14183833/understand-the-facts-about-uv-c-leds-and-germicidal-applications-magazine> (accessed 2023-09-06.554Z).
- (15) Winkler, H.; Bodrogi, P.; Trinh, Q.; Khanh, T. Q., Eds. *LED lighting: Technology and perception*; Wiley-VCH, 2015. DOI: 10.1002/9783527670147.
- (16) Kaya, K.; Kiliclar, H. C.; Yagci, Y. Photochemically generated ionic species for cationic and step-growth polymerizations. *European Polymer Journal* **2023**, 190, 112000. DOI: 10.1016/j.eurpolymj.2023.112000.
- (17) Sun, K.; Xiao, P.; Dumur, F.; Lalevée, J. Organic dye-based photoinitiating systems for visible-light-induced photopolymerization. *Journal of Polymer Science* **2021**, 59 (13), 1338–1389. DOI: 10.1002/pol.20210225.
- (18) Wang, Q.; Popov, S.; Strehmel, V.; Gutmann, J. S.; Strehmel, B. NIR-sensitized hybrid radical and cationic photopolymerization of several cyanines in combination with diaryliodonium bis(trifluoromethyl)sulfonyl imide. *Polym. Chem.* **2023**, 14 (2), 116–125. DOI: 10.1039/D2PY01186G.
- (19) Husár, B.; Ligon, S. C.; Wutzel, H.; Hoffmann, H.; Liska, R. The formulator's guide to anti-oxygen inhibition additives. *Progress in Organic Coatings* **2014**, 77 (11), 1789–1798. DOI: 10.1016/j.porgcoat.2014.06.005.
- (20) Ligon, S. C.; Husár, B.; Wutzel, H.; Holman, R.; Liska, R. Strategies to reduce oxygen inhibition in photoinduced polymerization. *Chemical reviews* **2014**, 114 (1), 557–589. DOI: 10.1021/cr3005197. Published Online: Oct. 1, 2013.
- (21) Crivello, J. V. Effect of Temperature on the Cationic Photopolymerization of Epoxides. *Journal of Macromolecular Science, Part A* **2008**, 45 (8), 591–598. DOI: 10.1080/10601320802168710.
- (22) Wagner, A.; Mühlberger, M.; Paulik, C. Photoinitiator-free photopolymerization of acrylate-bismaleimide mixtures and their application for inkjet printing. *J Appl Polym Sci* **2019**, 136 (29), 47789. DOI: 10.1002/app.47789.
- (23) Dumur, F. Recent advances on photobleachable visible light photoinitiators of polymerization. *European Polymer Journal* **2023**, 186, 111874. DOI: 10.1016/j.eurpolymj.2023.111874.

- (24) Müller, S. M.; Schlögl, S.; Wiesner, T.; Haas, M.; Griesser, T. Recent Advances in Type I Photoinitiators for Visible Light Induced Photopolymerization. *ChemPhotoChem* **2022**, 6 (11). DOI: 10.1002/cptc.202200091.
- (25) Petko, F.; Świeży, A.; Jankowska, M.; Stalmach, P.; Ortyl, J. Push–pull coumarin-based one-component iodonium photoinitiators for cationic nanocomposite 3D-VAT printing. *Polym. Chem.* **2023**, 14 (25), 3018–3034. DOI: 10.1039/D3PY00359K.
- (26) Bulut, U.; Crivello, J. V. Investigation of the Reactivity of Epoxide Monomers in Photoinitiated Cationic Polymerization. *Macromolecules* **2005**, 38 (9), 3584–3595. DOI: 10.1021/ma050106k.
- (27) Crivello, J. V. Cationic polymerization — Iodonium and sulfonium salt photoinitiators. In *Initiators - Poly-Reactions - Optical Activity*; Cantow, H.-J., Dall'Asta, G., Dušek, K., Ferry, J. D., Fujita, H., Gordon, M., Henrici-Olivé, G., Heublein, H. G., Höcker, H., Kennedy, J. P., Kern, W., Okamura, S., Olivé, S., Overberger, C. G., Saegusa, T., Schulz, G. V., Slichter, W. P., Stille, J. K., Eds.; Advances in Polymer Science, Vol. 62; Springer, 1984; pp 1–48. DOI: 10.1007/BFb0024034.
- (28) Park, S.; Kilgallon, L. J.; Yang, Z.; Du Ryu, Y.; Ryu, C. Y. Molecular Origin of the Induction Period in Photoinitiated Cationic Polymerization of Epoxies and Oxetanes. *Macromolecules* **2019**, 52 (3), 1158–1165. DOI: 10.1021/acs.macromol.8b02486.
- (29) Sangermano, M. Advances in cationic photopolymerization. *Pure and Applied Chemistry* **2012**, 84 (10), 2089–2101. DOI: 10.1351/PAC-CON-12-04-11.
- (30) Sangermano, M.; Razza, N.; Crivello, J. V. Cationic UV-Curing: Technology and Applications. *Macromol. Mater. Eng.* **2014**, 299 (7), 775–793. DOI: 10.1002/mame.201300349.
- (31) Pham, H. Q.; Marks, M. J. Epoxy Resins. In *Ullmann's encyclopedia of industrial chemistry*, 6., compl. rev. ed.; Bohnet, M., Ullmann, F., Eds.; Wiley-VCH, 2003. DOI: 10.1002/14356007.a09_547.pub2.
- (32) Bulut, U.; Crivello, J. V. Reactivity of oxetane monomers in photoinitiated cationic polymerization. *J. Polym. Sci. A Polym. Chem.* **2005**, 43 (15), 3205–3220. DOI: 10.1002/pola.20723.

- (33) Crivello, J. V.; Bulut, U. Photoactivated cationic ring-opening frontal polymerizations of oxetanes. *Designed Monomers and Polymers* **2005**, *8* (6), 517–531. DOI: 10.1163/156855505774597803.
- (34) Klikovits, N.; Knaack, P.; Bomze, D.; Krossing, I.; Liska, R. Novel photoacid generators for cationic photopolymerization. *Polym. Chem.* **2017**, *8* (30), 4414–4421. DOI: 10.1039/C7PY00855D.
- (35) Zivic, N.; Kuroishi, P. K.; Dumur, F.; Gigmès, D.; Dove, A. P.; Sardon, H. Recent Advances and Challenges in the Design of Organic Photoacid and Photobase Generators for Polymerizations. *Angewandte Chemie (International ed. in English)* **2019**, *58* (31), 10410–10422. DOI: 10.1002/anie.201810118. Published Online: Apr. 29, 2019.
- (36) Crivello, J. V. The discovery and development of onium salt cationic photoinitiators. *J. Polym. Sci. A Polym. Chem.* **1999**, *37* (23), 4241–4254. DOI: 10.1002/(SICI)1099-0518(19991201)37:23<4241:AID-POLA1>3.0.CO;2-R.
- (37) Taschner, R.; Liska, R.; Knaack, P. Evaluation of suitable onium tetrafluoroborates for cationic polymerization of epoxides. *Polymer International* **2022**, *71* (7), 804–816. DOI: 10.1002/pi.6330.
- (38) Irshadeen, I. M.; Walden, S. L.; Wegener, M.; Truong, V. X.; Frisch, H.; Blinco, J. P.; Barner-Kowollik, C. Action Plots in Action: In-Depth Insights into Photochemical Reactivity. *Journal of the American Chemical Society* **2021**, *143* (50), 21113–21126. DOI: 10.1021/jacs.1c09419. Published Online: Dec. 3, 2021.
- (39) Dumur, F. Recent advances on diaryliodonium-based monocomponent photoinitiating systems. *European Polymer Journal* **2023**, *195*, 112193. DOI: 10.1016/j.eurpolymj.2023.112193.
- (40) Kirschner, J.; Paillard, J.; Bouzrati-Zerelli, M.; Becht, J.-M.; Klee, J. E.; Chelli, S.; Lakhdar, S.; Lalevée, J. Aryliodonium Ylides as Novel and Efficient Additives for Radical Chemistry: Example in Camphorquinone (CQ)/Amine Based Photoinitiating Systems. *Molecules (Basel, Switzerland)* **2019**, *24* (16). DOI: 10.3390/molecules24162913. Published Online: Aug. 11, 2019.
- (41) Zhang, L.; Li, L.; Chen, Y.; Pi, J.; Liu, R.; Zhu, Y. Recent Advances and Challenges in Long Wavelength Sensitive Cationic Photoinitiating Systems. *Polymers* **2023**, *15* (11). DOI: 10.3390/polym15112524. Published Online: May. 30, 2023.
- (42) Fařcasu, D.; Hâncu, D. Acid strength of tetrafluoroboric acid The hydronium ion as a superacid and the inapplicability of water as an indicator

of acid strength. *Faraday Trans.* **1997**, 93 (12), 2161–2165. DOI: 10.1039/a700798a.

(43) Petko, F.; Galek, M.; Hola, E.; Popielarz, R.; Ortyl, J. One-Component Cationic Photoinitiators from Tunable Benzylidene Scaffolds for 3D Printing Applications. *Macromolecules* **2021**, 54 (15), 7070–7087. DOI: 10.1021/acs.macromol.1c01048.

(44) Michaudel, Q.; Kottisch, V.; Fors, B. P. Cationic Polymerization: From Photoinitiation to Photocontrol. *Angewandte Chemie (International ed. in English)* **2017**, 56 (33), 9670–9679. DOI: 10.1002/anie.201701425. Published Online: Jun. 30, 2017.

(45) Höfer, M.; Liska, R. Photochemistry and initiation behavior of phenylethynyl onium salts as cationic photoinitiators. *J. Polym. Sci. A Polym. Chem.* **2009**, 47 (13), 3419–3430. DOI: 10.1002/pola.23423.

(46) Boonlert-Uthai, T.; Taki, K.; Somwangthanaroj, A. Curing Behavior, Rheological, and Thermal Properties of DGEBA Modified with Synthesized BPA/PEG Hyperbranched Epoxy after Their Photo-Initiated Cationic Polymerization. *Polymers* **2020**, 12 (10). DOI: 10.3390/polym12102240. Published Online: Sep. 29, 2020.

(47) Kubisa, P. Hyperbranched polyethers by ring-opening polymerization: Contribution of activated monomer mechanism. *J. Polym. Sci. A Polym. Chem.* **2003**, 41 (4), 457–468. DOI: 10.1002/pola.10605.

(48) Penczek, S.; Pretula, J. Activated Monomer Mechanism (AMM) in Cationic Ring-Opening Polymerization. The Origin of the AMM and Further Development in Polymerization of Cyclic Esters. *ACS macro letters* **2021**, 10 (11), 1377–1397. DOI: 10.1021/acsmacrolett.1c00509. Published Online: Oct. 19, 2021.

(49) Sciancalepore, C.; Bondioli, F.; Messori, M. Non-hydrolytic sol–gel synthesis and reactive suspension method: an innovative approach to obtain magnetite–epoxy nanocomposite materials. *J Sol-Gel Sci Technol* **2017**, 81 (1), 69–83. DOI: 10.1007/s10971-016-4095-z.

(50) Mokbel, H.; Anderson, D.; Plenderleith, R.; Dietlin, C.; Morlet-Savary, F.; Dumur, F.; Gigmès, D.; Fouassier, J. P.; Lalevée, J. Simultaneous initiation of radical and cationic polymerization reactions using the “G1” copper complex as photoredox catalyst: Applications of free radical/cationic hybrid photopolymerization in the composites and 3D printing fields. *Progress in Organic Coatings* **2019**, 132, 50–61. DOI: 10.1016/j.porgcoat.2019.02.044.

- (51) Malik, M. S.; Schlögl, S.; Wolfahrt, M.; Sangermano, M. Review on UV-Induced Cationic Frontal Polymerization of Epoxy Monomers. *Polymers* **2020**, *12* (9). DOI: 10.3390/polym12092146. Published Online: Sep. 20, 2020.
- (52) Menzel, J. P.; Noble, B. B.; Blinco, J. P.; Barner-Kowollik, C. Predicting wavelength-dependent photochemical reactivity and selectivity. *Nature communications* **2021**, *12* (1), 1691. DOI: 10.1038/s41467-021-21797-x. Published Online: Mar. 16, 2021.
- (53) Abdallah, M.; Hijazi, A.; Dumur, F.; Lalevée, J. Coumarins as Powerful Photosensitizers for the Cationic Polymerization of Epoxy-Silicones under Near-UV and Visible Light and Applications for 3D Printing Technology. *Molecules (Basel, Switzerland)* **2020**, *25* (9). DOI: 10.3390/molecules25092063. Published Online: Apr. 28, 2020.
- (54) Dumur, F. Recent advances on ferrocene-based photoinitiating systems. *European Polymer Journal* **2021**, *147*, 110328. DOI: 10.1016/j.eurpolymj.2021.110328.
- (55) Erdur, S.; Yilmaz, G.; Goen Colak, D.; Cianga, I.; Yagci, Y. Poly(phenylenevinylene)s as Sensitizers for Visible Light Induced Cationic Polymerization. *Macromolecules* **2014**, *47* (21), 7296–7302. DOI: 10.1021/ma5019457.
- (56) Hola, E.; Fiedor, P.; Dzienia, A.; Ortyl, J. Visible-Light Amine Thioxanthone Derivatives as Photoredox Catalysts for Photopolymerization Processes. *ACS Appl. Polym. Mater.* **2021**, *3* (11), 5547–5558. DOI: 10.1021/acsapm.1c00886.
- (57) Hola, E.; Pilch, M.; Ortyl, J. Thioxanthone Derivatives as a New Class of Organic Photocatalysts for Photopolymerisation Processes and the 3D Printing of Photocurable Resins under Visible Light. *Catalysts* **2020**, *10* (8), 903. DOI: 10.3390/catal10080903.
- (58) Peter Pappas, S.; Pappas, B. C.; Gatechair, L. R.; Jilek, J. H.; Schnabel, W. Photoinitiation of cationic polymerization. IV. Direct and sensitized photolysis of aryl iodonium and sulfonium salts. *Polymer Photochemistry* **1984**, *5* (1), 1–22. DOI: 10.1016/0144-2880(84)90018-6.
- (59) Coban, Z. G.; Kiliclar, H. C.; Yagci, Y. Photoinitiated Cationic Ring-Opening Polymerization of Octamethylcyclotetrasiloxane. *Molecules (Basel, Switzerland)* **2023**, *28* (3). DOI: 10.3390/molecules28031299. Published Online: Jan. 29, 2023.

- (60) Wang, D.; Garra, P.; Fouassier, J. P.; Lalevée, J. Silane/iodonium salt as redox/thermal/photoinitiating systems in radical and cationic polymerizations for laser write and composites. *Polym. Chem.* **2020**, *11* (4), 857–866. DOI: 10.1039/C9PY01819K.
- (61) Pang, Y.; Jiao, H.; Zou, Y.; Strehmel, B. The NIR-sensitized cationic photopolymerization of oxetanes in combination with epoxide and acrylate monomers. *Polym. Chem.* **2021**, *12* (40), 5752–5759. DOI: 10.1039/D1PY00999K.
- (62) Xin, Y.; Xiao, S.; Pang, Y.; Zou, Y. NIR-sensitized cationic frontal polymerization of vinyl ether and epoxy monomers. *Progress in Organic Coatings* **2021**, *153*, 106149. DOI: 10.1016/j.porgcoat.2021.106149.
- (63) Chen, G.; Vahidifar, A.; Yu, S.; Mekonnen, T. H. Optimization of silane modification and moisture curing for EPDM toward improved physicomechanical properties. *Reactive and Functional Polymers* **2023**, *182*, 105467. DOI: 10.1016/j.reactfunctpolym.2022.105467.
- (64) Narewska, J.; Strzelczyk, R.; Podsiadły, R. Fluoroflavin dyes as electron transfer photosensitizers for onium salt induced cationic photopolymerization. *Journal of Photochemistry and Photobiology A: Chemistry* **2010**, *212* (1), 68–74. DOI: 10.1016/j.jphotochem.2010.03.018.
- (65) Brusciotti, F.; Snihirova, D. V.; Xue, H.; Montemor, M. F.; Lamaka, S. V.; Ferreira, M. G.S. Hybrid epoxy–silane coatings for improved corrosion protection of Mg alloy. *Corrosion Science* **2013**, *67*, 82–90. DOI: 10.1016/j.corsci.2012.10.013.
- (66) Seok, W. C.; Park, J. H.; Song, H. J. Effect of silane acrylate on the surface properties, adhesive performance, and rheological behavior of acrylic pressure sensitive adhesives for flexible displays. *Journal of Industrial and Engineering Chemistry* **2022**, *111*, 98–110. DOI: 10.1016/j.jiec.2022.03.040.
- (67) Babu, L. K.; Mishra, K.; Hamim, S. U.; Singh, R. P. Effect of excess silane on the viscoelastic behavior of epoxy under hygrothermal conditions. *International Journal of Adhesion and Adhesives* **2018**, *84*, 80–85. DOI: 10.1016/j.ijadhadh.2018.03.002.
- (68) Berzins, R.; Merijs-Meri, R.; Zicans, J. Research of Potential Catalysts for Two-Component Silyl-Terminated Prepolymer/Epoxy Resin Adhesives. *Polymers* **2023**, *15* (10). DOI: 10.3390/polym15102269. Published Online: May. 11, 2023.

- (69) Cullen, M.; Kaworek, A.; Mohan, J.; Duffy, B.; Oubaha, M. An investigation into the Role of the Acid Catalyst on the Structure and Anticorrosion Properties of Hybrid Sol-Gel Coatings. *Thin Solid Films* **2021**, *729*, 138703. DOI: 10.1016/j.tsf.2021.138703.
- (70) Al-Saadi, S.; Singh Raman, R. K. Silane Coatings for Corrosion and Microbiologically Influenced Corrosion Resistance of Mild Steel: A Review. *Materials (Basel, Switzerland)* **2022**, *15* (21). DOI: 10.3390/ma15217809. Published Online: Nov. 5, 2022.
- (71) Alamán, J.; López-Valdeolivas, M.; Alicante, R.; Medel, F. J.; Silva-Treviño, J.; Peña, J. I.; Sánchez-Somolinos, C. Photoacid catalyzed organic–inorganic hybrid inks for the manufacturing of inkjet-printed photonic devices. *J. Mater. Chem. C* **2018**, *6* (15), 3882–3894. DOI: 10.1039/C7TC05178F.
- (72) Chemtob, A.; Belon, C.; Croutxé-Barghorn, C.; Brendlé, J.; Soulard, M.; Rigolet, S.; Le Houérou, V.; Gauthier, C. Bridged polysilsesquioxane films via photoinduced sol–gel chemistry. *New J. Chem.* **2010**, *34* (6), 1068. DOI: 10.1039/b9nj00763f.
- (73) Kowalewska, A. Photoacid catalyzed sol–gel process. *J. Mater. Chem.* **2005**, *15* (47), 4997. DOI: 10.1039/b508212a.
- (74) Oku, A.; Okano, M.; Oda, R. The Peroxide-induced Polymerization of Epoxides. *BCSJ* **1964**, *37* (4), 570–575. DOI: 10.1246/bcsj.37.570.
- (75) Vega, J.; Aguilar, M.; Peón, J.; Pastor, D.; Martínez-Salazar, J. Effect of long chain branching on linear-viscoelastic melt properties of polyolefins. *e-Polymers* **2002**, *2* (1). DOI: 10.1515/epoly.2002.2.1.624.
- (76) Kaur, G.; Agboluaje, M.; Hutchinson, R. A. Measurement and Modeling of Semi-Batch Solution Radical Copolymerization of N-tert-Butyl Acrylamide with Methyl Acrylate in Ethanol/Water. *Polymers* **2022**, *15* (1). DOI: 10.3390/polym15010215. Published Online: Dec. 31, 2022.
- (77) Nguyen, T. P. T.; Barroca-Aubry, N.; Aymes-Chodur, C.; Dragoe, D.; Pembouong, G.; Roger, P. Copolymers Derived from Two Active Esters: Synthesis, Characterization, Thermal Properties, and Reactivity in Post-Modification. *Molecules (Basel, Switzerland)* **2022**, *27* (20). DOI: 10.3390/molecules27206827. Published Online: Oct. 12, 2022.
- (78) Li, L.; Wan, M.; Li, Z.; Luo, Y.; Wu, S.; Liu, X.; Yagci, Y. Coumarinacyl Anilinium Salt: A Versatile Visible and NIR Photoinitiator for Cationic and

Step-Growth Polymerizations. *ACS macro letters* **2023**, 12 (2), 263–268. DOI: 10.1021/acsmacrolett.2c00675. Published Online: Feb. 3, 2023.

(79) Sangermano, M.; Roppolo, I.; Chiappone, A. New Horizons in Cationic Photopolymerization. *Polymers* **2018**, 10 (2). DOI: 10.3390/polym10020136. Published Online: Jan. 31, 2018.

(80) Noè, C.; Hakkarainen, M.; Sangermano, M. Cationic UV-Curing of Epoxidized Biobased Resins. *Polymers* **2020**, 13 (1). DOI: 10.3390/polym13010089. Published Online: Dec. 28, 2020.

(81) Liu, S.; Borjigin, T.; Schmitt, M.; Morlet-Savary, F.; Xiao, P.; Lalevée, J. High-Performance Photoinitiating Systems for LED-Induced Photopolymerization. *Polymers* **2023**, 15 (2). DOI: 10.3390/polym15020342. Published Online: Jan. 9, 2023.

(82) Stiles, A.; Tison, T.-A.; Pruitt, L.; Vaidya, U. Photoinitiator Selection and Concentration in Photopolymer Formulations towards Large-Format Additive Manufacturing. *Polymers* **2022**, 14 (13). DOI: 10.3390/polym14132708. Published Online: Jul. 1, 2022.

(83) Lebedevaite, M.; Ostrauskaite, J.; Skliutas, E.; Malinauskas, M. Photocross-linked polymers based on plant-derived monomers for potential application in optical 3D printing. *J Appl Polym Sci* **2020**, 137 (20). DOI: 10.1002/app.48708.

(84) Yang, L.; Yang, J.; Nie, J.; Zhu, X. Temperature controlled cationic photocuring of a thick, dark composite. *RSC Adv.* **2017**, 7 (7), 4046–4053. DOI: 10.1039/C6RA25346F.

(85) Ghazali, S. K.; Adrus, N.; Majid, R. A.; Ali, F.; Jamaluddin, J. UV-LED as a New Emerging Tool for Curable Polyurethane Acrylate Hydrophobic Coating. *Polymers* **2021**, 13 (4). DOI: 10.3390/polym13040487. Published Online: Feb. 4, 2021.

(86) Golaz, B.; Michaud, V.; Leterrier, Y.; Manson, J.-A.E. UV intensity, temperature and dark-curing effects in cationic photo-polymerization of a cycloaliphatic epoxy resin. *Polymer* **2012**, 53 (10), 2038–2048. DOI: 10.1016/j.polymer.2012.03.025.

(87) Dorléans, V.; Delille, R.; Notta-Cuvier, D.; Lauro, F.; Michau, E. Time-temperature superposition in viscoelasticity and viscoplasticity for thermoplastics. *Polymer Testing* **2021**, 101, 107287. DOI: 10.1016/j.polymertesting.2021.107287.

- (88) Aoshima, S.; Kanaoka, S. A renaissance in living cationic polymerization. *Chemical reviews* **2009**, *109* (11), 5245–5287. DOI: 10.1021/cr900225g.
- (89) Penczek, S.; Pretula, J.; Slomkowski, S. Ring-opening polymerization. *Chemistry Teacher International* **2021**, *3* (2), 33–57. DOI: 10.1515/cti-2020-0028.
- (90) Matyjaszewski, K. *Cationic Polymerizations: Mechanisms, Synthesis and Applications*; Plastics Engineering Ser, v.35; Taylor & Francis Group, 1996.
- (91) Professor Paula Hammond. *Lecture 25: “Living” Cationic Polymerizations, Examples of Cationic Polymerization, Isobutyl Rubber Synthesis, Polyvinyl Ethers*: 10.569 *Synthesis of Polymers Fall 2006 materials*, 2023.
- (92) Hoti, G.; Caldera, F.; Cecone, C.; Rubin Pedrazzo, A.; Anceschi, A.; Appleton, S. L.; Khazaei Monfared, Y.; Trotta, F. Effect of the Cross-Linking Density on the Swelling and Rheological Behavior of Ester-Bridged β - Cyclodextrin Nanosponges. *Materials (Basel, Switzerland)* **2021**, *14* (3). DOI: 10.3390/ma14030478. Published Online: Jan. 20, 2021.
- (93) Lee, J.-H.; Shim, G.-S.; Park, J.-W.; Kim, H.-J.; Kim, Y. Adhesion performance and recovery of acrylic pressure-sensitive adhesives thermally crosslinked with styrene–isoprene–styrene elastomer blends for flexible display applications. *Journal of Industrial and Engineering Chemistry* **2019**, *78*, 461–467. DOI: 10.1016/j.jiec.2019.05.019.
- (94) Tsuji, Y.; Li, X.; Shibayama, M. Evaluation of Mesh Size in Model Polymer Networks Consisting of Tetra-Arm and Linear Poly(ethylene glycol)s. *Gels (Basel, Switzerland)* **2018**, *4* (2). DOI: 10.3390/gels4020050. Published Online: May. 25, 2018.
- (95) Finlayson, L.; Barnard, I. R. M.; McMillan, L.; Ibbotson, S. H.; Brown, C. T. A.; Eadie, E.; Wood, K. Depth Penetration of Light into Skin as a Function of Wavelength from 200 to 1000 nm. *Photochemistry and photobiology* **2022**, *98* (4), 974–981. DOI: 10.1111/php.13550. Published Online: Nov. 9, 2021.
- (96) Elias, H.-G., Ed. *Chemical structures and syntheses*, 1. ed., 1. reprint; Macromolecules / Hans-Georg Elias, Vol. 1; Wiley-VCH, 2010. DOI: 10.1002/9783527627219.
- (97) Fordham, P. J.; Gramshaw, J. W.; Castle, L. Analysis for organic residues from aids to polymerization used to make plastics intended for food contact. *Food additives and contaminants* **2001**, *18* (5), 461–471. DOI: 10.1080/02652030119958.

- (98) Moad, G. A Critical Assessment of the Kinetics and Mechanism of Initiation of Radical Polymerization with Commercially Available Dialkyldiazene Initiators. *Progress in Polymer Science* **2019**, *88*, 130–188. DOI: 10.1016/j.progpolymsci.2018.08.003.
- (99) Upadhyay, L. S. B.; Kumar, N. Chapter 21 - Nanocarriers: A boon to the drug delivery systems. In *Advances in nanotechnology-based drug delivery systems*; Talukdar, A. D., Sarker, S. D., Patra, J. K., Eds.; Nanotechnology in biomedicine; Elsevier, 2022; pp 555–584. DOI: 10.1016/B978-0-323-88450-1.00019-3.
- (100) Chang, N.-F.; Chen, Y.-S.; Lin, Y.-J.; Tai, T.-H.; Chen, A.-N.; Huang, C.-H.; Lin, C.-C. Study of Hydroquinone Mediated Cytotoxicity and Hypopigmentation Effects from UVB-Irradiated Arbutin and DeoxyArbutin. *International journal of molecular sciences* **2017**, *18* (5). DOI: 10.3390/ijms18050969. Published Online: May. 3, 2017.
- (101) Lima, M. S.; Costa, C. S. M. F.; Coelho, J. F. J.; Fonseca, A. C.; Serra, A. C. A simple strategy toward the substitution of styrene by sobrerol-based monomers in unsaturated polyester resins. *Green Chem.* **2018**, *20* (21), 4880–4890. DOI: 10.1039/C8GC01214H.
- (102) Wutzel, H.; Jarvid, M.; Bjuggren, J. M.; Johansson, A.; Englund, V.; Gubanski, S.; Andersson, M. R. Thioxanthone derivatives as stabilizers against electrical breakdown in cross-linked polyethylene for high voltage cable applications. *Polymer Degradation and Stability* **2015**, *112*, 63–69. DOI: 10.1016/j.polymdegradstab.2014.12.002.
- (103) Zunker, S.; R  he, J. Photo-Crosslinking of Thioxanthone Group Containing Copolymers for Surface Modification and Bioanalytics. *Macromolecules* **2020**, *53* (5), 1752–1759. DOI: 10.1021/acs.macromol.9b01503.
- (104) Veith, C.; Diot-N  ant, F.; Miller, S. A.; Allais, F. Synthesis and polymerization of bio-based acrylates: a review. *Polym. Chem.* **2020**, *11* (47), 7452–7470. DOI: 10.1039/D0PY01222J.
- (105) Di Lorenzo, F.; Seiffert, S. Nanostructural heterogeneity in polymer networks and gels. *Polym. Chem.* **2015**, *6* (31), 5515–5528. DOI: 10.1039/C4PY01677G.
- (106) Gruijl, F. R. de; van der Leun, J. C. Environment and health: 3. Ozone depletion and ultraviolet radiation. *CMAJ: Canadian Medical Association Journal* **2000**, *163* (7), 851–855.

- (107) Rostami, N.; Graf, D.; Schranzhofer, L.; Hild, S.; Hanemann, T. Overcoming oxygen inhibition effect by TODA in acrylate-based ceramic-filled inks. *Progress in Organic Coatings* **2019**, *130*, 221–225. DOI: 10.1016/j.porgcoat.2019.01.048.
- (108) Stevens, K. A.; Smith, Z. P.; Gleason, K. L.; Galizia, M.; Paul, D. R.; Freeman, B. D. Influence of temperature on gas solubility in thermally rearranged (TR) polymers. *Journal of Membrane Science* **2017**, *533*, 75–83. DOI: 10.1016/j.memsci.2017.03.005.
- (109) *Startseite - Leitfaden der Union zur Verordnung (EU) Nr. 10/2011 über Materialien und Gegenstände aus Kunststoff, die dazu bestimmt sind, mit Lebensmitteln in Berührung zu kommen.* https://www.bvl.bund.de/SharedDocs/Downloads/03_Verbraucherprodukte/lebensmittelkontaktmaterialien/leitfaden_eu_10_2011_Kunststoff.html (accessed 2023-11-02.264Z).
- (110) ISO. *ISO - Search.* <https://www.iso.org/search.html?q=10993> (accessed 2023-11-02.799Z).
- (111) Rothenbacher, T.; Baumann, M.; Fögel, D. 2-Isopropylthioxanthone (2-ITX) in food and food packaging materials on the German market. *Food additives and contaminants* **2007**, *24* (4), 438–444. DOI: 10.1080/02652030601182664.
- (112) Lee, S. Y.; Kim, J. S.; Lim, S. H.; Jang, S. H.; Kim, D. H.; Park, N.-H.; Jung, J. W.; Choi, J. The Investigation of the Silica-Reinforced Rubber Polymers with the Methoxy Type Silane Coupling Agents. *Polymers* **2020**, *12* (12). DOI: 10.3390/polym12123058. Published Online: Dec. 20, 2020.
- (113) Xie, Y.; Hill, C. A.S.; Xiao, Z.; Militz, H.; Mai, C. Silane coupling agents used for natural fiber/polymer composites: A review. *Composites Part A: Applied Science and Manufacturing* **2010**, *41* (7), 806–819. DOI: 10.1016/j.compositesa.2010.03.005.
- (114) Kumar, S.; Samal, S. K.; Mohanty, S.; Nayak, S. K. Recent Development of Biobased Epoxy Resins: A Review. *Polymer-Plastics Technology and Engineering* **2018**, *57* (3), 133–155. DOI: 10.1080/03602559.2016.1253742.
- (115) Jin, F.-L.; Li, X.; Park, S.-J. Synthesis and application of epoxy resins: A review. *Journal of Industrial and Engineering Chemistry* **2015**, *29*, 1–11. DOI: 10.1016/j.jiec.2015.03.026.
- (116) Sugane, K.; Mishima, T.; Shibata, M. Biobased epoxy nanocomposites composed of sorbitol polyglycidyl ether, biobased carboxylic acids and

microfibrillated cellulose. *J Polym Res* **2021**, 28 (7). DOI: 10.1007/s10965-021-02595-x.

(117) Terry, J. S.; Taylor, A. C. The properties and suitability of commercial bio-based epoxies for use in fiber-reinforced composites. *J Appl Polym Sci* **2021**, 138 (20). DOI: 10.1002/app.50417.

(118) Allen, K. W., Ed. *Adhesion 12*; Springer Netherlands, 1988. DOI: 10.1007/978-94-009-1349-3.

(119) D. J. Yarusso. Chapter 13 - Effect of rheology on PSA performance **2002**.

(120) Foltyn, P.; Restle, F.; Wissmann, M.; Hengsbach, S.; Weigand, B. The Effect of Patterned Micro-Structure on the Apparent Contact Angle and Three-Dimensional Contact Line. *Fluids* **2021**, 6 (2), 92. DOI: 10.3390/fluids6020092.

(121) Pradeep, S. A.; Iyer, R. K.; Kazan, H.; Pilla, S. 30 - Automotive Applications of Plastics: Past, Present, and Future. In *Applied plastics engineering handbook: Processing, materials, and applications*, Second edition; Kutz, M., Ed.; Plastics design library series; William Andrew, 2017; pp 651–673. DOI: 10.1016/B978-0-323-39040-8.00031-6.

(122) *Verordnung - 10/2011 - EN - EUR-Lex*. <https://eur-lex.europa.eu/legal-content/DE/TXT/?uri=celex%3A32011R0010> (accessed 2024-04-07.028Z).

(123) *Test Methods / Afera*. https://books.google.de/books/about/FINAT_Technical_Handbook.html?id=Rn3VjgEACAAJ&redir_esc=y (accessed 2023-11-03.950Z).

(124) Park, H.-W.; Seo, H.-S.; Kwon, K.; Lee, J.-H.; Shin, S. Enhanced Heat Resistance of Acrylic Pressure-Sensitive Adhesive by Incorporating Silicone Blocks Using Silicone-Based Macro-Azo-Initiator. *Polymers* **2020**, 12 (10). DOI: 10.3390/polym12102410. Published Online: Oct. 19, 2020.

(125) Zhang, A.; Ha, Z.; Xia, Y.; Chen, X.; Oliver, S.; Lei, L.; Shi, S. Synergistic improvement on both the oil-resistance and heat-resistance performance of a single-component acrylic pressure-sensitive adhesive. *Progress in Organic Coatings* **2022**, 172, 107096. DOI: 10.1016/j.porgcoat.2022.107096.

(126) FINAT. *FINAT Technical Handbook: Test Methods*; Finat, 2009.

(127) Yamada, M.; Takahashi, K.; Fujimura, N.; Nakamura, T. Generalized characteristics of peel tests independent of peel angle and tape thickness.

Engineering Fracture Mechanics **2022**, 271, 108653. DOI: 10.1016/j.engfracmech.2022.108653.

(128) Rau, D. A.; Reynolds, J. P.; Bryant, J. S.; Bortner, M. J.; Williams, C. B. A rheological approach for measuring cure depth of filled and unfilled photopolymers at additive manufacturing relevant length scales. *Additive Manufacturing* **2022**, 60, 103207. DOI: 10.1016/j.addma.2022.103207.

(129) Jiang, F.; Wörz, A.; Romeis, M.; Drummer, D. Analysis of UV-Assisted direct ink writing rheological properties and curing degree. *Polymer Testing* **2022**, 105, 107428. DOI: 10.1016/j.polymertesting.2021.107428.

(130) Park, J.; Lee, D. W.; Noh, S. M.; Jung, H. W. Optimal combination of UV - induced cationic ring opening polymerization monomers for light-weight automotive plastic coating. *J Appl Polym Sci* **2023**, 140 (25). DOI: 10.1002/app.53980.

(131) Gorsche, C.; Harikrishna, R.; Baudis, S.; Knaack, P.; Husar, B.; Laeuger, J.; Hoffmann, H.; Liska, R. Real Time-NIR/MIR-Photorheology: A Versatile Tool for the in Situ Characterization of Photopolymerization Reactions. *Analytical chemistry* **2017**, 89 (9), 4958–4968. DOI: 10.1021/acs.analchem.7b00272. Published Online: Apr. 19, 2017.

(132) Altgelt, K. H., Ed. *Gel permeation chromatography*; M. Dekker, 1971.

(133) Stuart, B. H. *Infrared spectroscopy: Fundamentals and applications*; Analytical techniques in the sciences; Wiley-Interscience, 2005. DOI: 10.1002/0470011149.

(134) Lambert, J. B.; Mazzola, E. P.; Ridge, C. D. *Nuclear magnetic resonance spectroscopy: An introduction to principles, applications, and experimental methods*, Second edition; John Wiley & Sons, 2019.

(135) Menczel, J. D.; Grebowicz, J., Eds. *Handbook of differential scanning calorimetry: Techniques, instrumentation, inorganic, organic and pharmaceutical substances*; Butterworth-Heinemann, 2023.

(136) Hinderer, F. *UV/Vis-Absorptions- und Fluoreszenz-Spektroskopie*; Springer Fachmedien Wiesbaden, 2020. DOI: 10.1007/978-3-658-25441-4.

(137) Voigtländer, B. *Atomic Force Microscopy*; Springer International Publishing, 2019. DOI: 10.1007/978-3-030-13654-3.

8. Appendix

8.1 List of abbreviations

¹³C NMR – 13-Carbon nuclear magnetic resonance

¹H NMR – Proton nuclear magnetic resonance

2-EHA – 2-Ethylhexyl Acrylate

3-HF – 3-Hydroxyflavone

ACEM – Activated chain end mechanism

AC-ITX – 3-(1-Methylethyl)-9-oxo-9H-thioxanthen-2-yl 2-propenoate

ACS-M – 3-(Trimethoxysilyl)propylacrylate

AF – Adhesion failure

AFM – Atomic force microscopy

AIBN – 2,2'-Azobis(isobutyronitrile)

AILED-P – (2,4-dimethoxyphenyl)phenyliodonium 2-naphthaleneacetonitrile hexafluorophosphate

AlAcAc – Aluminum acetyl acetonate

AMM – Activated monomer mechanism

BA – Butylacrylate

BPAE – Bisphenol A based Epoxide

BP-MA – 4-(Acryloyloxy)benzophenone

BPO – Phenyl bis(2,4,6-trimethylbenzoyl)-phosphine oxide

CAES-E – 2-(3,4-epoxycyclohexyl)ethyltriethoxysilane

CAESO-B – bis[2-(3,4-epoxycyclohexyl)ethyl]-tetramethyldisiloxane

CAESO-Q – tetrakis[(epoxycyclohexyl)ethyl]tetramethyl-cyclotetrasiloxane

CF – Cohesive failure

CILED-P – 7-methoxy-4-methylcoumarin-3-yl phenyliodonium hexafluorophosphate

CILED-Sb – 7-methoxy-4-methylcoumarin-3-yl phenyliodonium hexafluoroantimonate

CMR – Carcinogenic, mutagenic and reprotoxic

DBA – 9,10-Dibutoxyanthracene

DCM – Dichloromethane

DEMC – 7-Diethylamino-4-Methylcumarin

DMA – Dynamic mechanical analysis

DMSO-d6 – Deuterated Dimethyl sulfoxide

DMSO-d6 – Dimethylsulfoxid-d6

DSC – Differential scanning calorimetry

DTC – 4,6-bis (dodecylthiomethyl)-o-cresol

EPB – Epoxidized Polybutadiene

EPOMA – 3, 4-epoxycyclohexylmethyl methacrylate

EtOAc – Ethylacetate

GC – MS – Gas chromatography coupled with Mass spectrometry

GPC – Gel permeation chromatography

HBPAE – Hydrogenated (Bisphenol A) based Epoxide

HOMO – Highest Occupied Molecular Orbital

HTP – High throughput reactor

IP – Intellectual property

IR – Infrared spectroscopy

ITX – Isopropylthioxanthone

LC – MS – Liquid chromatography coupled with Mass spectrometry

LED – Light emitting diode

LSE – Low surface energy

LUMO – Lowest Unoccupied Molecular Orbital

MA – Methacrylate

OH-ITX – 2-Hydroxy-3-(1-methylethyl)-9H-thioxanthen-9-one

PE – Polyethylene

PET – Polyethylene terephthalate

POX – tert-Butyl peroxy-2-ethylhexanoate

PP – Polypropylene

PSA – Pressure sensitive adhesive

SAFT – Shear adhesion failure temperature

SOBE – Sorbitol based Epoxide

TAS-P – Triarylsulphonium hexafluoro phosphate salts (mixture)

TAS-Sb – Triarylsulphonium hexafluoro antimonate salts (mixture)

T_g – Glass transition temperature

TMSN – Tetramethylsuccinonitril

TPO – Diphenyl(2,4,6-trimethylbenzoyl)phosphine oxide

TS – Total solid

VMOX – Vinyl methyl oxazolidinone

8.2 Acknowledgements

This dissertation was created between 2020 and 2023 in the laboratories of Henkel AG & Co. KGaA.

First of all, I would like to thank Dr. Anja Schneider, Dr. Andreas Taden, Thomas Roschkowski and Dr. Dirk Kasper in particular for their trust in me to embark on this journey together and the interesting research topic. I would also like to thank the HHU Düsseldorf, in particular Professor Dr. Laura Hartmann and PD Dr. Klaus Schaper, for their continuous and encouraging support. I would also like to thank them for their generous trust and openness towards the selection of topics as well as the ongoing project planning.

Special thanks are due to the entire APP PSA PD+AE team. In the past three years I always had the feeling that I could count on each and every one of you and that I always got an open ear for technical as well as interpersonal questions and that technical discussions were not only promising but were accompanied by a lot of fun as well. Thank you for hundreds of rounds of table football together, the "butterfly attack" will go down in history, I am sure. Both our meetings with many laughs and the team events I will not forget. I think the hardcover book in the prison cell of the Escape Room has been removed in the meantime. Unfortunately, I decided to run with a career as a Chemist and not as a Locksmith. Who will actually stand at the grill from now on?

Also many thanks to our US colleagues and the Project Lead. Without you, a scale-up would not have been possible. In addition, many thanks to our Business Development for the encouraging words. I am infinitely grateful to Henkel Analytics for performing countless analyses, some of which were not commonplace. Thank you for often prioritizing my samples so to not waste time.

Lastly, I would like to thank my parents Michaela and Michael, my sister Caroline, my grandparents and my girlfriend Kathi. Without you, the last three years would not have been possible. You have not only supported me financially, but have always been there for me, in ups and in downs. Your tolerance and dedication have made this work possible.